Human leukocyte transcriptome changes in response to altered gravity environments: investigations using bed rest participants and astronauts aboard the International Space Station

Daniel Stratis

A thesis submitted in partial fulfillment for a Master of Science in Biology

Department of Biology

Faculty of Science

University of Ottawa

Preface

This thesis investigates two studies: (1) the Toulouse Cocktail Bed Rest Study and (2) the MARROW spaceflight study. Research ethics for the first study were obtained from the Comité de protection des personnes Sud-ouest et outre-mer (ID-RCB:2016-A00401-50) and reviewed by the Ottawa Health Science Network Research Ethics Board (#20160925-01H). Funding was provided by the European Space Agency (ESA), the Centre National d'Etudes Spatiales and the Canadian Space Agency (CSA). For the second study, ethics was obtained from NASA Human Research Multilateral Review (#Pro1283), Johnson Space Center Institutional Review Board, European Space Agency Medical Board, Japanese Aerospace Exploration Agency (JAXA), and the Ottawa Health Science Network Research Ethics Board (#2009646-01H). This study was funded by the Canadian Space Agency. All participants from both studies provided written informed consent. For both research articles contained in this thesis, I was first author. My contributions were as follows: analysis of data, interpretation of results, preparation of figures, drafting of manuscripts, editing and revision of manuscripts, and approval of final version of articles.

In consultation with the journals, I retain the right as an author to include published articles as part of this thesis and post to thesis repositories. Copyright permissions have been included in Appendix II, and articles have been properly referenced with the respective journals as the original source.

Abstract

Introduction: Space is an extreme environment exposing astronauts to microgravity and cosmic radiation resulting in immune dysfunction. To overcome the complex challenges of studying astronauts in space, bed rest studies represent an alternative model simulating microgravity exposure on Earth. We sought to characterize the steady-state transcriptome changes in leukocytes isolated from two microgravity models: (1) participants to 60 days of bed rest and (2) astronauts to ~6 months of spaceflight. **Methods:** The bed rest study recruited twenty healthy men receiving a nutritional supplement or not; the spaceflight study had fourteen male and female astronauts participate. For both studies, ten blood samples were collected over three study phases, leukocytes were isolated, and transcriptomes were quantified using high throughput RNA-sequencing. My pipeline of data analysis applied differential expression (DE) methods and functional enrichment to identify gene expression changes and pathways responding to the altered gravity environments of both bed rest and spaceflight models. **Results:** Temporal differential expression identified transcriptome modulation reflecting multisystem shifts and immune dysregulation in response to the transitions to and from bed rest (2,415 DE genes) and spaceflight (247 DE genes). Interestingly, later bed rest and in-flight timepoints trended towards stable RNA levels with no differential expression. The bed rest study found the nutritional intervention had no mitigating effects on transcriptome changes (0 DE genes), and the spaceflight study revealed down-regulation in response to spaceflight followed by an opposite up-regulation upon return to Earth. **Conclusion:** The altered gravity environments of bed rest and spaceflight significantly modulated leukocyte transcriptome compositions revealing immune dysfunction at the molecular level. Future analyses utilizing the higher quality bed rest dataset is required to isolate the effect of microgravity from other space stressors and apply validation experiments to develop gene biomarkers indicative of immune deconditioning.

Résumé

Introduction: L'espace constitue un environnement extrême exposant les astronautes à la microgravité et au rayonnement cosmique entraînant un dysfonctionnement immunitaire. Pour surmonter les défis complexes de l'étude des astronautes dans l'espace, les études d'alitement représentent un modèle alternatif simulant l'exposition à la microgravité sur Terre. Nous avons cherché à caractériser les modifications du transcriptome à l'état d'équilibre dans les leucocytes isolés de deux modèles d'étude: (1) participants à 60 jours d'alitement et (2) astronautes séjournant environ 6 mois dans l'espace. **Méthodes:** L'étude d'alitement a recruté vingt hommes en bonne santé recevant ou non un supplément nutritionnel; l'étude de vols spatiaux a inclus la participation de quatorze astronautes; 11 hommes et 3 femmes. Pour les deux études, dix échantillons de sang ont été prélevés au cours des trois phases d'étude, les leucocytes ont été isolés et les transcriptomes ont été quantifiés à l'aide du séquençage de l'ARN à haut débit. Ma stratégie d'analyse de données a appliqué des méthodes de mesure d'expression différentielle (ED) et d'enrichissement fonctionnel pour identifier les changements d'expression génique et les voies répondant aux environnements de gravité différents associés aux modèles d'alitement et de vol spatial. **Résultats:** L'expression différentielle temporelle a identifié la modulation du transcriptome reflétant les changements multisystémiques et une dérégulation immunitaire en réponse aux transitions vers et à la sortie de l'alitement (2 415 gènes DE) et aux vols spatiaux (247 gènes DE). Fait intéressant, l'alitement prolongé et les temps de récolte en vol tendaient vers des niveaux d'ARN stables soit sans expression différentielle. L'étude d'alitement a révélé que l'intervention nutritionnelle n'avait aucun effet atténuant sur les changements du transcriptome (gènes 0 DE), et l'étude des vols spatiaux a révélé une régulation à la baisse en réponse au vol dans l'espace suivie d'une régulation à la hausse opposée lors du retour sur Terre. **Conclusion:** Les environnements de gravité modifiés d'alitement et de vols spatiaux ont modulé de manière significative les compositions du transcriptome des leucocytes, révélant un dysfonctionnement immunitaire au niveau moléculaire. De

futures analyses utilisant l'ensemble de données d'alitement qui est de qualité supérieure sont nécessaires pour isoler l'effet de la microgravité des autres facteurs associés au stress spatiaux et effectuer des expériences de validation pour identifier des biomarqueurs génétiques indicatifs du déconditionnement immunitaire.

Acknowledgments

Firstly, I would like to express my immense gratitude to my supervising professor Dr. Odette Laneuville for her commitment, support, and belief in my abilities throughout my research journey. She has provided me with invaluable guidance and lessons that have not only shaped my academic pursuits but also left a lasting impact on my personal growth as an individual.

I would like to thank Dr. Martin Pelchat for his exceptional teachings and guidance in the fields of bioinformatics and computer science. I will fondly remember our meetings with Dr. Laneuville as both productive and entertaining.

I appreciate my thesis advisory committee members, Dr. Julien Martin and Dr. Marc Ekker for their valuable feedback and insightful suggestions throughout my degree. I'd also like to acknowledge their excellent teachings of advanced statistics and molecular methods respectively.

I am grateful for all the enjoyable lunches and great company from students both within and outside the Laneuville lab. I'd especially like to express my gratitude to Dr. Haodong Zhou for his mentorship and shared experience as a graduate student guiding me through my degree.

Funding for my degree included support from the University of Ottawa. Funding for this research was provided by the European Space Agency, the Centre National d'Etudes Spatiales, and the Canadian Space Agency awarded to Dr. Odette Laneuville and Dr. Guy Trudel.

Lastly, my academic journey would not have been possible without the unwavering support, encouragement, and love from my family and friends. They have been a constant source of inspiration and strength providing meaning to this achievement.

Table of Contents

List of Tables

Chapter 2

Supplemental Table

List of Figures

Abbreviations

ANODEV	Analysis of deviance
ANOVA	Analysis of variance
BDC	Baseline Data Collection
C	Cluster
CD	Cluster of Differentiation
CLT	Central Limit Theorem
CMV	Cytomegalovirus
CSA	Canadian Space Station
DE	Differentially Expressed
EBV	Epstein-Barr Virus
ELISA	Enzyme-Linked Immunosorbent Assay
ESA	European Space Station
FDR	False Discovery Rate
GLM	Generalized Linear Model
GO	Gene Ontology
GRO-seq	Global Run-On sequencing
GSEA	Gene Set Enrichment Analysis
HAD	Hospital Acquired Deconditioning
HDT	Head Down Tilt
HSV	Herpes Simplex Virus
IAA	International Academy of Astronautics
IF	In-Flight

IHW	Independent Hypothesis Weighting
IQR	Interquartile Range
ISS	International Space Station
JAXA	Japanese Aerospace Exploration Agency
LFC	Log2 Fold Change
LINC	Long Intergenic Non-Protein Coding
LRT	Likelihood Ratio Test
MARROW	Marrow Adipose Reaction: Red or White
ML	Machine Learning
NASA	National Aeronautics and Space Administration
NES	Normalized Enrichment Score
NGS	Next Generation Sequencing
NK	Natural Killer
ORA	Overrepresentation Analysis
PBMC	Peripheral Blood Mononuclear Cell
PCA	Principal Component Analysis
PF	Pre-Flight
PST	Plasma Separator Tube
R	Reambulation/Return to Earth
RIN	RNA Integrity Number
RNA-seq	Ribonucleic Acid sequencing
SANS	Spaceflight-Associated Neuro-Ocular Syndrome
SBS	Sequencing-By-Synthesis
sEV	secreted Extracellular Vesicles

SSE	Sum of Squared Error
TEC	To be Experimentally Confirmed
TNF	Tumor Necrosis Factor
VFF	Vertebral Fat Fraction
VST	Variance Stabilizing Transformation
VZV	Varicella Zoster Virus
ZAP	Zinc-Finger Antiviral Protein
ZNF	Zinc-Finger Protein

Introduction

Spaceflight-induced deconditioning

Short and long-term spaceflight is an extreme environment exposing the human body to cosmic radiation and microgravity. Most physiological functions are negatively affected leading to the deconditioning and reduced functional capacity of multiple organ systems (1,2). For astronauts sojourning in space, the most rapid physiological change occurring within days in microgravity is the redistribution of blood and bodily fluids from the lower to upper part of the body (3,4). In microgravity, the loss of gravitational pull downwards means the body's hydrostatic pressure gradient disappears and blood moves upwards toward the head and upper body by the actions of smooth muscles and veins (5). This creates the appearance of "puffy face bird leg" syndrome observed in astronauts from facial edema and decreased leg volume (Figure 0.1) (4).This also results in symptoms of "space motion sickness" including anorexia, vomiting, nausea, headache, and malaise caused by altered responses of baroreceptors, nervous and endocrine systems (6). Additionally, the headward fluid shift has been proposed as an etiology for spaceflight-associated neuro-ocular syndrome (SANS); ophthalmic abnormalities in astronauts after long-duration spaceflight caused by increased intracranial pressure (7,8). At the cellular level, loss of hydrostatic pressure gradients alters the Starling-Landis equilibrium of blood plasma, causing it to shift towards extravascular tissues including the lymphatic system resulting in pronounced diuresis and plasma volume reduction by 10-15% within 24-48 h in space (9,10). Reduced plasma volume implies increased concentration of blood cells that must be returned to normal homeostatic levels achieved through hemolysis, which has been proposed as a major contributor to anemia observed in astronauts (11,12).

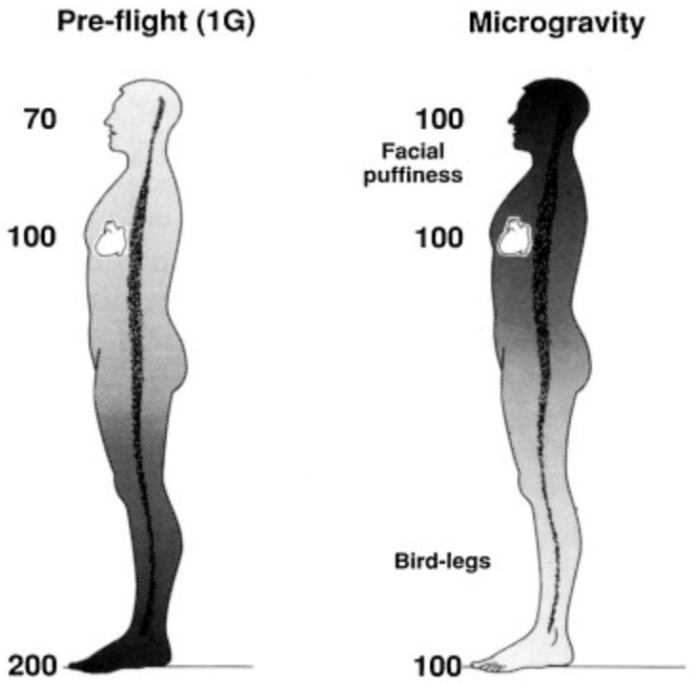

Figure 0.1 | Headward fluid shift during spaceflight. Expected distributions of body fluids (shading) and mean arterial pressure (numerical values in mm Hg) at the head, heart and feet during pre-flight (left) and microgravity (right). Figure modified from Watenpaugh and Hargen, 1996 (5).

Spaceflight also affects the musculoskeletal system, mainly resulting in loss of bone and muscle mass attributed to the unloaded state of microgravity (13). These effects are dependent on the role of each body region in counteracting gravity. For instance, sites that support weight bearing in normal gravity such as the legs and lower extremities typically show greater degeneration than in regions that are non-weight bearing such as the neck (14,15). Bone density loss experienced in microgravity occurs at an average rate of about 1-1.5% per month resulting in increased risk of bone fracture post-flight (16). Skylab missions from the 1970s have shown increased bone resorption and reduction in Ca^{2+} balance (17). Bone formation is typically unchanged or decreases during spaceflight without effective exercise-induced bone loading (18). Taken together, increased bone resorption and decreased or unchanged bone

formation yield a negative calcium balance that results in bone loss and increased risk of developing kidney stones (19).

Muscle atrophy is driven by a reduction in fiber size and protein synthesis, bearing similarities to catabolic patients undergoing metabolic breakdown (1,2). The National Aeronautics and Space administration (NASA) Twins Study collected samples from an astronaut during a one-year mission aboard the International Space Station (ISS) with comparisons to his identical Earth-bound twin (20). Biochemical profiling of blood samples collected on day 1 of post-flight found significant rises in inflammatory cytokines IL-6, IL-10, IL-1ra, CCL2 and CRP when compared to pre-flight. These cytokines are associated with muscle metabolism and suggests muscle regeneration in response to microgravity (21). Twin's studies provide the unique opportunity of controlling for genetic variation; however, these findings are limited in generalizability to the broader population given the sample size was n = 1.

Despite the strong health and preventive isolation of astronauts from terrestrial pathogens before and during spaceflight missions, they still experience complicated patterns of immune system dysregulation mostly manifesting at the subclinical level; mainly from changes of leukocyte cell distributions, reduced function of leukocyte sub-populations, and altered cytokine profiles (1). However, these outcomes can trigger adverse clinical events in some astronauts including infections from bacteria and viruses, chronic inflammation, atypical allergies, and atopic dermatitis (22). For instance, Th1/Th2 cytokine imbalances lead to shifts in Th2-cell mediated immunity and persistent inflammation resulting in subclinical reactivation and shedding of herpesvirus particles (23–25). At the molecular level, the underlying mechanisms responsible for these outcomes are less understood. One study measured transcript level changes for 234 known stress-response genes in the blood of six astronauts before and after spaceflight, and found differentially regulated transcripts involved in DNA repair, oxidative stress, and protein folding (26). However, this study lacked in-flight measurements and used an older technique of microarrays that does not allow genome-wide measures of transcript levels. The NASA Twins study

found inflammation-associated transcriptomic signatures in peripheral blood mononuclear cells (PMBCs) (20), consistent with increases of inflammatory cytokines in the plasma of astronauts (21,25). Another study isolated blood exosomes from three astronauts who flew short missions to the ISS (~5-13 days) and identified 27 differentially regulated long non-coding RNAs (lncRNA) with previously documented activities regulating gene expression (27). However, this study also lacked in-flight measurements. More studies with larger sample sizes of astronauts sampled during spaceflight are required for a more comprehensive understanding of the biological processes underlying immune deconditioning in astronauts during spaceflight.

Studying long-term space travel

The Artemis Lunar Missions aim to return humans to the Moon including plans to build the Gateway Lunar Outpost for long-term crewed missions (28). Several agencies and private companies have expressed interest in conducting long-term crewed missions to Mars lasting several years (29). Besides lunar and Mars missions, there is a growing interest in deep space exploration to destinations in our solar system such as asteroids or moons of Jupiter and Saturn. Additionally, there are many commercial space initiatives to build private space stations and even develop space tourism. Given the growing demand for manned long-term space exploration, there must be a proportional need for biomedical research to further understand and mitigate spaceflight-induced deconditioning. The Marrow Adipose Reaction: Red or White (MARROW) project lead by my laboratory represents one such initiative focusing on the bone marrow and blood cell changes occurring during spaceflight (11). This longitudinal study recruited fourteen male and female astronauts scheduled for ~6-month long missions aboard the ISS and collected biological samples during pre-flight, in-flight, and up to one-year post-flight (Figure 2.1) (30). The study design, samples collection days, and collection protocols were all controlled and dictated by NASA. Collected samples included breath, stool, and blood to study various biological systems

including bone, microbiome, hematology, and immunology. The focus of my thesis is on total RNA measures extracted from leukocytes within the blood (Chapter 2) (30).

Studying astronauts during spaceflight provides invaluable and unique opportunities to gain knowledge on human physiology while adapting to the extreme environment of space. However, this process is far from straightforward and entails complex logistical and technical challenges that are difficult to overcome; mainly low sample sizes, and technical obstacles for sample collection and processing in microgravity. Astronaut samples are scarce given the current infrequency of human space travel. Typically, there is only 3 or 6 people onboard the ISS at any given time (https://www.nasa.gov/feature/facts-and-figures). Sample collection is also associated with numerous technical challenges, including both natural barriers imposed by the space environment or artificially by NASA protocol. In addition to microgravity, astronauts face many other spaceflight hazards and stressors including confinement and isolation, hostile and closed environments, and exposure to cosmic radiation (1). All these hazards induce downstream physiological and psychological issues making it impossible to isolate the effect of microgravity on its own. Given the tight constraints and environmental hazards associated with in-flight studies, ground-based analogs are both practical and attractive to isolate the microgravity effect.

Bed rest model: an Earth-based microgravity analog

The bed rest model confines healthy participants to 24/7 bed rest in the horizontal supine or head-down tilt (HDT) position for prolonged periods of time. This is an experimental analog designed to simulate microgravity exposure through unloading and hypokinesia of the body by altering the gravity vector experienced by participants and induce physiological adaptations similar to those experienced by astronauts during spaceflight (31,32). Bed rest study standardizations to enhance reliability, repeatability and validity of studies have been published by the *International Academy of Astronautics* (IAA) with a

report entitled “Guidelines for standardization of Bed Rest Studies in the Spaceflight Context” (https://www.nasa.gov/hrp/important_documents). Guidelines include study durations, position (HDT), management, nomenclature, subject inclusion and exclusion criteria, subject monitoring, physiotherapy, medical care, psychological support, ethics, nutritional intake, and handling of biological samples (31). However, its important to note that all bed rest studies vary in experimental design, lengths, and tested interventions (2). For instance, the use of -6° head-down tilt has become an informal standard over time, with the purpose of mimicking the headward fluid shift experienced by astronauts (Figure 0.2) (31). Studies typically recruit 9-25 participants of one sex with most studies using only males, but female only studies have been conducted (33). Study designs usually include three phases: before, during and after bed rest with each phase varying in the number of days. Bed rest durations vary from 5-90 days in bed, with most studies using 60 days. Lastly, essentially all bed rest studies test a different countermeasure involving exercise regimens, artificial gravity, pharmacological or nutritional interventions attempting to mitigate the negative effects of unloading (2).

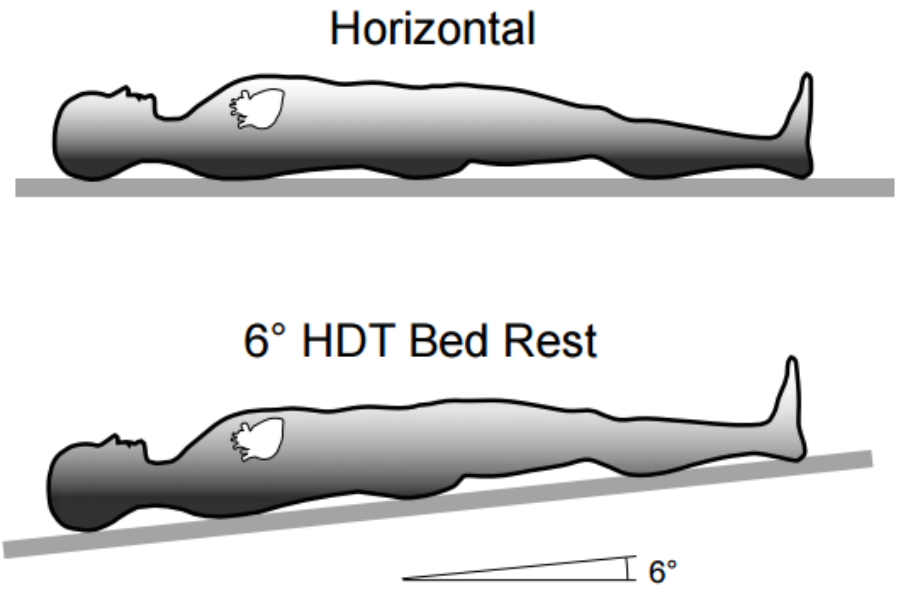

Figure 0.2 | -6° head down-tilt (HDT) bed rest model. Expected distributions of body fluids (shading) at the head, heart and feet for bed rest participants in the horizontal (top) and head down-tilt positions (bottom). Figure modified from Hargens and Vico, 2016 (9).

The advantages of using ground-based microgravity analogs such as the bed rest model to study the impact of microgravity on health are numerous. As discussed above, bed rest study standardization for participant recruitment increases reproducibility between experiments and reduces confounding variables. Controlled study environments under 24/7 medical surveillance also contributes to the reduction of confounders and greatly improves technical support to measure more biological outcomes. Experimental hazards are fewer relative to spaceflight and there are less constraints imposed on researchers for biological measures. Sample sizes are larger given the substantial increase in recruitment pools compared to astronauts. Lastly, bed rest models offer the opportunity to develop and test countermeasures to mitigate the negative effects of microgravity. Overall, insights gained from bed rest studies can inform and enhance future space missions, contributing to astronaut health and performance in space.

Many of the physiological changes observed in astronauts during spaceflight are also observed in bed rest participants. However, these changes are usually not as severe and are subclinical in many cases (9). For instance, head down-tilt bed rest induces a headward fluid shift resulting in a 10-15% plasma volume reduction similar to astronauts (34), but no immediate symptoms of headache, nausea, or vomiting occur. Additionally, evidence of ocular impairments during bed rest have only been reported at the cellular level (9,35), and low-grade hemolysis has been measured during bed rest but with no symptoms of anemia (36). Bone modifications in both bed rest and spaceflight studies are characterized by diminished bone mineral densities, augmented calcium in urine, and increased risk of renal stone formation (37). Although reported changes are often more severe during spaceflight than with bed rest (9). Skeletal muscle changes are also similar between bed rest and spaceflight models including major losses of fiber mass and force that's greater in the weight-bearing regions such as the legs (38,39). Clinical immune symptoms or evidence of infection have not been reported in bed rest participants, the only evidence of immune dysfunction occurs at the cellular and molecular levels. Immune cell count changes are mixed with reports of no significant changes in lymphocyte subsets or B-cell homeostasis (40) but increases in granulocytes and natural killer T cells with decreases in $CD4^+$ and $CD8^+$ T cells during bed rest (41,42). This is consistent with astronaut studies showing no changes in specific adaptive immunity during spaceflight (25). Inflammatory changes are consistently reported with neutrophil shedding of L-selectin, increases in the number of polymorphonuclear cells, and shifts in various cytokine concentrations (43,44). The bed rest model simulates many aspects of microgravity but cannot account for all other spaceflight hazards that likely contribute to deconditioning. This makes many of the immune function changes to only manifest at the subclinical level stressing the importance of focusing on the molecular aspects of immune deconditioning during bed rest.

The Toulouse Cocktail Bed Rest Study was conducted in Toulouse, France between 2017 and 2018. Twenty healthy male participants were recruited to undergo a three phase bed rest study: 15 days

in baseline, 60 days in -6° head-down tilt bed rest, and 30 days in reambulation. To test the efficacy of a nutritional intervention at mitigating bed rest-induced deconditioning, participants were divided into two equal groups: “control” and “cocktail”. The “cocktail” group received a daily oral dosage of pills containing anti-inflammatories, anti-oxidants, and vitamins during the bed rest phase (45). Details on the contents of the nutritional intervention can be found in the methods section of Chapter 1. Various biological samples and data were collected from 16 different international research teams during baseline, bed rest, and up to 30 days reambulation (Figure 1.1) (45). The European Space Agency (ESA) financed the study and dictated participant recruitment, study design, blood sample collection days, and integration of all protocols. Our lab collected blood samples to extract the total RNA from leukocytes and measure the transcriptome changes over time (Chapter 1) (45).

Transcriptomics: genome-wide expression analysis

The transcriptome is defined as the set of all RNA transcripts (coding and non-coding) produced by a population of cells (46). It represents the steady-state of RNA transcript levels as a consequence of multiple processes within the cell, mainly RNA transcription and degradation (47). Steady-state analysis hinders the distinction between transcriptional and post-transcriptional strategies to regulate RNA levels. Nevertheless, measuring transcriptome changes provides valuable insight into the dynamic gene expression patterns and molecular responses that underly the physiological processes when cells adapt to novel conditions (48). As such, measuring the transcriptome changes in blood leukocytes offers a molecular understanding of immune system deconditioning resulting from spaceflight and bed rest. Additionally, leukocytes circulate throughout the entire body contacting multiple organ systems and thus may reflect multisystem changes outside of the immune system. For future applications, blood sampling represents a simple and convenient method for measuring gene biomarkers to monitor physiological or

subclinical changes, assess efficacy of interventions, and provide personalized interventions for astronauts during space travel (49).

RNA-sequencing (RNA-seq) is the combination of high-throughput sequencing with computational methods to capture and quantify genome-wide transcript levels (50). Currently, RNA-seq is the superior and dominant method to quantify transcriptomics over microarrays with advantages such as wider dynamic ranges, genome-wide profiling, increased sensitivity, improved accuracy and precision, greater statistical power, and decreasing costs (50,51). Figure 0.3 depicts an oversimplified summary of the steps of RNA-seq. *In vitro* steps include library preparation and sequencing: extracted RNA is fragmented, and reverse transcribes it into complimentary (c) DNA, which are sequenced producing millions of short read sequences. Sequencing was performed at the Genome Quebec Innovation Center in Montreal, Canada using the NovaSeq6000 system to perform Next Generation Sequencing (NGS). Specifically, this system utilizes the sequencing-by-synthesis (SBS) method to process multiple samples simultaneously while also applying paired-end sequencing that sequences both ends of a DNA fragment (52). *In silico* mapping then aligns these read sequences to a reference genome to quantify relative transcript abundance (Figure 0.3) (50). Read mapping accuracy is improved with paired-end sequencing, which also provides the necessary information to detect and characterize splice variants by defining intron-exon boundaries (53).

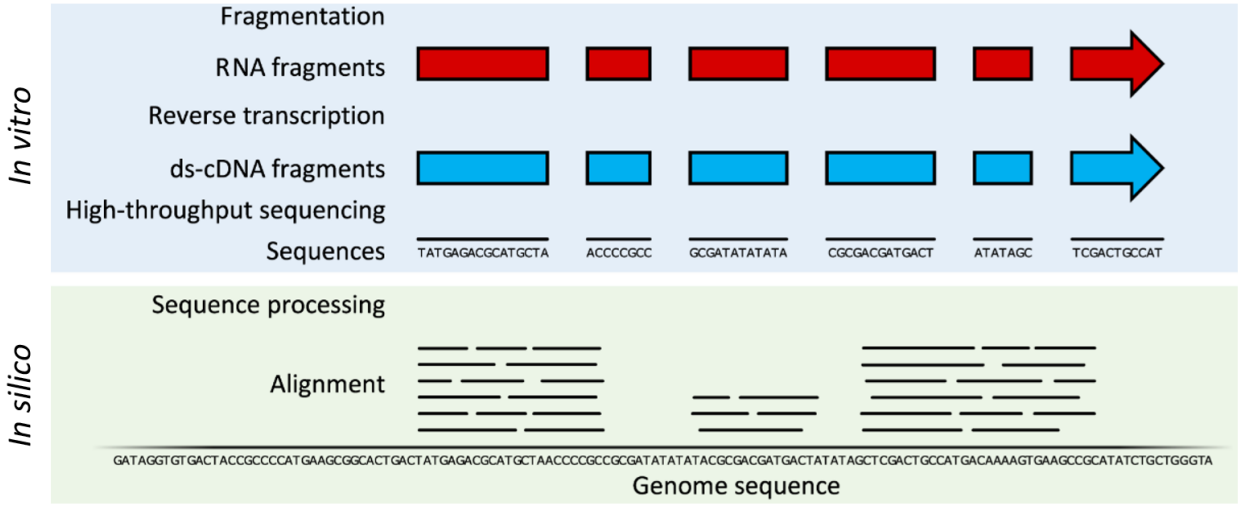

Figure 0.3 | RNA-sequencing summary. In vitro steps (blue). Library preparation: extracted RNA from a population of cells is fragmented, then reverse transcribed into double-stranded complimentary (ds-c) DNA; sequencing: ds-cDNA fragments are sequenced using Next Generation Sequencing (NGS) methods producing millions of short read sequences. In silico steps (green). Mapping: reads are aligned to a reference genome sequence to annotate relative levels of gene expression. Figure modified from Lowe et al, 2017 (50).

Other computational methods exist for different experimental purposes such as *de novo* assembly of reads to identify novel transcripts, or transcript and exon-level mapping to study alternative splicing events (54). However, these were not the focus of my thesis, which was focused on gene-level mapping to annotated genes and quantify their expression level changes. Gene-level mapping resulted in a matrix of integer read counts for tens of thousands of genes in each RNA sample. The data analysis of read count tables marks the start of my involvement in the Toulouse bed rest and MARROW spaceflight projects.

Pipeline of data analysis

The first step of my analyses was to normalize the raw read count for between-sample effects, mainly read depth and RNA composition (Figure 0.4). Accounting for these technical effects is necessary to ensure the read count data is accurately reflecting differences in expression (55). Read depth refers to the total number of reads in a sample, which usually differs between samples as the result of sequencing variability (Figure 0.4 *left*) (56). Ignoring this effect results in inaccurate sample comparisons and biased differential expression results (55). RNA composition refers to several highly differentially expressed genes between samples that skews the expression of other genes (Figure 0.4 *right*) (57). To account for both read depth and RNA composition, I used the *size factor normalization* method from the *DESeq2* package in R (58). In summary, this method estimated size factors for each sample, divided the raw count data by these size factors, and applied a log transformation to stabilize variance across expression values (59). Read normalization was necessary for gene differential expression analyses, but also essential for exploratory analyses or data visualizations whenever between sample comparisons were made.

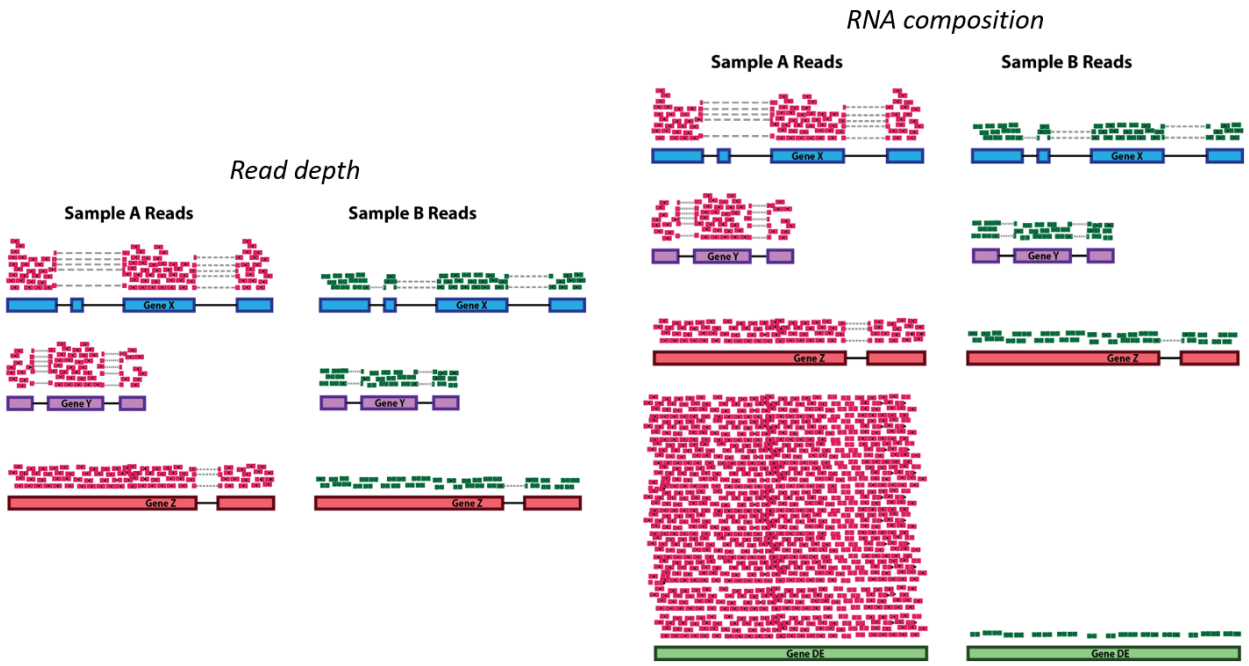

Figure 0.4 | Read count normalization for between-sample effects. Left, read depth differences between samples. Genes in *Sample A* appear to have more reads relative to *Sample B*, however this is a consequence of *Sample A* having a higher read depth. Right, RNA composition differences between samples. The differentially expressed (DE) gene takes up most of the read counts in *Sample A*, but not *Sample B*. Normalizing each sample by dividing by the total number of read counts would make most other genes in *Sample A* appear less expressed than those same genes in *Sample B*. Pink and green rectangles represent reads aligned to a gene. Reads connected by dashed lines connect to a read spanning an intron. Source from: https://hbctraining.github.io/DGE_workshop/lessons/02_DGE_count_normalization.html

To quantify significant changes in gene expression levels, I used the *DESeq2* package in R (58) to identify specific gene candidates responding to bed rest and spaceflight. The main advantage of *DESeq2's* statistical strategies are to address the limitations of low read count genes represented in RNA-seq data. Low read count genes are more susceptible to sampling variability and technical noise introducing higher

levels of variation (60). Essentially, low read count genes have poor signal to noise ratios making statistical analysis more unreliable. To overcome this issue, *DESeq2* includes a preprocessing step that employs independent filtering to remove low count or uninformative genes. Gene-specific dispersion is then estimated and encompasses both biological and technical variability in gene expression (57,61). Generalized linear models assuming negative binomial distributions are fitted and statistical testing accounting for multiple comparisons yield genes considered differentially expressed (58). Further interpretations can be made from gene log2 fold changes (LFC) with the option to shrink them to improve the precision of lowly expressed genes (58). Conventional transcriptome studies with longitudinal study designs have typically focused on the differential expression changes at specific timepoint comparisons and rarely integrate time-dependent analyses that capture temporal patterns and expression trajectories. This is true for the NASA Twins study, which segregated in-flight from pre-flight, post-flight and ground samples focusing on differential expression between pre-flight/ground vs in-flight and post-flight (20). This approach missed the expression trends and patterns over time, specifically failing to uncover any transitional responses to and from spaceflight and did not take advantage of the multiple timepoints collected during each study phase of the mission. My main goal was to overcome these limitations by incorporating temporal differential expression analyses integrating all three phases of both studies: Toulouse bed rest (baseline, bed rest, and reambulation); MARROW spaceflight (pre-flight, in-flight, and post-flight). For both studies, I used the same statistical strategies and *DESeq2* to find specific genes that were differentially expressed between any timepoint and plotted the expression values for these genes across time to reveal their temporal expression changes. For the MARROW spaceflight study, I included further differential expression analyses of certain timepoint comparisons selected based on the temporal results. Mainly, the focus of these comparisons was on the transition periods to and from spaceflight.

Summarizing the biological functions of differentially expressed genes was achieved through the enrichment of gene ontology (GO) terms, which are standardized annotations describing functional attributes and biological properties of genes (62). GO terms are developed and maintained by the GO Consortium and stored in the GO database for public access (63). One widely used strategy for extracting GO terms that are significantly enriched is through an overrepresentation analysis (ORA). This compares the number of differentially expressed genes within a particular GO term to the total number of genes in the genome associated with that term. The Fisher Exact Test is then applied to calculate statistical significance and determines if a GO term is more prevalent in a list of differentially expressed genes than expected by chance (64). The ORA functional enrichment method utilized the lists of differentially expressed genes from both studies to identify functional themes responsive to both bed rest and spaceflight environments. Another common approach is the Gene Set Enrichment Analysis (GSEA) (65). This approach requires a list of genes ranked based on numerical values such as LFC or normalized read counts, which are used to calculate normalized enrichment scores (NES) that measure the cumulative deviation of the gene list from the expected distribution. NES values are then compared to a null distribution of enrichment scores determined through permutations testing and statistical significance is calculated to yield enriched GO terms from the ranked list of genes. GSEA was only performed on the bed rest transcriptome at baseline.

Overall, I used a pipeline of data transformations and statistical techniques to normalize read counts, isolate differentially expressed gene candidates changing over time, and summarize the biological functions of those gene candidates. Figure 0.5 depicts the pipeline of data analysis I used to investigate the transcriptome changes in leukocytes taken from bed rest participants and astronauts in space.

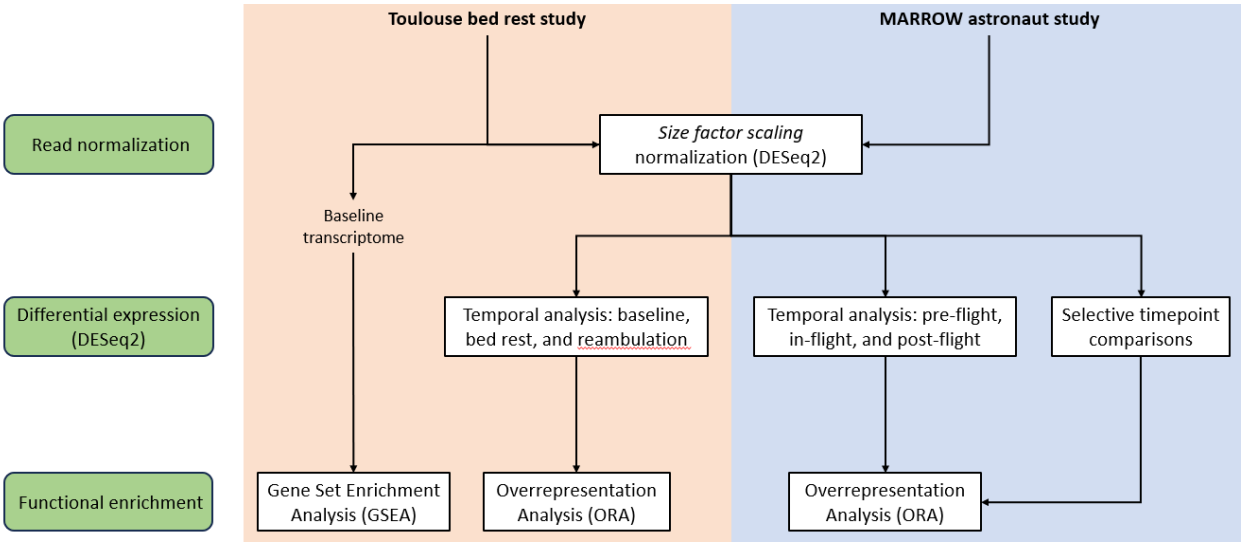

Figure 0.5 | Pipeline of read count data analysis. Strategies for read normalization, differential expression, and functional enrichment for both the Toulouse bed rest (orange) and MARROW astronaut studies (blue).

Purpose and objectives

The purpose of my thesis was to characterize the composition of human blood leukocyte transcriptome changes over time in response to altered gravity environments using two experimental models: participants to 60 days in bed rest (Chapter 1), and astronauts to ~6 months in spaceflight (Chapter 2). Chapter 1 is a hypothesis-generating study examining the temporal response of leukocyte transcriptome changes in healthy participants to a 60-day bed rest study combined with a hypothesis-testing aspect measuring any mitigating effect of a nutritional intervention (45). My hypothesis is the nutritional intervention will not alter the transcriptome over time and predict transcriptome changes will not differ between control and cocktail groups. Chapter 2 does not test any countermeasure and is therefore solely hypothesis-generating evaluating the temporal expression changes with focus on selective timepoint comparisons to capture transcriptional shifts in astronauts during the transition to and from ~6 months of spaceflight (30).

Chapter 1

The characteristic response of the human leukocyte transcriptome to 60 days of bed rest and to reambulation

Medicine & Science in Sports & Exercise

Daniel Stratis[1]; Guy Trudel[2,3,4]; Lynda Rocheleau[4]; Martin Pelchat[4]; Odette Laneuville[1,2]

[1] Department of Biology, Faculty of Science, University of Ottawa, Ottawa, Ontario, Canada

[2] Bone and Joint Research Laboratory, Ottawa Hospital Research Institute, Ottawa, Ontario, Canada

[3] Department of Medicine, Division of Physiatry, Faculty of Medicine, University of Ottawa, Ottawa, Ontario, Canada

[4] Department of Biochemistry, Microbiology and Immunology, Faculty of Medicine, University of Ottawa, Ottawa, Ontario, Canada

Stratis, Daniel; Trudel, Guy; Rocheleau, Lynda; Pelchat, Martin; Laneuville, Odette. The Characteristic Response of the Human Leukocyte Transcriptome to 60 Days of Bed Rest and to Reambulation. *Medicine & Science in Sports & Exercise*. 2023; 55(3): 365-375. DOI: 10.1249/MSS.0000000000003071

Keywords: Bed rest; reambulation; transcriptome; leukocytes; immunity genes; cellular stress.

ABSTRACT

Introduction: We sought to isolate the microgravity effect of spaceflight from other space stressors by characterizing the leukocytes' transcriptome of participants to a 60-d bed rest study; an Earth model of microgravity. **Methods:** Twenty healthy men received a nutritional supplement or not and 10 blood samples were collected throughout three study phases: baseline data collection (BDC) (BDC-12, BDC-11), head-down tilt (HDT) bed rest (HDT1, HDT2, HDT30, HDT60), and reambulation (R1, R2, R12, R30). We measured gene expression through RNA sequencing of leukocytes, applied generalized linear models to assess differential expression followed by enrichment analysis to identify temporal changes (model 1) and to measure the impact of a nutritional supplement (model 2). **Results:** Baseline transcriptomes included 14,624 protein-coding transcripts and showed both high intra-individual correlations (mean Kendall coefficient, 0.91 ± 0.04) and inter-individual homogeneity (0.89 ± 0.03). We identified 2,415 differentially expressed protein-coding transcripts grouping into six clusters (C1-C6). At phase transitions, clusters showed either a decrease-then-increase (C3 and C5) or an increase-then-decrease (C1, C2, C6) pattern. All six clusters converged toward average expression at HDT30 and HDT60. Gene ontology terms at baseline related to immune functions while in bed rest and reambulation related to sequestration of ions, immune response, cellular stress, and mineralization. The nutritional intervention had no effect. **Conclusions:** The temporal profiles of leukocytes' transcriptomes emphasized the dynamic nature of gene expression occurring during and after bed rest. Enriched biological processes among the differentially expressed genes included immune related and unrelated responses. The convergence toward no differential expression at days 30 and 60 of bed rest suggests a hypometabolic state. Current findings can guide future work on the complex responses and adaptation mechanisms to microgravity.

INTRODUCTION

Space is a challenging environment for the human body affecting multiple organs and systems simultaneously (1-4). Spaceflight is also associated with adverse effects, such as muscle atrophy, bone-density loss, and impaired immune response (5-8). Astronauts are prone to bacterial and viral infections shortly after returning to Earth (9, 10). Infections, mild inflammation, atopic dermatitis, and the reactivation of latent herpes viruses characterize the reduced ability of astronauts to fight pathogens (10-12). At the cellular level, in-orbit measurements conducted during a 6-month mission onboard of the International Space Station was associated with elevated circulating white blood cells counts, primarily granulocytes and lymphocytes, and impairments of immune cell functions upon returning to Earth (13). In a different study, a transient increase in neutrophils (the first responder to infection) along with reduced lymphocyte counts, specifically a decrease in T- and B-cell counts was reported postflight (14). Overall, an increase in granulocytes is consistently reported in space travel studies, whereas changes of lymphocyte subpopulations are inconsistent. Discrepancies have been attributed to spaceflight characteristics, such as mission duration and astronaut inter-individual variations characterizing the immune system (15). Elucidating the mechanisms involved in the regulation of the immune response in microgravity is of importance for space traveling.

At the molecular level, few studies have examined gene differential expression in circulating immune cells exposed to microgravity. The NASA Twins Study included a longitudinal assessment of the immune system through gene expression in white blood cells combined with measures of blood cytokine concentrations (16). Differentially expressed genes associated with immune-related pathways included the adaptive immune system, innate immune response, and NK cell-mediated immunity (16) but source of samples was limited to two individuals. The scarcity of astronauts' biological samples and technical challenges hampers our ability to monitor blood cells and study the mechanisms of altered cellular functions while in microgravity. However, bed rest studies represent an Earth-based analog to

microgravity with advantages such as direct access to participants for sample collection and technologies for analyses. Healthy volunteers are confined to 24/7 bed rest with the head at a -6° inclination over predefined durations in a highly controlled environment with continuous medical monitoring (17-20). In addition, bed rest experimental designs can incorporate the testing of specific countermeasures to mitigate the negative effects (e.g.; nutrition, exercise) (17, 18).

The multisystem nature of space-induced physiological adaptations requires a temporal design combined with genome wide molecular approaches to decipher the cellular and molecular mechanisms involved (16). Peripheral blood constitutes a source of biological material containing a reservoir of cells that circulate throughout the body and as such are in contact with multiple organs. Transcriptional changes measured in leukocytes may thus reflect multisystem changes, making them rich in information to probe and assess the status of health and disease. When combined with an integrated time-dependent analysis, gene expression captures longitudinal processes better than studying the physiological state at a particular time point. In the current study, we harvested circulating leukocytes of healthy men transitioning to bed, during 60 d of head-down tilt bed rest and transitioning to reambulation to establish their transcriptome responses. Half of the participants received a polyphenol dietary supplement. The purpose of our study was to characterize the temporal effects of bed rest by investigating the leukocyte transcriptome of healthy participants to a 60-d bed rest study and to measure the effect of a nutritional intervention. We hypothesized that the expression of protein-coding transcripts will change in response to transitioning to bed rest and reambulation after bed rest, and the nutritional intervention will not alter the transcriptome over time.

METHODS

Participants and ethics statements

Twenty male subjects were recruited according to the selection criteria listed in the Guidelines for Standardization of Bed Rest Studies in the Spaceflight Context (20). The selection process included medical and psychological examination and was conducted at the Space Clinic of the Institute of Space Medicine and Physiology (MEDES-IMPS, Rangueil Hospital) in Toulouse (France). Participants remained in the facility from the start of the baseline data collection (BDC) phase until day 14 of the reambulation (R) phase and returned for the last sample collection at R30. Selected participants had no medical history, were not taking drugs or medications, and were nonsmokers. Average age was 34 ± 8 yr and weight 73.5 ± 1.5 kg. Research ethics approval was obtained from the Comité de protection des personnes Sud-ouest et outre-mer (ID-RCB:2016-A00401-50) and was registered at ClinicalTrials.gov (A New Nutritional Countermeasure to Prevent the Deconditioning Induced by 60 Days of Antiorthostatic Bed Rest [LTBRCocktail] [NCT03594799]). The current investigation was conducted as a substudy within the "cocktail" bed rest head-down tilt (HDT) trial and reviewed by the ethics committee at the Ottawa Health Science Network REB (20160925-01H). All participants gave informed consent and were continuously monitored by a medical team.

Study design

The "cocktail" Bed Rest Study consisted of three consecutive phases: 14 d of BDC, followed by 60 d of -6° HDT bed rest, and reambulation (R) for 14 d within the facility plus 16 d outside the facility (Figure 1.1). The study tested the efficacy of a nutritional intervention to mitigate the negative effects of bed rest. The study ran two identical campaigns of 10 participants each starting 8 months apart between January 2017 and January 2018. For each campaign, five participants were randomly assigned to the "control" group and five participants were part of the "cocktail" group receiving daily pills containing 741

mg of bioactive polyphenols, 2.1 g of omega-3 and 138 mg vitamin E coupled with 80 µg selenium (XXS-2A-BR2 nutrient cocktail; Spiral Cie, Dijon, France) throughout the HDT phase (detailed nutrient cocktail composition in Culliton et al.) (21).

Blood collection and leukocyte capture

For each participant, ~4 mL of venous blood was collected in the morning after an overnight fast on the following days: BDC (-12, -11), HDT (1, 2, 30, 60), R (1, 2, 12, 30). Blood was collected in a Vacutainer with plasma separator tube (PST) gel and 83 units of lithium heparin (8362534; Becton Dickinson, Franklin Lakes, NJ). The fresh blood samples were passed through a LeukoLOCK™ filter (AM1923; ThermoFisher Scientific, Waltham, MA) to capture the leukocytes. The filters were flushed with 3 mL of phosphate-buffered saline to remove residual red blood cells and then with 3 mL of RNAlater solution (ThermoFisher Scientific) to stabilize leukocyte RNA. The two filter ports were sealed, the filters were frozen at −80°C and shipped to our laboratory for RNA isolation.

RNA isolation, library preparation, and sequencing

RNA isolation from leukocytes immobilized on the filter was performed using the LeukoLOCK™ total RNA isolation system and manufacturer's protocol (AM1923; ThermoFisher Scientific). Total RNA was suspended in 50 µL of RNAase-free water and quality assessed using the Agilent BioAnalyzer 2100. Samples with RNA Integrity Number (RIN) ≥ 8.0 were used to generate RNA sequencing libraries (23). Of the 200 samples collected, 3 had RIN ≤ 8.0 and were not further analyzed (cocktail group: B1-3, D1-4, and control group: G1-3). RNA sequencing libraries were prepared from 1 µg of total RNA using the Illumina Stranded mRNA Prep kit, and instructions from the manufacturer (AM1923; ThermoFisher Scientific). Library quality was assessed using the Agilent BioAnalyzer 2100 and 197 samples passed the quality metrics for sequencing, including a concentration above 10 nM. Libraries (125 pM) were

multiplexed and sequenced with 100 paired-end reads to a depth of ~50 million reads per sample using the Illumina NovaSeq 6000 System. Library preparation, quality assessment, high-throughput sequencing and de-multiplexing were performed at Genome Quebec Innovation Center (Montreal, Canada).

RNA-Seq data analysis

Reads were aligned to the publicly available human transcriptome and genome (GRCh38.84) using *TopHat* with default parameters (version 2.0.13) (24). Transcript abundance calculations were performed using *HTSeq* with default parameters (version 0.6.1) (25). The expression dataset corresponded to all transcripts from protein coding and non-protein coding genes measured at individual study timepoints for each participant. Read count data for the two baseline timepoints (BDC-12 and BDC-11) and for all 20 participants (total 40 baseline samples) were used to assess inter-individual participant variability. Independent filtering using the DESeq2 package in R (26) excluded genes with mean normalized read counts <2 resulting in 14,624 protein coding genes representing the baseline transcriptome. The normalized read counts from each gene were averaged across the two baseline timepoints to produce one combined baseline timepoint for each participant. The baseline transcriptomes for each participant were then pairwise correlated generating a nonparametric Kendall rank correlation matrix represented by a symmetrical heatmap to visualize the inter-individual participant transcriptome variability. All sequence analyses and result visualizations were conducted using the R environment (https://cran.r-project.org/doc/manuals/r-release/R-intro.html) and custom scripts.

Principal component analysis

The variance stabilizing transformation (log2-transformation reducing variance of low read counts) was applied to the normalized read counts using the *vst()* function built within the *DESeq2*

package in R (26). The VST normalized read counts were used to calculate each sample's principal component scores using the *prcomp()* function in R. This was done for the subset of baseline samples (40 samples) and for every sample across all study phases (197 samples). Samples were then plotted along PC1 and PC2 to visualize the variance explained by the individual participants, baseline timepoints and individual study phases.

Temporal differential expression analysis

Temporal differential expression analysis across all timepoints of the study was generated using the *DESeq2* package in R (26) and two fixed-effect generalized linear models were fitted treating time as factorial:

Model 1: read counts ~ replicate + group + time point + ε

Model 2: read counts ~ replicate + group + time point + group:time point + ε

Model 1 asks "what is the effect across time?," whereas model 2 asks "what is the effect of the nutritional intervention across time?" Repeated measures were controlled by including the "replicate" term, which accounts for the number of biological replicates in each participant. The element "group" refers to control or cocktail and the element "time point" reflects the inclusion of all 10 timepoints in the differential expression analysis. The tests are conceptually similar to an analysis of variance (ANOVA) but instead represent an analysis of deviance because *DESeq2* estimates dispersion not variance. Briefly, *DESeq2* performed gene count normalization, sample dispersion estimation, model fitting and significance testing using the likelihood ratio test generating one P value per gene (26). Adjustment for multiple statistical tests was done using the Benjamini-Hochberg correction (27). Genes with false discovery rate (FDR) adjusted P values <0.001 were considered statistically significant and identified as

gene candidates that were differentially expressed between any time point across the three phases of the study (model 1) or between nutritional and control groups over time (model 2). Of these identified protein-coding genes, normalized read counts were averaged among the 20 participants at each time point and scaled across genes as z-scores.

Gene cluster analysis

Gene candidates identified with Model 1 were further analyzed to extract clusters of genes displaying similar profiles of expression changes throughout the entire study. Briefly, the Euclidean distance between each of the model 1 gene candidates were calculated using the z scores scaled normalized read counts from each sample across time. These values were then hierarchically clustered using the *hclust()* function in R creating a tree dendrogram to visualize the gene clusters, which were resolved by a static tree cut (Supplemental Figure 1.1A). The optimal number of clusters was determined by visual inspection of the tree dendrogram and support from the "elbow method" (Supplemental Figure 1.1B) (28).

Enrichment analysis

Two enrichment analyses were performed separately; one for baseline timepoints only (BDC-12 and BDC-11) using gene set enrichment analysis (GSEA) (29), and one for all 10 timepoints across the three study phases (BDC, HDT, and R), using overrepresentation analysis (ORA) (22). Gene set enrichment analysis used the normalized read counts from the baseline transcripts' list consisting of 14,624 protein-coding genes averaged across the two baseline timepoints and biological replicates. Baseline GSEA was done through *clusterProfiler 4.0's gseGO()* function with the min and max gene set size set to 100 and 500, respectively, and enriched gene ontology (GO) terms grouped under "Biological Processes" at any level. The enrichment analysis across time for the three study phases used the list of

individual differentially expressed gene clusters over time and 14,624 protein-coding genes as the reference list to perform an ORA with custom R scripts to detect significantly overrepresented GO terms over time. Gene cluster ORA utilized *clusterProfiler 4.0's groupGO()* function to map genes from each cluster to their associated level 4 GO terms grouped under "Biological Processes." Using custom R code, a Fisher's exact test was applied to test for significantly overrepresented GO terms between gene clusters and the reference list. After adjustment for multiple comparisons using the Benjamini–Hochberg correction, P values with FDR <0.05 were considered statistically significant. The list of temporal differentially expressed genes was further analyzed to identify genes related to the ORA enriched GO term "regulation of immune system process." Expression levels of identified genes were averaged across replicates for each timepoint, and log2 fold change values relative to baseline (BDC) were calculated for each timepoint within HDT and R phases. A heatmap was then created using the *pheatmap* package in R to display the log2 fold changes for each gene across all HDT and R timepoints (https://cran.r-hub. io/web/packages/pheatmap/pheatmap.pdf).

RESULTS

Transcriptome Variability at Baseline

Transcriptomes at baseline were compared to assess participant intraindividual and interindividual variability. Baseline transcriptomes consisted of 14,624 protein-coding genes measured at both baseline timepoints, BDC-12 and BDC-11. For intraindividual variability, the average of individual Kendall correlation coefficients was 0.91 ± 0.04. Correlation plots of the two baseline samples from the same participant and Kendall correlation coefficients are displayed in Supplemental Figure 1.2A. To further assess variability of transcriptomes at baseline, a principal component analysis (PCA) was performed with the 14,624 protein-coding genes and resulted in PC1 (47.4%) and PC2 (6.5%); explaining 53.9% of total read count variance (Supplemental Figure 1.2B). The 95% confidence ellipses of the two baseline samples overlapped significantly; 15 of the 20 baseline values were included in the overlapping region of the two ellipses (Supplemental Figure 1.2B) further demonstrating the reproducibility of transcriptomes between the two baseline timepoints. The high intraparticipant correlation justified the combination of the two baseline timepoints for interindividual variability analysis using pairwise correlations of participants transcriptomes. The mean ± SD of the pairwise Kendall correlation coefficients was 0.89 ± 0.03 for the 20 participants, indicating a high participant homogeneity of transcriptomes at baseline. Results from individual pairwise comparisons of the 20 participants' transcriptomes at baseline are illustrated as a symmetrical correlation heatmap (Supplemental Figure 1.3).

Temporal Differential Expression Analysis

To measure the effect of time on transcriptomes, differential expression of protein-coding genes was measured using two generalized linear models applied to all 10 timepoints of the study. Model 1 identified 2,415 protein-coding genes differentially expressed between any timepoint of the study. In

model 2, transcriptomes of the 10 timepoints were also compared, and in addition, the model tested for the interaction between the nutritional intervention and timepoints. Model 2 identified 0 protein-coding genes differentially expressed between nutritional intervention and control groups across any timepoint. The lack of significant effect of the nutritional intervention on transcriptomes over time justified the combination of participants from control and cocktail groups in subsequent analyses.

Temporal changes of protein-coding genes

Visualization of the temporal changes of expression for the individual 2,415 differentially expressed protein-coding genes are shown in Figure 1.2A, which plots the mean transcript levels for each gene across all 10 timepoints of the study. Gene transcript levels are reported as z-scores, which centered and scaled the normalized read counts for each gene by the mean and standard deviation across the 2,415 protein-coding genes ensuring comparable scaling and visualization for all genes. A positive z-score was interpreted as above average gene expression, a negative z-score indicated below average gene expression, and zero corresponded to average levels. At 30 d (HDT30) and at 60 d (HDT60) of bed rest, the levels of most mRNA showed convergent transcription toward average levels compared with bed rest day 1 (HDT1) and day 2 (HDT2) (Figure 1.2A). Changes in gene expression during reambulation after bed rest displayed variability at all four timepoints (R1, R2, R12, R30) (Figure 1.2A). The dynamic changes in levels of protein-coding transcripts throughout the three phases of the bed rest study was reiterated in Figure 1.2B, showing violin plots of scaled normalized read counts expressed as z-scores and at each individual timepoint. The spread of average transcript levels at HDT30 and HDT60 displayed the smallest interquartile range compared with all other timepoints.

Gene cluster analysis

Hierarchical cluster analysis of the 2,415 temporal differentially expressed transcripts identified six gene clusters based on the similarity of expression changes across all three bed rest study phases (Figure 1.2A) (Supplemental Figure 1.1A). Interestingly, gene clusters showed an inverse pattern of expression changes at the onset of bed rest (HDT1 and HDT2) and reambulation phases (R 12). For clusters 1, 2, and 6, the pattern of differential expression was characterized by an increase of expression at the transition to the bed rest HDT phase and by a decrease of expression at reambulation day 12 (Figure 1.2A). We named this cluster profile a pattern of "increase-then-decrease" differential expression. Conversely, clusters 3 and 5 displayed a pattern of decreased expression at the transition to bed rest and subsequent increased expression at reambulation day 12 after bed rest, referring to a "decrease-then-increase" pattern of differential gene expression (Figure 1.2A).

Principal Component Analysis

Principal component analysis was used to visualize differences in transcriptome variability between all three phases of the study; BDC, HDT, and R. The analysis included the differentially expressed 2,415 protein-coding genes across all 10 timepoints of the study and identified principal components 1 and 2 (PC1 and PC2) corresponding to 55.0% and 8.5% respectively, explaining 63.5% of total read count variance (Supplemental Figure 1.4). This was 9.6% higher than the PCA using the baseline transcriptome consisting of 14,624 protein-coding genes, which indicates variations in expression changes are better encapsulated by the profile of 2,415 differentially expressed genes than the baseline profile of 14,624 genes. In addition, the 95% confidence ellipses show more overlap between BDC and HDT transcriptomes compared with the overlap between baseline and reambulation. This indicated a larger variability of changes in transcript levels during the reambulation phase compared with the BDC and HDT phases (Supplemental Figure 1.4).

Enrichment Analysis

For insight into the biological functions of expressed genes, two enrichment analysis of leukocyte transcriptomes were performed separately: one for baseline transcriptomes only and one for differentially expressed genes over time. For baseline transcriptomes, the normalized read counts of the 14,624 protein-coding genes at timepoints BDC-12 and BDC-11 were analyzed for the enrichment of function using GSEA. At baseline, GSEA resulted in 20 GO terms including terms mainly describing leukocyte functions (Figure 1.3A). The terms “immune effector process” and “response to bacterium” had the largest gene counts (Figure 1.3A). Additional biological processes represented in baseline transcriptomes included “circulatory system process,” “taxis” and “response to wounding” (Figure 1.3A). The second enrichment analysis was conducted on differentially expressed genes measured across all 10 timepoints grouped in the six clusters, which were then analyzed individually using ORA. Results for the enrichment analysis of the differentially expressed genes over time are displayed in Figure 1.3B. The highest gene counts were in Cluster 6 and included the terms “regulation of signaling,” “cellular response to stress,” and “cell population proliferation” among the most represented biological processes. Cluster 4 comprised immune-related biological processes including: “IL-6 production” and “regulation of cytokine production.” The most represented terms for cluster 2 related to oxidative phosphorylation. In cluster 1, the most represented biological processes had low gene counts and included terms related to “sequestration of metal ions.” Biological processes related to biomineralization characterized three of the six most represented terms in cluster 5. The most represented terms in cluster 3 included “protein localization.”

In an additional analysis of the 2,415 protein-coding genes differentially expressed over time, we performed an ORA enrichment of genes related to immune functions. A total of 155 protein-coding genes mapped to the GO term “regulation of immune system process”; 85 genes from C1, 32 genes from C3 and 38 genes from C5. Temporal changes of these genes are expressed as log2 fold changes relative

to baseline and displayed in a heatmap (Figure 1.4). The profiles of changes of expression for most immune-related genes had characteristics similar to patterns displayed by the six gene clusters identified from the 2,415 differentially expressed genes. Similarities included changes in the patterns of expression at study phase transitions characterized by either a “decrease-then-increase” pattern or an “increase-then decrease” pattern. The near zero differential expression at days 30 and 60 of the bed rest HDT phase relative to baseline was also a characteristic of immune-related genes (Figure 1.4).

DISCUSSION

We conducted serial RNA sequencing on circulating leukocytes from 20 healthy male participants transitioning to and from 60 d of bed rest to identify key protein-coding genes and enriched biological terms characteristic of bed rest and to measure the impact of a nutritional intervention. Our primary findings were: 1) Participants' transcriptomes at baseline were homogeneous; 2) differentially expressed genes over time grouped into six clusters displaying either decrease-then increase or increase-then-decrease patterns of differential expression at phase transitions: baseline to bed rest and bed rest to reambulation; 3) immune-related processes were most represented in leukocyte transcriptomes at baseline while biological processes enriched among the differentially expressed genes at any timepoint included; sequestration of ions, immune response, cellular stress, and mineralization; 4) transcripts levels converged toward average levels after 30 and 60 d in bed; 5) the nutritional intervention did not affect the expression profile of protein-coding genes throughout the bed rest study.

Baseline transcriptomes and interindividual variability

The high intraindividual correlations comparing transcriptomes from samples collected at two consecutive days of the baseline phase (Supplemental Figure 1.2) testified to robust and reproducible methods. In addition, the high inter-individual correlations comparing transcriptomes of the 20 participants at baseline (Supplemental Figure 1.3) is indicative of leukocyte transcriptome homogeneity in our cohort, which is consistent with the stringent recruitment standards for this study limited to healthy men within a narrow age range (20). But the transcriptome's homogeneity at baseline is inconsistent with immune variability characterizing healthy adult populations. A meta-analysis of 1,575 healthy adults across multiple cohorts documented differences in leukocyte subpopulations, cytokine profile, and functional response indicating immune heterogeneity characterizing healthy adults (30). However, immune variability was attributed to nonheritable influences such as exposure to pathogens

rather than heritable factors as described in monozygotic twins (31). Interestingly, a report on the same 20 participants from our study showed no significant frequency changes in leukocytes, total lymphocytes, B-cell concentrations during bed rest (32). This points to the controlled experimental environment of bed rest studies contributing to immune transcriptome homogeneity. Future experiments are necessary to validate leukocytes' transcriptome homogeneity in larger populations of healthy adults. Our experimental approach yielding both high intra-participant reproducibility and high inter-participant homogeneity support the validity of the leukocyte gene expression to characterize the effects of bed rest and of reambulation after bed rest.

Transcriptomes during bed rest and reambulation

The temporal profiles of leukocytes' transcriptomes emphasized the dynamic nature of gene expression occurring during and after bed rest. Differentially expressed genes over time clustered into 6 profiles and underwent major changes of expression timed with phase transitions: baseline to bed rest and bed rest to reambulation. Remarkably, the gene clusters C3 and C5 displaying decreased expression when going to bed rest, showed increased expression at reambulation day 1 (C5) and day 2 (C3 and C5). In contrast, the gene clusters C1, C2, and C6 increased expression when going to bed, then decreased expression at reambulation day 12. The timing and patterns of clusters at phase transitions coincided with skeletal unloading and inactive antigravity muscles during bed rest, while loading and activation of gravity muscles occurring at reambulation. Transcriptome changes suggest that specific biological systems and processes are responsive to verticalization and weight bearing while other are more active during rest in the horizontal position. Blood circulation, muscle action and bone stimulation constitute examples of activity-, position- and gravity-dependent systems (33-35). More specific to circulating leukocytes, the minus 6-° antiorthostatic bed rest position induced a fluid shift (2). Blood shifting cephalad from the lower limbs triggers a 10% to 15% plasma volume reduction resulting in

hemoconcentration (2). Leukocytes cellular stress pathways related to hemoconcentration may activate intrinsic mechanisms to preserve function and adjust cell population (21) as will be discussed in the functional enrichment analysis below. The display of transcriptome decrease-then-increase changes in and out of bed rest would suggest that genes clusters are related to processes necessary during activity, verticalization or gravity. Conversely, genes from the increase-then-decrease clusters would be related to processes active during the horizontal unloaded state of bed rest.

The next transcriptome findings pertain to the phase after 60 d of bed rest when our cohort initiated reambulation and gradually returned to their habitual level of physical activity. The reambulation phase corresponded to the return from microgravity and integration of physiological responses from multiple systems. Using a principal component analysis to compare transcriptomes during the three phases, the current study found more variability at reambulation compared with baseline and bed rest phases (Supplemental Figure 1.4). This finding suggests that despite participant transcriptomic homogeneity at baseline, transcriptomes are variable at reambulation.

Bed rest and reambulation caused marked changes in leukocyte biological processes

During bed rest, the enrichment analysis pointed to gene differential expression unrelated to leukocyte function as detected at baseline. An enrichment analysis of the 14,624 genes expressed at baseline identified biological functions related to immunity, response to bacterium, circulatory system processes, taxis and wounding; all typical and expected of leukocytes. However, the 2,415 differentially expressed genes in response to bed rest and reambulation indicated a significant adjustment in transcriptomes. GO terms “signaling,” “response to stress,” “regulation of cell population,” “oxidative phosphorylation,” “mineralization” and “cytokine production” dominated the leukocyte functions modulated by bed rest and reambulation after bed rest. The altered transcriptome may indicate a shift in

circulating leukocyte activity to address cellular stresses and adaptation to hemoconcentration and then hemodilution, bone unloading then reloading typical of the bed rest model (21, 35).

In agreement with previously reported physiological changes of bed rest protocols, the current study identified bone morphogenesis and muscle cell development as significant biological events associated with HDT bed rest and reambulation (35-37). Genes from clusters 3 and 5 (decrease-then-increase pattern) were associated with GO term descriptions such as dendrite development, synaptic plasticity, regulation of growth, biomineralization, tooth mineralization, and biomineral tissue development. Central nervous and bone systems are typically stimulated by limb movement and coordination during activity, verticalization, and weightbearing (38, 39). Bed confinement abolishing these actions is compatible with their strong down regulation of the transcriptomic response to bed rest. Similarly, at reambulation, return to the vertical position and weightbearing may explain the switching to increase expression of genes in clusters 3 and 5. These results connect with literature on bone demineralization with bed rest and bone mass and mineralization accrual with weightbearing and return to activity (39, 40). On the contrary, gene clusters 1, 2, and 6 with increased expression at bed rest and reduced expression at reambulation included regulation of cell population and sequestering of metal ions, among others. Blood cell population regulation is required with the fluid shifts inducing hemoconcentration then hemodilution as previously measured with the bed rest model (17, 21). In addition, skeletal unloading and bone demineralization during bed rest increases calcium and phosphate ions availability into circulation (34, 37, 41). In these 20 participants, increased availability of ferrous ions from increased hemolysis was previously reported during the bed rest phase (21). The significant enrichment of the GO term “sequestering of metal ion” among cluster 1 genes correlates with a leukocytes’ response to free heme release secondary to red blood cell hemolysis previously reported in the same participants (21).

Differential expression of "regulation of immune system process" genes

The transcriptomic response indicated that the immune system of healthy participants was impacted by bed rest and reambulation. The representation of the GO term "regulation of immune system process" corresponded to 6.4% (155/2415) of all the differentially expressed genes over time. Of interest, three genes of the tumor necrosis factor (TNF) family; TNFSF13B, TNFAIP8L2, and TNFSF14 all increased at reambulation. TNFSF14 is known as a herpesvirus entry mediator acting as a costimulatory factor for the activation of lymphoid cells and as a deterrent to infection by herpesvirus (9). Upregulation of TNFSF14 at reambulation day 1 might contribute to the protection against herpesvirus reactivation observed in astronauts upon returning on Earth (11). Latent herpes virus reactivation was not reported after 90 d of bed rest (10, 11). The bed rest model was designed and is used as an Earth-based microgravity analog because it mimics many of the physiological changes taking place in microgravity (17, 20). A second group of immune system genes identified in the current study corresponds to members of the complement system. Complement 1q (C1q) can activate the classical pathway of the complement system allowing protection against infections by targeting antigen-bound immunoglobulins, C-reactive protein and apoptotic cells (42). The profiles of expression of genes C1QA, C1QB, C1QC, and C2 suggest a repression of the complement system during bed rest and potentially explaining the vulnerability to infection induced by bed rest in healthy adults.

No differential expression after prolonged bed rest

A striking characteristic of transcriptome changes was the convergence toward average expression at days 30 and 60 of bed rest. This convergence was a path common to all 20 participants. To our knowledge, such a phenomenon reported here for the first time and the biological meaning of this discovery is unclear. The reduced level of physical activity, inherent to bed rest, and reduced energy expenditure during the bed rest phase represent potential causal factors for transcriptome convergence

toward no change. The general lack of expression changes after prolonged bed rest represents an adaptation and is indicative of global mechanisms yet to be identified limiting variations of mRNA levels in leukocytes. The transcriptomic convergence may indicate a generalized hypometabolic state and a reduced energy expenditure compatible with the main clinical use of bed rest (43). Reversal of the convergence during reambulation demonstrated a high degree of transcriptome flexibility with participants adapting their transcriptomes to periods of bed rest and physical activity.

Nutritional intervention does not affect bed rest induced transcriptome changes

The current study tested the efficiency of a nutritional supplement in polyphenol, omega-3, vitamin E, and selenium at mitigating the negative impact of bed rest in healthy male participants. Our results are consistent with independent reports documenting a lack of effect of the nutritional supplement on: cardiac circadian rhythms (44), muscle deconditioning (45), oxidative damage, mitochondrial content and protein balance (45), lumbar vertebral fat fraction (46), hemolysis (21), bone formation and resorption (41), neurobehavior (47), and B-cell homeostasis (32) on the same participants. Austermann et al. (41) attributed the lack of effect of the nutritional intervention to the well-controlled diet of bed rest participants containing sufficient amounts of micronutrients and therefore the supplement might not have provided additional benefits on any outcome measured.

Limitations

We obtained and analyzed 10 blood samples at key moments over the 104 experimental days of the bed rest study. Important changes happening in-between blood draws would have been missed; preventing us from, for example, establishing the start time of convergence of transcriptome toward no differential expression in late bed rest. We report changes of transcript levels, which represent steady state levels, limiting our ability to comment on dynamic transcriptional and posttranscriptional changes

including RNA degradation, and translation. The number of individuals was limited to 20 participants. The stringent anthropomorphic and demographic recruitment criteria prevent extrapolation to a wider, heterogeneous or ill population. Importantly, the male-only cohort used in this study prevents the extrapolation of results to women and preclude any sex-based comparisons. Finally, our gene expression analysis was performed on circulating leukocytes; it is therefore not possible to allocate the individual contribution of cell subpopulations; e.g., lymphocytes, neutrophils, monocytes, etc., to the expression profiles.

CONCLUSIONS

Temporal leukocyte transcriptome variations reflect the significant biologic perturbations caused by microgravity. Leukocyte biological processes changing from immune function to stress reactions may explain the vulnerability of astronauts to infections. Our study demonstrates that genetic tools accurately mapped key elements of bed rest protocols with potential applications for space travelers. Particularly at phase transition; entering bed rest and later reambulation constituted major stressors to circulating leukocytes identified from differentially expressed genes represented by six cluster profiles and a shift in biological functions. In addition, gene clusters presented transcriptomic convergence after 30 and 60 d of bed rest potentially reflecting common path to generalized hypometabolism related to preserving energy. Gene clusters also presented transcriptomic decrease-then-increase and increase-then-decrease patterns at transitions to bed and to ambulation after bed rest possibly distinguishing metabolic pathways responsive to rest and unloading and to opposite activities, verticalization and weight bearing. Current findings can guide future work on the nature of the complex response to microgravity and integrated responses from multiple systems toward homeostasis.

Acknowledgements

The authors would like to acknowledge financial support from the Canadian Space Agency (grants 15EXPBEDST and 19FAOTTB24 to O. L. and G. T.). The bed rest study was funded by the European Space Agency, the Centre National d'Etudes Spatiales and the Canadian Space Agency (CSA). The authors would like to thank the volunteers for their participation, the staff at the Medes Institute for Space Medicine and Physiology especially Marie-Pierre Bareille, Arnaud Beck, Marie-Claude Costes-Salon, Patrick Person, and Corinne Lombard for support during the study, Theresa Backlund, Téa Backlund, for their assistance with sample collection.

Author Contributions

G. T. and O. L. participated in the concept and design. All authors participated in the acquisition, analysis, or interpretation of data. D. S., G. T., O. L. participated in the drafting of the article. All authors participated in the critical revision of the article for important intellectual content. D. S. and O. L. participated in the statistical analysis. G. T. and O. L. participated in the funding acquisition. The European Space Agency established the study design, dates, sample size, and duration of the bed rest study.

Conflicts of Interest

The authors declare no competing interests. The results of the study are presented clearly, honestly, and without fabrication, falsification, or inappropriate data manipulation. The results of the present study do not constitute endorsement by the American College of Sports Medicine.

References

1. Scott JM, Stoudemire J, Dolan L, Downs M. Leveraging spaceflight to advance cardiovascular research on earth. *Circ Res*. 2022;130(6): 942–57.
2. Norsk P, Asmar A, Damgaard M, Christensen NJ. Fluid shifts, vasodilatation and ambulatory blood pressure reduction during long duration spaceflight. *J Physiol*. 2015;593(3):573–84.
3. Demontis GC, Germani MM, Caiani EG, Barravecchia I, Passino C, Angeloni D. Human pathophysiological adaptations to the space environment. *Front Physiol*. 2017;8:547.
4. Pavez Loriè E, Baatout S, Choukér A, et al. The future of personalized medicine in space: from observations to countermeasures. *Front Bioeng Biotechnol*. 2021;9:739747.
5. Lee PHU, Chung M, Ren Z, Mair DB, Kim DH. Factors mediating spaceflight-induced skeletal muscle atrophy. *Am J Phys Cell Phys*. 2022;322(3):C567–80.

6. Frippiat JP, Crucian BE, de Quervain DJF, et al. Towards human exploration of space: the THESEUS review series on immunology research priorities. *NPJ Microgravity*. 2016;2:16040.
7. Sonnenfeld G, Shearer WT. Immune function during space flight. *Nutrition*. 2002;18(10):899–903.
8. Patel S. The effects of microgravity and space radiation on cardiovascular health: from low-earth orbit and beyond. *Int J Cardiol Heart Vasc*. 2020;30:100595.
9. Wang S, Ljubimov A, Jin L, Pfeffer K, Kronenberg M, Ghiasi H. Herpes simplex virus 1 latency and the kinetics of reactivation are regulated by a complex network of interactions between the herpesvirus entry mediator, its ligands (gD, BTLA, LIGHT, and CD160), and the latency-associated transcript. *J Virol*. 2018;92(24): e01451–18.
10. Mehta SK, Laudenslager ML, Stowe RP, et al. Latent virus reactivation in astronauts on the international space station. *NPJ Microgravity*. 2017;3:11.
11. Rooney BV, Crucian BE, Pierson DL, Laudenslager ML, Mehta SK. Herpes virus reactivation in astronauts during spaceflight and its application on earth. *Front Microbiol*. 2019;10:16.
12. Crucian B, Simpson RJ, Mehta S, et al. Terrestrial stress analogs for spaceflight associated immune system dysregulation. *Brain Behav Immun*. 2014;39:23–32.
13. Crucian BE, Choukèr A, Simpson RJ, et al. Immune system dysregulation during spaceflight: potential countermeasures for deep space exploration missions. *Front Immunol*. 2018;9:1437.
14. Paul AM, Mhatre SD, Cekanaviciute E, et al. Neutrophil-to-lymphocyte ratio: a biomarker to monitor the immune status of astronauts. *Front Immunol*. 2020;11:564950.
15. Elgindi M, Sapudom J, Ibrahim IH, et al. May the force be with you (or not): the immune system under microgravity. *Cell*. 2021;10(8):1941.
16. Garrett-Bakelman FE, Darshi M, Green SJ, et al. The NASA Twins Study: a multidimensional analysis of a year-long human spaceflight. *Science*. 2019;364(6436):eaau8650.

17. Pandiarajan M, Hargens AR. Ground-based analogs for human spaceflight. *Front Physiol*. 2020;11:716.
18. Ploutz-Snyder LL, Downs M, Goetchius E, et al. Exercise training mitigates multisystem deconditioning during bed rest. *Med Sci Sports Exerc*. 2018;50(9):1920–8.
19. Böcker J, Schmitz MT, Mittag U, Jordan J, Rittweger J. Betweensubject and within-subject variation of muscle atrophy and bone loss in response to experimental bed rest. *Front Physiol*. 2022;12:743876.
20. Sundblad P, Orlov O, Angerer O, Larina I, Cromwell R. Standardization of bed rest studies in the spaceflight context. *J Appl Physiol* (1985). 2016;121(1):348–9.
21. Culliton K, Louati H, Laneuville O, Ramsay T, Trudel G. Six degrees head-down tilt bed rest caused low-grade hemolysis: a prospective randomized clinical trial. *NPJ Microgravity*. 2021;7(1):4.
22. Boyle J. Gene-expression omnibus integration and clustering tools in SeqExpress. *Bioinformatics*. 2005;21(10):2550–1.
23. Schroeder A, Mueller O, Stocker S, et al. The RIN: an RNA integrity number for assigning integrity values to RNA measurements. *BMC Mol Biol*. 2006;7:3.
24. Kim D, Pertea G, Trapnell C, Pimentel H, Kelley R, Salzberg SL. TopHat2: accurate alignment of transcriptomes in the presence of insertions, deletions and gene fusions. *Genome Biol*. 2013;14(4):R36.
25. Anders S, Pyl PT, Huber W. HTSeq—a Python framework to work with high-throughput sequencing data. *Bioinformatics*. 2015;31(2):166–9.
26. Love MI, Huber W, Anders S. Moderated estimation of fold change and dispersion for RNA-seq data with DESeq2. *Genome Biol*. 2014; 15(12):550.
27. Benjamini Y, Hochberg Y. Controlling the false discovery rate: a practical and powerful approach to multiple testing. *J R Stat Soc B Stat Methodol*. 1995;57(1):289–300.

28. Thorndike RL. Who belongs in the family? *Psychometrika*. 1953; 18(4):267–76.
29. Subramanian A, Tamayo P, Mootha VK, et al. Gene set enrichment analysis: a knowledge-based approach for interpreting genome-wide expression profiles. *Proc Natl Acad Sci U S A*. 2005;102(430): 15545–50.
30. Kaczorowski KJ, Shekhar K, Nkulikiyimfura D, et al. Continuous immunotypes describe human immune variation and predict diverse responses. *Proc Natl Acad Sci U S A*. 2017;114(30):E6097–106.
31. Carr EJ, Dooley J, Garcia-Perez JE, et al. The cellular composition of the human immune system is shaped by age and cohabitation. *Nat Immunol*. 2016;17(4):461–8.
32. Bonnefoy J, Baselet B, Moser D, et al. B-cell homeostasis is maintained during two months of head-down tilt bed rest with or without antioxidant supplementation. *Front Immunol*. 2022;13:830662.
33. Hargens AR, Vico L. Long-duration bed rest as an analog to microgravity. *J Appl Physiol* (1985). 2016;120(8):891–903.
34. Konda NN, Karri RS, Winnard A, et al. A comparison of exercise interventions from bed rest studies for the prevention of musculoskeletal loss. *NPJ Microgravity*. 2019;5(1):12.
35. Pavy-Le Traon A, Heer M, Narici MV, Rittweger J, Vernikos J. From space to earth: advances in human physiology from 20 years of bed rest studies (1986–2006). *Eur J Appl Physiol*. 2007;101(2):143–94.
36. Trudel G, Uhthoff HK, Laneuville O. Hemolysis during and after 21 days of head-down-tilt bed rest. *Phys Rep*. 2017;5(24):e13469.
37. Krause AR, Speacht TA, Steiner JL, Lang CH, Donahue HJ. Mechanical loading recovers bone but not muscle lost during unloading. *NPJ Microgravity*. 2020;6(1):36.

38. Rittweger J, Felsenberg D. Recovery of muscle atrophy and bone loss from 90 days bed rest: results from a one-year follow-up. *Bone*. 2009; 44(2):214–24.
39. Kakuris KK, Yaroshenko YN, Charapakhin KP, Neofitov NH. Chronic head-down-tilt sleeping as physiological regulator of bone remodelling during diminished muscular activity in humans. *Clin Physiol Funct Imaging*. 2017;37(4):428–36.
40. Laneuville O, Rocheleau L, Chan Chun Kong D, Pelchat M, Trudel G. Effect of rehabilitation on biologic and transcriptomic responses after hospital-acquired deconditioning: a prospective longitudinal feasibility study. *Disabil Rehabil*. 2021;44(14):3623–31.
41. Austermann K, Baecker N, Zwart SR, et al. Antioxidant supplementation does not affect bone turnover markers during 60 days of 6° head-down tilt bed rest: results from an exploratory randomized controlled trial. *J Nutr*. 2021;151(6):1527–38.
42. van de Bovenkamp FS, Dijkstra DJ, van Kooten C, Gelderman KA, Trouw LA. Circulating C1q levels in health and disease, more than just a biomarker. *Mol Immunol*. 2021;140:206–16.
43. Zuccarelli L, Baldassarre G, Magnesa B, et al. Peripheral impairments of oxidative metabolism after a 10-day bed rest are upstream of mitochondrial respiration. *J Physiol*. 2021;599(21): 4813–29.
44. Solbiati S, Landreani F, Turcato M, et al. Analysis of changes in cardiac circadian rhythms of RR and QT induced by a 60-day headdown bed rest with and without nutritional countermeasure. *Eur J Appl Physiol*. 2020;120(7):1699–710.
45. Arc-Chagnaud C, Py G, Fovet T, et al. Evaluation of an antioxidant and anti-inflammatory cocktail against human hypoactivity-induced skeletal muscle deconditioning. *Front Physiol*. 2020;11:71.
46. Liu T, Melkus G, Ramsay T, Sheikh A, Laneuville O, Trudel G. Bone marrow reconversion with reambulation: a prospective clinical trial. *Investig Radiol*. 2021;56(4):215–23.

47. Brauns K, Friedl-Werner A, Gunga HC, Stahn AC. Effects of two months of bed rest and antioxidant supplementation on attentional processing. *Cortex*. 2021;141:81–93.

Figures

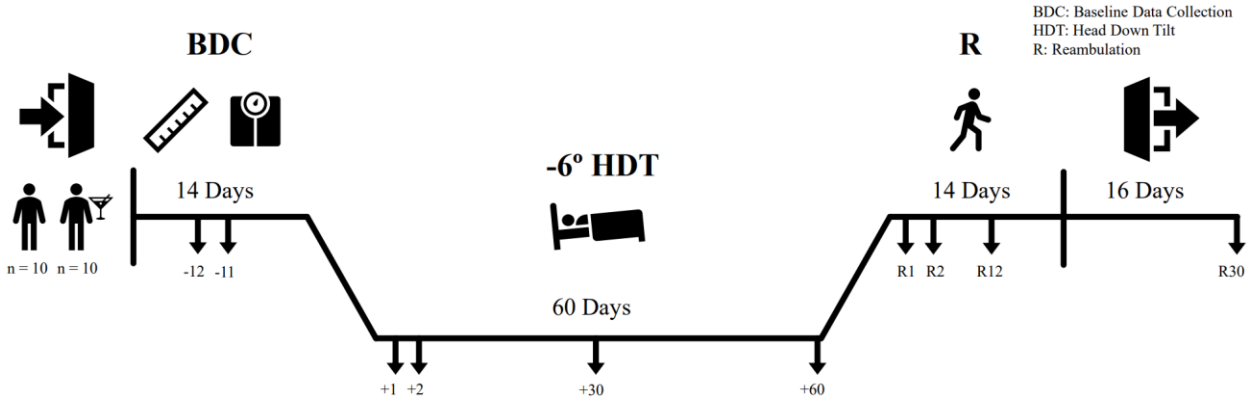

Figure 1.1 | Experimental design. Twenty healthy male participants were randomly assigned to either the “control” (n = 10) or “cocktail” (n = 10) and underwent a three-phase bed rest study; 14 d in baseline (BDC), 60 d in −6° HDT bed rest, and 30 d of reambulation (R). The “cocktail” group received a daily oral dosage of an antioxidant/anti-inflammatory cocktail at mealtime throughout the HDT bed rest phase as a nutritional intervention. For each participant, venous blood was collected in the morning after an overnight fast at 10 different timepoints (indicated by arrows); two baseline samples 12 and 11 d before HDT bed rest (BDC-12, −11), four samples during the HDT phase (HDT1, 2, 30, 60), and four samples after HDT phase (R1, 2, 12, 30).

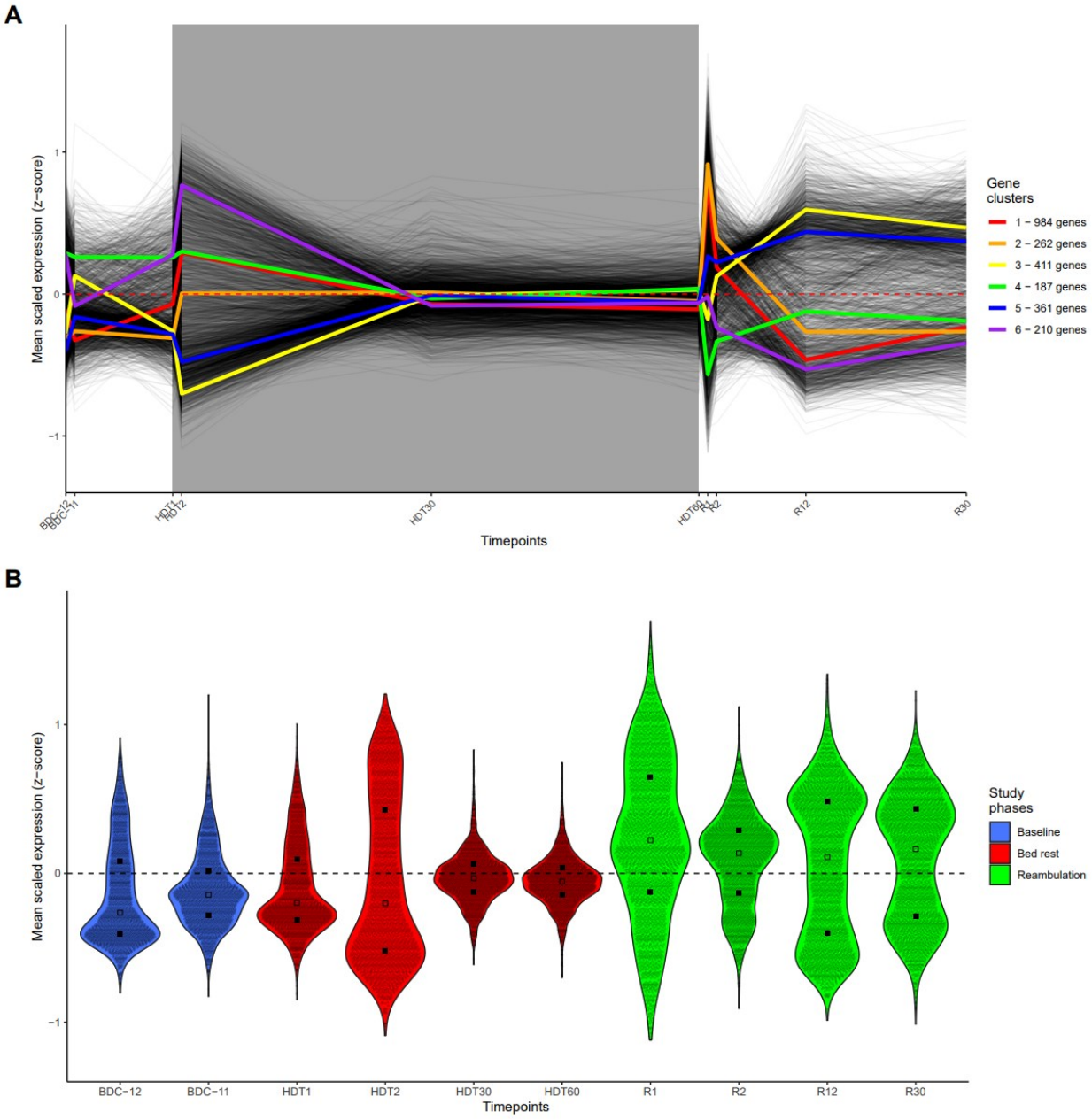

Figure 1.2 | Temporal profiles of differential gene expression during the three phases of the bed rest study. Gene expression values represent the mean scaled normalized read counts for the 2415 protein-coding transcripts differentially expressed between any timepoint. A, Transcript levels represent the average of normalized read counts for the 20 participants at individual timepoints and expressed as z scores. Black lines follow individual transcripts and colored lines represent the profiles of the six gene clusters identified through hierarchical clustering. The number of protein-coding genes identified in each

cluster is indicated. The shaded area represents the HDT phase. B, Levels of the differentially expressed 2415 protein-coding transcripts measured at individual timepoints displayed as violin plots of z scores: medians indicated by open squares and upper and lower quartiles indicated by black squares. Colors denote the study phase. BDC (blue), HDT (red), and R (green).

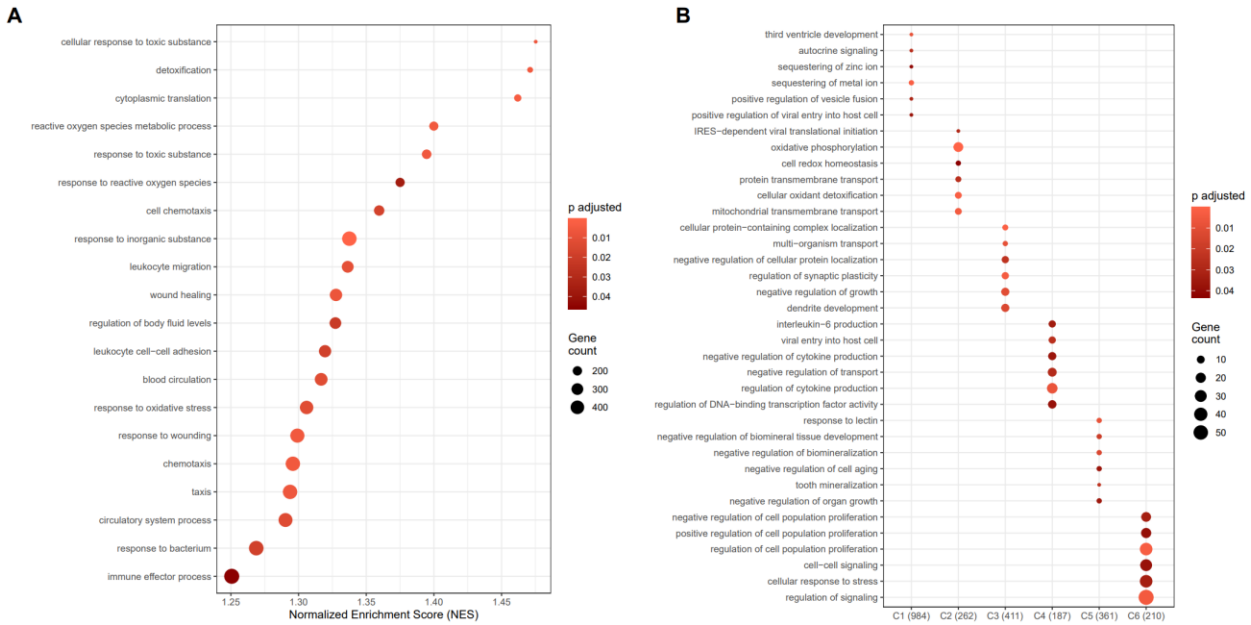

Figure 1.3 | Functional enrichment analysis. Dot plots displaying the GO terms obtained from the GSEA of baseline timepoints only (BDC-12 and BDC-11) (A) and ORA of gene clusters across all study phases (B). For both plots, the size of each dot is proportional to the number of genes mapping to that specific GO term. The color of each dot is based on the FDR adjusted P values, where brighter points have lower values (color scale). Panel A displays the enrichment results for the baseline transcriptomes only and all 20 statistically significant GO terms obtained from GSEA. NES are based on the weighted KS statistic. Panel B displays the top six most enriched GO terms for each cluster of differentially expressed genes at any timepoint of the study and obtained from ORA. Enrichment corresponds to the ratio of mapped gene counts to a given GO term between each gene cluster (C1-C6) and the reference list. Enriched GO terms were grouped under “Biological Processes” at level 4. Using the Benjamini-Hochberg correction for multiple comparisons, P values with FDR < 0.05 were considered statistically significant. NES, normalized enrichment score; KS, Kolmogorov-Smirnov.

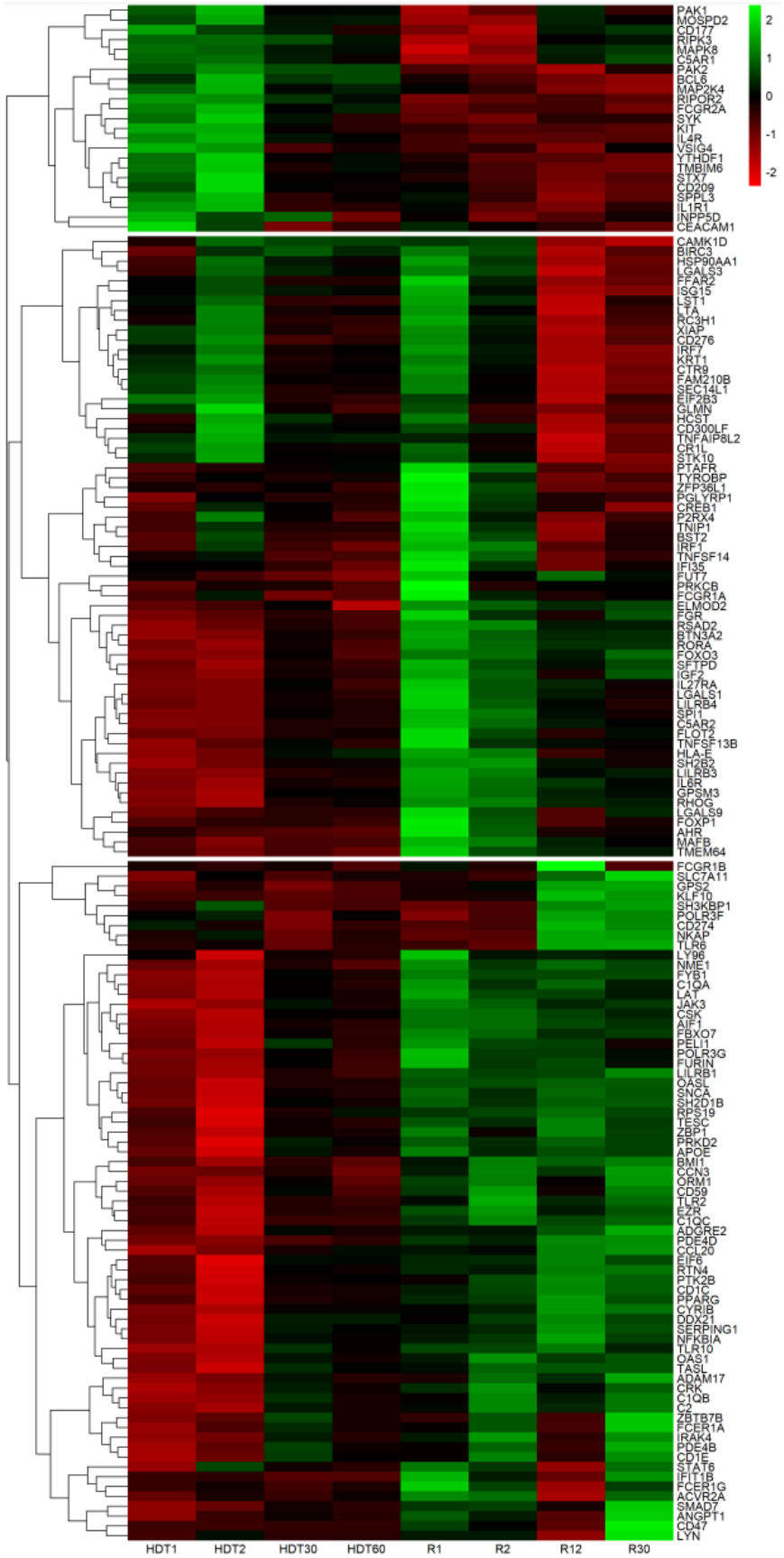
PAK1
MOSPD2
CD177
RIPK3
MAPK8
C5AR1
PAK2
BCL6
MAP2K4
RIPOR2
FCGR2A
SYK
KIT
IL4R
VSIG4
YTHDF1
TMBIM6
STX7
CD209
SPPL3
IL1R1
INPP5D
CEACAM1
CAMK1D
BIRC3
HSP90AA1
LGALS3
FFAR2
ISG15
LST1
LTA
RC3H1
XIAP
CD276
IRF7
KRT1
CTR9
FAM210B
SEC14L1
EIF2B3
GLMN
HCST
CD300LF
TNFAIP8L2
CR1L
STK10
PTAFR
TYROBP
ZFP36L1
PGLYRP1
CREB1
P2RX4
TNIP1
BST2
IRF1
TNFSF14
IFI35
FUT7
PRKCB
FCGR1A
ELMOD2
FGR
RSAD2
BTN3A2
RORA
FOXO3
SFTPD
IGF2
IL27RA
LGALS1
LILRB4
SPI1
C5AR2
FLOT2
TNFSF13B
HLA-E
SH2B2
LILRB3
IL6R
GPSM3
RHOG
LGALS9
FOXP1
AHR
MAFB
TMEM64
FCGR1B
SLC7A11
GPS2
KLF10
SH3KBP1
POLR3F
CD274
NKAP
TLR6
LY96
NME1
FYB1
C1QA
LAT
JAK3
CSK
AIF1
FBXO7
PELI1
POLR3G
FURIN
LILRB1
OASL
SNCA
SH2D1B
RPS19
TESC
ZBP1
PRKD2
APOE
BMI1
CCN3
ORM1
CD59
TLR2
EZR
C1QC
ADGRE2
PDE4D
CCL20
EIF6
RTN4
PTK2B
CD1C
PPARG
CYRIB
DDX21
SERPING1
NFKBIA
TLR10
OAS1
TASL
ADAM17
CRK
C1QB
C2
ZBTB7B
FCER1A
IRAK4
PDE4B
CD1E
STAT6
IFIT1B
FCER1G
ACVR2A
SMAD7
ANGPT1
CD47
LYN
2
1
0
-1
-2
HDT1
HDT2
HDT30
HDT60
R1
R2
R12
R30

Figure 1.4 | Differential expression of immune processing genes at bed rest HDT and reambulation (R). Heat map illustration of the log2-fold changes of expression at HDT bed rest and R relative to baseline levels for differentially expressed genes involved in the regulation of immune processes. Among the 2415 differentially expressed genes at any timepoint of the study, 155 were represented in “regulation of immune system process” GO term. Expression levels of individual genes at HDT and reambulation relative to BDC values and expressed as log2-fold changes displayed as a heatmap. The color bar represents values of log2-fold changes ranging from −2 (red) to +2 (green).

Supplemental Digital Content

- Supplemental Figure 1.1
- Supplemental Figure 1.2
- Supplemental Figure 1.3
- Supplemental Figure 1.4

Chapter 2

The transcriptome response of astronaut leukocytes to long missions aboard the International Space Station reveals immune modulation

Fronters in Immunology

Daniel Stratis[1]; Guy Trudel[2,3,4]; Lynda Rocheleau[4]; Martin Pelchat[4]; Odette Laneuville[1,2]

[1] Department of Biology, Faculty of Science, University of Ottawa, Ottawa, Ontario, Canada

[2] Bone and Joint Research Laboratory, Ottawa Hospital Research Institute, Ottawa, Ontario, Canada

[3] Department of Medicine, Division of Physiatry, Faculty of Medicine, University of Ottawa, Ottawa, Ontario, Canada

[4] Department of Biochemistry, Microbiology and Immunology, Faculty of Medicine, University of Ottawa, Ottawa, Ontario, Canada

Stratis, Daniel; Trudel, Guy; Rocheleau, Lynda; Pelchat, Martin; Laneuville, Odette. The transcriptome response of astronaut leukocytes to long missions aboard the International Space Station reveals immune modulation. *Frontiers in Immunology*. 2023; 14:1771103. DOI: 10.3389/fimmu.2023.1171103

Keywords: Astronauts; spaceflight adaptation; leukocytes; immune gene expression; fluid shift; herpesvirus; transcriptome (RNA-seq)

ABSTRACT

Introduction: Spaceflight leads to the deconditioning of multiple body systems including the immune system. We sought to characterize the molecular response involved by capturing changes in leukocyte transcriptomes from astronauts transitioning to and from long-duration spaceflight. **Methods:** Fourteen male and female astronauts with ~6-month long missions aboard the International Space Station (ISS) had 10 blood samples collected throughout the three phases of the study: one pre-flight (PF), four in-flight (IF) while onboard the ISS, and five upon return to Earth (R). We measured gene expression through RNA sequencing of leukocytes and applied generalized linear modeling to assess differential expression across all 10 time points followed by the analysis of selected time points and functional enrichment of changing genes to identify shifts in biological processes. **Results:** Our temporal analysis identified 276 differentially expressed transcripts grouped into two clusters (C) showing opposite profiles of expression with transitions to and from spaceflight: (C1) decrease-then-increase and (C2) increase-then-decrease. Both clusters converged toward average expression between ~2 and ~6 months in space. Further analysis of spaceflight transitions identified the decrease-then-increase pattern with most changes: 112 downregulated genes between PF and early spaceflight and 135 upregulated genes between late IF and R. Interestingly, 100 genes were both downregulated when reaching space and upregulated when landing on Earth. Functional enrichment at the transition to space related to immune suppression increased cell housekeeping functions and reduced cell proliferation. In contrast, egress to Earth is related to immune reactivation. **Conclusion:** The leukocytes' transcriptome changes describe rapid adaptations in response to entering space followed by opposite changes upon returning to Earth. These results shed light on immune modulation in space and highlight the major adaptive changes in cellular activity engaged to adapt to extreme environments.

INTRODUCTION

The journey to space and sojourn in this extreme environment expose astronauts to health hazards such as cosmic radiations and microgravity (1). Short- and long-term spaceflight negatively affects most physiological functions: musculoskeletal, cardiovascular, respiratory, metabolic, endocrine, cognitive, gastrointestinal, microbial, genito-urinary, dermatological, ocular, and immune (1-3). A rapid physiological change occurring immediately upon entering space is the prompt redistribution of blood from the lower to upper part of the body (4). In response, plasma shifts toward extravascular tissues including the lymphatic system, resulting in diuresis and reduction in blood volume by ~10%-15% within the first days in microgravity (5). An opposite response occurs upon return to Earth; blood redistributes to the lower limbs, requiring an increase of total blood volume achieved by increasing fluid intake (6). These fluid shifts represent opposite physiological adaptations when transitioning to and from microgravity environments.

At the cellular level, plasma volume redistribution during spaceflight alters blood cell concentration –triggering mechanisms to restore homeostasis. An analysis of astronaut blood samples collected onboard the International Space Station (ISS) reported a ~17% elevation in white blood cell counts persisting during long-term spaceflight and accompanied by impairments of immune cell functions upon returning to Earth (7, 8). Early studies have also reported that, within 1 week in microgravity, red blood cell mass decreases ~10% (9). In a recent study, a temporal analysis including before, during, and after mission measurements of hemoglobin from 14 astronauts sojourning onboard of the ISS for ~6 months documented ongoing hemolysis in space (10). At the molecular level, studies have focused on the transcriptomic changes of astronauts during spaceflight. The National Aeronautics and Space Administration (NASA) Twin Study monitored simultaneously one twin experiencing spaceflight for ~1 year and compared data to his twin brother in the terrestrial environment. Transcriptional changes were found in multiple immune cell types including Peripheral Blood

Mononuclear Cells (PBMCs), CD4 and CD8 T lymphocytes, and CD19 B lymphocytes. Gene expression in lymphocytes remained disrupted even after spaceflight (11). Those studies offered valuable insight into the molecular interactions occurring during spaceflight but suffer from small astronaut sample sizes and lack an integrated time-dependent analysis.

Genome-wide expression analysis provides a rich source of information to characterize molecular processes that underlie physiological adaptions associated with spaceflight (11). Peripheral blood cells are an ideal candidate to probe systemic effects due to their contact with multiple organ systems through blood circulation. Transcriptional changes in circulating blood cells may thus reflect multisystem changes rich in information to assess astronaut health in response to the space environment and guide the design of personalized interventions. In the current study, we took advantage of the rare opportunity to sample a cohort of 14 astronauts onboard the ISS for ~6-month missions. We harvested the circulating leukocytes of ISS crewmembers before, during, and after spaceflight to establish the transcriptional composition and dynamic changes. This hypothesis-generating study combined an integrated time-course analysis followed by a time-point analysis at phase transitions to ISS missions. This approach captured the longitudinal changes in transcript levels and characterized the effect of transitioning to and from space, the adaptation in space, and state up to 1-year post-flight. We predict that the greatest transcriptional changes will occur at phase transitions entering spaceflight and returning to Earth, whereas minimal changes will be observed later in spaceflight.

METHODS

Participant selection, study design, and ethics

Twenty astronauts scheduled to travel to the ISS voluntarily attended a presentation of the Marrow Adipose Reaction: Red Or White (MARROW) project approximately 1 year before an astronaut's scheduled flight. Inclusion criteria included male or female astronauts that were non-smokers, without any metal implants, and were scheduled to remain on the ISS for a minimum of four months. Fourteen astronauts, 11 men (46.7 ± 7.3 years old) and three women (39.7 ± 2.1 years old) consented to participating in the study on the temporal analysis of the leukocyte transcriptomes from blood samples collected throughout the three phases of their mission: pre-flight (PF), in-flight (IF), and return to Earth (R). All participants gave informed consent and were monitored by a medical team at NASA. Ethics approval was obtained from the NASA Human Research Multilateral Review (#Pro1283), Johnson Space Center Institutional Review Board (JSCIRB), European Space Agency Medical Board, Japanese Aerospace Exploration Agency, and the Ottawa Health Science Network Research Ethics Board (#2009646-01H).

Blood sample collection and storage

Ten blood samples were collected from each astronaut: one sample at PF between 90 and 60 days before liftoff, four samples IF onboard the ISS (IF1: between days 4 and 6; IF2: between days 8 and 12; IF3: between days 65 and 95; IF4: 30 to 1 day before returning on Earth), and five samples upon return to Earth (R) (R1: day 1; R2: between days 3 and 7; R3: between days 12 and 15; R4: between days 23 and 37; R5: between days 335 and 395) (Figure 2.1). Approximately 4 ml of venous blood was collected after an overnight fast in a Vacutainer with plasma separator tube gel and 83 units of lithium heparin (#8362534, Becton Dickinson, Franklin Lakes, NJ, USA). Immediately after harvesting, blood tubes were inverted, centrifuged at 1,500g for 15 min at room temperature, and stored at -80°C. PF and post-flight blood samples were collected and centrifuged at the NASA Johnson Space Center in Houston

Texas (USA) by a certified phlebotomist, and IF samples were collected, centrifuged, and frozen by crewmembers. The protocol for blood collection, centrifugation, and storage was the same for all blood samples including those collected onboard of the ISS. Frozen samples were shipped to our institution within 2-3 months after collection. A total of 139 blood samples were collected from 14 crewmembers during 12 different ISS missions (Supplementary Figure 2.1).

Leukocyte capture, RNA isolation, library preparation, and sequencing

Frozen blood samples were thawed at room temperature for ~15 min, and leukocytes layered on top of the gel were resuspended by gentle inversion of the tube. Total RNA was isolated from leukocytes using the LeukoLOCK™ total RNA isolation system and manufacturer's protocol (#AM1923, ThermoFisher Scientific, Waltham, MA, USA). Total RNA was suspended in 20 mL of RNAse-free water, and quality was assessed using the Agilent BioAnalyzer 2100 (Model G2939B, Agilent, Santa Clara, CA, USA). All 139 samples had RNA integrity number (RIN) ≥ 8.0. RNA sequencing libraries were depleted of rRNA using the NEBNext® ribosomal RNA (rRNA) Depletion Kit (Human/ Mouse/Rat) (#6310L, Ipswich, MA, USA) or using the NEBNext® Ultra™ II Directional RNA (rRNA) Library Prep Kit for Illumina® (#E7760L, Ipswich, MA, USA). Library quality was assessed using the Agilent BioAnalyzer 2100, and 72 samples passed the quality metrics for sequencing including a concentration above 10 nM (Supplementary Figure 2.1). Details of the inventory of libraries included with randomly assigned astronaut identifiers and time points that passed quality metrics are provided in Table 2.1. Libraries (125 pM) were multiplexed and sequenced with 100-base paired-end reads to a depth of ~50 million reads per sample using the Illumina NovaSeq 6000 System (Illumina, San Diego, CA, USA). Library preparation, quality assessment, high-throughput sequencing, and de-multiplexing step were performed at Genome Quebec Innovation Center (Montreal, Canada).

RNA-seq mapping

Reads were aligned to the publicly available human transcriptome and genome (GRCh38.84) using HISAT with default parameters (v2.0.13) (12). Transcript abundance calculations were performed using HTSeq with default parameters (v0.6.1) (13). For consistency with rRNA depletion library preparation, rRNA genes were excluded leaving an expression dataset that corresponded to 59,901 transcripts from coding and non-coding genes measured at the individual study time points for each astronaut.

Sample quality control

Gene read counts for the 59,901 genes from each sample were normalized for sample read depth using *DESeq2's* median of ratios (14), and the variance stabilizing log2 transformation (VST) was applied reducing variance of low read counts for principal component analysis. Principal component scores were calculated using the *prcomp()* function in R for all 72 samples. Samples were then plotted along PC1 and PC2 to visualize the variance explained by the individual astronauts and study time points. This showed significant deviation of the PF sample a2068.1 from other samples (Supplementary Figure 2.2). Therefore, this sample was treated as a technical outlier and excluded from further analyses leaving 71 samples for analysis in silico. All sequence analyses and result visualizations were conducted using the R environment (https://cran.r-project.org/doc/manuals/r-release/R-intro.html) and custom scripts.

Differential expression analysis

Two separate differential expression analyses were completed with both using the same fixed-effect generalized linear model (GLM) within the *DESeq2* package in R environment (14).

Model: read counts ~ replicate + sex + cumulative time in space + time + ε

This model measures the effect across time treating the "time" variable as categorical and included all 10 time points of the study. Confounding variables —sex and astronaut cumulative lifetime in space— were controlled while also accounting for repeated measures of biological replicates. The first differential expression analysis tested the temporal effect through applying likelihood ratio testing (LRT) on the "time" variable using the normalized read counts of all 59,901 genes. The temporal analysis was conceptually similar to analysis of variance (ANOVA) but instead represented an analysis of deviance (ANODEV) because *DESeq2* estimates dispersion not variance. Adjustment for multiple comparisons was done through independent hypothesis weighting (IHW) using the *IHW* package in R environment (15). This method increased power by assigning weights to each hypothesis test while controlling for the false discovery rate using the Benjamini-Hochberg correction (16). Genes with adjusted p-values < 0.1 were considered statistically significant and identified as gene candidates that were differentially expressed between any time point of the study.

For more specific insight into the IF and post-flight specific effects, differential expression analyses were done on a subset of time points. This used the same GLM as in the temporal differential expression analysis but instead applied the Wald's test on log2 fold changes (LFCs) for significance testing followed by LFC shrinkage using the *ashr* method (17). Comparisons of selective time points were conceptually similar to a post-hoc analysis testing the effect of specific time points within the "time" variable. Adjustment for multiple comparisons was done using only the Benjamini-Hochberg correction (16). Genes with adjusted p-values < 0.1 and LFC values > |0.5| were identified as gene candidates differentially expressed between a given time-point comparison.

Transcriptome expression visualizations

The normalized read counts of gene candidates identified as differentially expressed between any of the 10 time points (temporal analysis) were averaged among all astronauts at each time point and

scaled across genes as z-scores. These genes were then further analyzed to extract gene clusters displaying similar patterns of expression throughout the entire study. Briefly, the Euclidean distance between each gene candidate was calculated using their z-score scaled normalized read counts from each sample across time. These values were then hierarchically clustered using the *hclust()* function in R environment creating a tree dendrogram to visualize the gene clusters, which were resolved by a static tree cut (Supplementary Figure 2.3). Gene z-scores of temporal gene clusters were then plotted across time using lines and split violin plots overlayed by box plots to visualize the relative expression of genes over the course of the study (Figure 2.2).

As part of the temporal analysis, independent filtering of genes using *DESeq2* excluded genes with mean normalized read counts < 45 resulting in a profile of 15,410 genes representing the expressed transcriptome across time. The normalized read counts for this profile of expressed genes were scaled separately as z-scores. Gene z-scores for the 15,410 genes were then plotted across time as violin plots (Supplementary Figure 2.4).

RNA bio-typing

Gene candidate profiles identified from both temporal and timepoint differential expression analyses were bio-typed according to the functionality of RNA transcribed from these genes. Bio-type annotation was done using the *biomaRt* package in R environment (18, 19), which utilized the Vega archive gene classifications (https:// vega.archive.ensembl.org/info/about/gene_and_transcript_ types.html). The relative proportions of RNA bio-types within each differentially expressed gene profile were then displayed as stacked bar plots (Figures 2.2B; 2.3C, F).

Log fold change heatmap

The LFC values relative to PF were calculated for a subset of gene candidates identified from the differential expression analysis of selective time points. This subset of genes was identified from the Venn diagram overlap between the differentially expressed gene profiles for PF vs. IF2 and IF4 vs. R1 (Figure 2.4A). LFC values relative to PF were then displayed as a heatmap across all IF and post-flight time points along with their gene identities (Figure 2.4B).

Enrichment analysis

For insight into the broader biological functions of the differentially expressed gene profiles, functional enrichment of leukocyte transcriptomes using two separate overrepresentation analyses (ORAs) (20) of gene ontology (GO) terms was performed: one is to assess the temporal effect across all time points using the differentially expressed gene clusters and the other is to assess the spaceflight phase transitions using the differentially expressed genes from the selective time-point comparisons. A custom R script was used to detect significantly overrepresented GO terms between the list of differentially expressed gene profiles and the 15,410 expressed genes used as the reference list. ORA utilized *clusterProfiler 4.0's groupGO()* function (21) to map genes to their associated level 4 GO terms grouped under "Biological Processes". A Fisher exact test was applied to test for significantly overrepresented GO terms between genes and the reference list. After adjustment for multiple comparisons using the Benjamini-Hochberg correction, GO terms with FDR p-values < 0.05 were considered statistically significant.

Significant GO terms from the temporal gene clusters with > 1.5 enrichment were displayed onto a dot plot. The median LFC values relative to PF for the genes mapping to a specific GO term were displayed as a heatmap across all IF and post-flight time points (Figure 2.2C). For differentially expressed genes between specific time-points, significant GO terms were summarized by cluster networks based

on semantic similarity (Figures 2.3B) using REVIGO via a web browser (https://revigo.irb.hr) (22). The GO term cluster networks were further processed for clarity and aesthetics using Cytoscape (v3.9.1.0) (23).

RESULTS

Temporal analysis of leukocyte transcriptomes

To report the effects of space mission to the ISS, we determined the composition of astronauts' transcriptomes and measured differential expression over time using a GLM within the *DESeq2* package. LRT of all 10 time points identified 276 genes differentially expressed between any time point of the study. In addition, we found 15,410 genes represented the expressed transcriptome of astronauts over all 10 time points and corresponded to genes with average normalized read counts > 45 according to *DESeq2's* independent filtering threshold.

Transcriptome changes at transition to and from space

Temporal changes for the 276 differentially expressed genes are shown in Figure 2.2, which plots the mean transcript level for each gene across all 10 time points of the study. Transcript levels were reported as z-scores, which centered and scaled the normalized read counts for each gene by the mean and standard deviation across the 276 genes, ensuring comparable scaling and visualization for all genes. A positive z-score was interpreted as above average gene expression, a negative z-score indicated below average gene expression, and zero corresponded to average levels. Hierarchical clustering identified two gene clusters (C) based on the similarity in z-score changes over time (Figure 2.2A; Supplementary Figure 2.3). The two gene clusters consisted of 247 (C1) and 29 (C2) genes, respectively, and mirrored each other; average levels changed in opposite directions at individual time points. Both showed inverse patterns of expression changes at transition to space and at the transition back to Earth (Figure 2.2A). Specifically, gene C1 was characterized by decreased expression after 8-12 days in space (IF2) followed by increased expression on day 1 after return to Earth (R1) (Figure 2.2A). Conversely, gene C2 displayed increased expression transitioning to space and decreased expression at return to Earth (Figure 2.2A).

Gene expression changes in C1 were less variable than C2 as shown by the narrower spread in violin plots and smaller interquartile ranges (IQR) of box plots (Figure 2.2A).

Protein-coding genes dominate temporal gene clusters

Bio-typing of gene RNA revealed distinct bio-type proportions of the two temporal gene clusters. C1 consisted mostly of protein-coding genes (68.8%), 19.4% long non-coding RNAs (lncRNA), and 11.7% genes coding for other various RNA biotypes (Figure 2.2B). C2 genes consisted mostly of protein-coding genes (93.1%), zero lncRNA, and 6.9% other RNAs (Figure 2.2B).

The two temporal gene clusters differ in biological function

Functional enrichment of the two differentially expressed gene clusters across all 10 time points produced terms describing different biological functions. Shown in a dot plot are the GO terms from each temporal gene cluster with an enrichment > 1.5 (Figure 2.2C). In C1, seven of the top eight most enriched terms described immune system and leukocyte functions. Among these, the terms “regulation of immune system”, “lymphoid organ development”, and “leukocyte and lymphocyte activation” had the largest gene counts (Figure 2.2C). In contrast, C2 was composed of terms describing diverse biological processes including anatomical structure and development and molecular regulation such as “DNA-binding transcription factor” (Figure 2.2.C). Interestingly, the second most enriched term of C2 was “regulation of body fluid levels” (Figure 2.2C). The heatmap in Figure 2.2C displays the median LFC values relative to baseline for the genes associated with a given GO term throughout IF and post-flight time points. LFC values reiterated the opposite profiles of changes characterizing the two clusters of genes: inverse pattern of expression at IF and post-flight transitions (Figure 2.2A).

Gene expression converges toward average levels after long-duration exposure to space

Gene expression between 2 and 6 months IF (IF3 and IF4) converged toward average levels. This pattern was observed for the 276 temporally differentially expressed genes (Figure 2.2A) and was also evident with the profile of 15,410 genes obtained from independent filtering in *DESeq2* (Supplementary Figure 2.4). The spread of average transcript levels for all expressed genes at IF3 and IF4 displayed the smallest IQR compared to all other time points (Supplementary Figure 2.4; Supplementary Table 2.1).

Leukocyte transcriptome at spaceflight phase transitions

To assess the effects of space transitions on astronauts' transcriptomes, four time-point comparisons were selected on the basis of the most important changes in transcript levels displayed in the temporal profiles of clusters (Figure 2.2A). The time-point comparisons included space phase transitions (PF vs. IF2 and IF4 vs. R1), transcriptional convergence after long-duration in space (IF3 vs. IF4), and 1 year after return from space (PF vs. IF5). The differential expression results for PF vs. IF2 and IF4 vs. R1 are shown in (Figures 2.3A, B respectively). All four differential expression results are summarized in Table 2.2.

Differential expression was strongest during transitions to space and return to Earth

Comparing transcriptomes at PF and IF2 time points, we identified 112 downregulated genes and eight upregulated genes (Figure 2.3A). The return to Earth was associated with 16 downregulated genes and 135 upregulated genes differentially expressed between IF4 and R1 transcriptomes (Figure 2.3D). Substantial gene expression changes at space transitions were dominated by genes downregulated during early spaceflight (IF2) and upregulated during the return to Earth (R1). These results confirm the decrease-then-increase pattern of gene C1 identified in the temporal gene cluster analysis (Figure 2.2). In addition, RNA bio-typing of the differentially expressed genes at space transitions

(PF vs. IF2 and IF4 vs. R1) replicated results from the temporal gene clusters with protein coding as most represented RNA (Figures 2.3C).

Space transition responses differ in biological function

Enrichment analysis of the 112 downregulated genes between PF and IF2 and 135 upregulated genes between IF4 and R1 identified biological functions differing between the transitions to and from space. GO terms are summarized in a cluster network on the basis of semantic similarity shown in Figures 2.3B, E. The transition to space enriched terms is related to cellular growth such as “cell population proliferation” (most enriched), “cell differentiation”, and “cellular component organization” (Figure 2.3B). In contrast, the return to Earth resulted in two clusters of enriched terms both describing different biological processes than the transition to space (Figure 2.3E). One cluster consisted of terms related to cellular transport such as “intracellular transport” and “protein transport and localization” (Figure 2.3E). The other cluster included terms describing the regulation of immune system processes such as “leukocyte activation” and “lymphoid organ development” (Figure 2.3E).

One hundred genes were both downregulated when reaching space and upregulated when landing on Earth

Among the 112 downregulated genes when reaching space and 135 upregulated genes when returning to Earth, 100 were the same genes (Figure 2.4A). Figure 2.4B lists the 100 genes along with a heatmap displaying the LFC values relative to PF for each gene. The three most represented gene families were Zinc-Finger Protein (ZNF) genes (n = 6), Cluster of Differentiation (CD) genes (n = 3), and Long Intergenic Non-Protein Coding (LINC) RNA (n = 3).

Leukocyte transcriptome in-flight and 1-year post-flight

No differential expression occurs during late in-flight

Our results found zero genes differentially expressed between 65-95 days IF and 30-1 day prior to return to Earth (IF3 vs. IF4) (Table 2.2). The convergence toward no changes later in flight is also evident from standardizing scaled expression to z-scores. The distribution of mean scaled expression (z-scores) for all genes at each time point are shown in Figure 2.2A; Supplementary Figure 2.4. Late IF time points corresponding to IF3 and IF4 had the lowest IQRs compared to all 10 time points (0.29 and 0.32, respectively) (Supplementary Table 2.1).

Transcriptome 1-year post-flight is similar to pre-flight

Analysis between PF and 1-year post-flight time points (PF vs. R5) revealed zero differentially expressed genes (Table 2.2). From the 15,410 expressed genes, transcriptional variability between PF and 1 year after returning from space appeared similar on the basis of the spread of violin plots and IQR (Supplementary Table 2.1; Supplementary Figure 2.4). However, Figure 2.2A shows C1 and C2 having reversed expression 1-year post-flight when compared to PF. C1 genes had above average expression PF but had below average expression 1-year post-flight, and vice versa for C2.

DISCUSSION

We analyzed the leukocyte transcriptome of 14 female and male astronauts before their launch to space, upon reaching the ISS, in space for 6 months, at egress to Earth, and up to 1 year after landing. Differential expression was measured using an integrated time-course analysis followed by a focused analysis of mission phase transition time points. The salient findings were as follows (1): temporal analysis identified the decrease-then-increase expression pattern at transitions to and from space as the main profile of change with immune system processes most represented; (2) phase transition analysis identified downregulated genes mainly associated with "regulation of cell population" and upregulated genes at the return to Earth associated with "regulation of immune system process"; (3) 100 genes were both downregulated when reaching space and upregulated upon returning to Earth; and (4) transcript levels converged toward average levels displaying no differential expression between ~2 and ~6 months IF.

Differential expression at phase transition

The first analysis of the leukocyte transcriptomes provided an overview of the relative transcriptional changes occurring at 10 time points across the three phases of a space mission: PF, IF, and R. Astronauts' leukocyte transcriptomes showed opposite directions of gene expression changes upon reaching the space environment compared to the return on Earth. Cluster analysis grouped the differentially expressed genes into two clusters characterized by major changes in opposing directions: (C1) decrease-then-increase and (C2) increase-then-decrease.

The biological processes represented among the 247 genes from C1 were mainly specialized leukocyte functions and immune system processes. Temporal transcriptome data indicated a reduction of immune functions when transiting to space and the opposite when returning on Earth: an increase of immune function. Our findings are consistent with previous reports of decreased immunity in space

including reductions in T-cell function, NK-cell function, altered plasma cytokine profiles, and persistent inflammation (7, 8, 24-26). Our analysis at both transition to a different gravitational environment revealed novel genes and pathways not previously documented in astronauts traveling to space. The decreased expression of the cell surface receptor CD3E and CD3G genes, both members of the CD3 T-cell receptor complex, is likely contributing to the reduced immunity while in space. The CD3 complex is involved in the recognition of antigens and subsequent signal transduction, leading to the activation of T lymphocytes (27, 28). The reduction of CD3 expression in response to microgravity was previously observed in vitro in a human cell line of T lymphocytes and Jurkat cells exposed to microgravity (29). Our data from astronauts' leukocytes provide additional evidence for the CD3 complex dynamic response to microgravity and changes occurring within the first few days after transitioning to and from space. Considering the rapid changes of CD3 complex gene expression, adaptive immunity such as the response to foreign antigens is likely affected by changing microgravity environments, rather than innate immune systems (30). The impact of the differential expression on the adaptive immune system can not be excluded as both immune systems are highly interconnected and previously documented to be impacted by microgravity (31, 32). Few studies have examined the dynamic changes of markers of adaptive and innate immune response throughout ISS missions, and published data are from either short-duration missions (8-15 days) or to comparisons between pre- and post- flight (33, 34). A comprehensive study of eight astronauts sojourning ~6 months onboard of the ISS reported no or very little effects on B-cell number, phenotype, and antibody output after returning on Earth (35). In this study, total B-cells and immunoglobulin A increased after 90 days in flights and returned to baseline at return day. Our data on leukocytes' transcriptome agree with the previous observations of transitional changes in immune cells while transitioning to and from space and the return toward baseline levels later after returning to Earth.

The lower number of genes in C2 (n = 29) limited the conclusions for enrichment analysis and identification of represented biological processes. Of interest, the biological term "regulation of body

fluid" represented in the short list of genes in C2 displayed a pattern of upregulation when reaching space. The gene SLC4A1 associated with the term "regulation of body fluid" encodes for an anion exchanger protein localized in the plasma membrane of erythrocytes and mediates carbon dioxide transport to the lungs (36). Increased expression of SLC4A1 gene when reaching space may respond to the increase of carbon dioxide levels in conditions of low red blood cell mass, with the latter being previously documented in astronauts (10). The gene AQP3 with changes in opposite directions at both phase transitions functions as a water and urea exit mechanism of antidiuresis in collecting duct cells —a mechanism regulating body fluids (37). Therefore, reaching space promoted leukocyte gene expression related to basic housekeeping cell functionality as well as specific space adaptations like headward body fluid shifts leading to loss in plasma volume and hemoconcentration (38). Restoring blood cells concentrations to homeostatic levels requires a decrease in the number of circulating leukocytes and red blood cells whose population is decreased by ~10% in the first 10 days in space (39). Therefore, in addition to immune functions, the leukocyte transcriptome identified cellular functions and physiological systems affected by spaceflight.

The opposite directions of expression changes in the gene clusters at space transitions replicated the results obtained from participants subjected to a microgravity analogue (40). The -6° head down tilt bedrest model replicates the microgravity component of spaceflight with many of the physiological changes happening in space including fluid shift, muscle atrophy, bone loss, and hemolysis (41-44). Transcriptome composition changed in opposite directions at transitions between ambulation and bedrest and between bedrest and re-ambulation in 20 healthy participants submitted to 60 days of bedrest (40). While the space missions were longer with an average of 6 months compared to the 60 days period in bed, the transcriptome changes at phase transition coincided. Comparable changes in the leukocyte transcriptome may, therefore, indicate a characteristic response to the negative mechanotransduction, inactivity, and fluid shift brought about by prolonged exposure to both bedrest

and space. Leukocyte transcriptomes are therefore highly sensitive to changes in the gravity vector and appear to mount an adaptive response toward restoring homeostasis.

The next characteristic of leukocyte transcriptome temporal changes observed was the transcriptional convergence toward average levels displaying no differential expression after 2 months of space exposure. This is a novel finding revealed through the temporal analysis. The biological meaning is unclear but indicative of global mechanisms yet to be identified that limit variations of mRNA levels in leukocytes in space. Interestingly, the gene expression convergence of astronauts replicated the results of participants to the 60 day bedrest study (40), supporting that gene expression convergence is related to inactivity and redirected gravity isolated from other space specific stressors. In addition, this might be compatible with a generalized loss of specialized cell functions upon removal of normally oriented gravity and activity. The lack of mechanotransduction and inactivity would then focus cellular activity on core housekeeping functions.

The comparison of transcriptomes between PF and 1-year postflight showed that the two gene clusters were reversed in expression. This may suggest that some molecular space adaptations acquired while living in space for 6 months were maintained for at least 1 year after return to life on Earth. This may bear physiological significance given the ~20% increases in hemolysis in the same astronauts 1 year after returning from space (10, 39).

Shift in biological functions at spaceflight transitions to and from microgravity

Transiting to and from microgravity was associated with the differential expression of 120 and 151 genes from the reference list of 15,410 genes expressed in leukocytes. The majority (93.3%) of the differentially expressed genes when reaching space were down regulated and 95.7% were up regulated when returning. Differential expression measured at mission transitions is consistent with the temporal profile of C1 characterized by down and up- expression. Downregulated genes identified between PF and

early IF were associated with the biological term “regulation of cellular population proliferation”. This transcriptomic response is consistent with the head ward fluid shift and subsequent hemoconcentration of blood cells occurring when entering space (38). A decrease in circulating red and white blood cells restores blood cell concentrations to maintain homeostasis, consistent with the downregulation of genes involved in cellular proliferation (10). A suppression of blood cell proliferation represents an adaptation to the reduced blood volume in space.

At transition from space to Earth, transcriptomes were characterized by an up regulation of expression, opposite to changes measured when reaching space. Enrichment analysis of the upregulated genes between late IF and return to Earth resulted in biological processes describing the regulation of immune system, leukocyte activation, and lymphoid organ development. Returning to Earth’s surface gravity after ~6 months in microgravity reversed the down regulation of genes involved in immune processes. Many immune alterations persist during long-duration spaceflight (8). Reactivation of immune- related genes in response to the re-entry to Earth is needed to reverse immune dysregulation occurring during spaceflight. The composition of the leukocytes’ transcriptome was influenced by the transition to the different gravity environments.

Of the 112 genes downregulated early IF, 100 (89.3%) of those same genes were upregulated immediately upon return to Earth. This means that the same genes responded to both transitions to and from microgravity despite the occurrence of different physiological changes. To our knowledge, this represents a novel finding. Most differentially expressed genes at space transitions coded for proteins with the second most important being long non-coding RNAs. The notable modulation of transcription factors (ZNF and CD) and lncRNAs that regulate expression of downstream target genes may explain why the same differentially expressed genes are regulating different physiological responses. Zinc Finger proteins are transcriptions factors that have a wide range of molecular functions including DNA recognition, RNA packaging, transcriptional activation, regulation of apoptosis, protein folding and

assembly, and lipid binding (45). Changes in ZNF expression would potentially alter these molecular processes that would then manifest at the cellular and physiological levels. For instance, we identified Zinc-Finger Antiviral Proteins (ZAP) ZNF776, ZNF585B, and ZNF83 as downregulated during early spaceflight and upregulated upon return to Earth. ZAPs help prevent the spread of viruses by targeting viral mRNA (46). The downregulation of these genes when reaching space corresponds to reported reactivation of herpesvirus in astronauts during spaceflight (27). Whereas, the following upregulation of ZAPs when returning to Earth may be a response to suppress the replication of herpes viral particles.

Contributions and limitations

Our access to unique astronauts' blood samples and RNA analysis of the leukocytes' transcriptome using high- throughput sequencing technique represents the strength of this study. The finding of genes responding to both the transition to and from space with decreased and then increased profile of changes that related to immune processes represents a novel finding. Our study also identified additional expression changes at phase transitions in genes unrelated to specific immune functions, such as cell population regulation. This provides evidence of changes at the molecular level by which the body adapts to the headward fluid shift observed in microgravity environments. This study bears a number of limitations. Blood draws were taken at 10 different time points throughout astronaut missions; changes of interest to establish the onset of transcriptional convergence in space timed in-between blood draws may have been missed. Technical limitations onboard the ISS hampered sample acquisition, processing, and analysis. For instance, blood samples were collected within a window of days rather than on a specific day that introduced variability. Leukocyte and RNA isolation were not possible on the ISS and blood samples were frozen at -80°C for their journey back to Earth, leading to cell lysis and RNA degradation. This resulted in samples with inadequate RNA quality for sequencing, which were rejected, leading to an unbalanced final sample size. In addition, a potential contribution of altered leukocyte

subpopulations to gene differential expression can not be excluded. RNA sequencing removed ribosomal RNA and was biased toward protein-coding genes; changes in other RNA biotypes would have been missed. The limited sample size and heterogeneous cohort of 14 astronauts with unequal sex distribution limited statistical power and prevented sex-specific comparisons.

CONCLUSIONS

The analysis of transcriptome composition identified changes during the transitions to and from space characterized mainly by a decrease and an increase of transcript levels respectively. When reaching space, the transcriptomic changes are indicative of decreased immune functions and increased basic cellular activities linked to adaptive changes. The transcriptomic changes egressing back to Earth were in opposite direction —increased expression, mainly for genes related to the immune system. These results shed light on immune modulation in space, the timing of differential expression at transition to and from space, and highlight the major adaptive changes in leukocyte activity engaged to adapt to extreme environments.

Data availability statement

The datasets presented in this article are not readily available because of ethical and privacy restrictions. Requests to access the datasets should be directed to the corresponding author/s. Aggregated data to understand and assess the conclusions of this research are available in the figures and Supplementary Tables. Aggregated data (read count tables and metadata) have been deposited in NASA's Life Sciences Data Archives (LSDA) under dataset name "MARROW payload". Investigators can request access to the astronaut data at jsc-lsda@mail.nasa.gov.

Ethics statement

The studies involving human participants were reviewed and approved by NASA Human Research Multilateral Review Board Johnson Space Center Institutional Review Board European Space Agency Medical Board Japanese Aerospace Exploration Agency Ottawa Health Science Network Research Ethics Board. The patients/participants provided their written informed consent to participate in this study.

Author contributions

GT and OL participated in the concept and design. All authors participated in the acquisition, analysis, or interpretation of data. DS, GT, OL participated in the drafting of the article. All authors participated in the critical revision of the article for important intellectual content. DS and OL participated in the statistical analysis. GT and OL participated in the funding acquisition. All authors contributed to the article and approved the submitted version.

Funding

This study was funded by the Canadian Space Agency (Contract No. 9F008-140254).

Conflict of interest

The authors declare that the research was conducted in the absence of any commercial or financial relationships that could be construed as a potential conflict of interest.

Publisher's note

All claims expressed in this article are solely those of the authors and do not necessarily represent those of their affiliated organizations, or those of the publisher, the editors, and the reviewers. Any product that may be evaluated in this article, or claim that may be made by its manufacturer, is not guaranteed, or endorsed by the publisher.

References

1. Afshinnekoo E, Scott RT, MacKay MJ, Pariset E, Cekanaviciute E, Barker R, et al. Fundamental biological features of spaceflight: advancing the field to enable deep-space exploration. Cell [Internet] (2020) 183(5):1162–84. doi: 10.1016/ j.cell.2020.10.050

2. Roberts DR, Asemani D, Nietert PJ, Eckert MA, Inglesby DC, Bloomberg JJ, et al. Prolonged microgravity affects human brain structure and function. Am J Neuroradiol (2019) 40(11):1878–85. doi: 10.3174/ajnr.A6249
3. Demontis GC, Germani MM, Caiani EG, Barravecchia I, Passino C, Angeloni D. Human pathophysiological adaptations to the space environment. Front Physiol (2017) 8(AUG):1–17. doi: 10.3389/fphys.2017.00547
4. Thornton WE, Moore TP, Pool SL. Fluid shifts in weightlessness. Aviat Sp Env Med (1987) 58(9 Pt 2):A86–90.
5. Leach CS, Alfrey CP, Suki WN, Leonard JI, Rambaut PC, Inners LD, et al. Regulation of body fluid compartments during short-term spaceflight. J Appl Physiol (1996) 81(1):105–16. doi: 10.1152/jappl.1996.81.1.105
6. Hargens AR, Richardson S. Cardiovascular adaptations, fluid shifts, and countermeasures related to space flight. Respir Physiol Neurobiol [Internet] (2009) 169(Suppl 1):S30–33. doi: 10.1016/j.resp.2009.07.005
7. Bigley AB, Agha NH, Baker FL, Spielmann G, Kunz HE, Mylabathula PL, et al. NK cell function is impaired during long-duration spaceflight. J Appl Physiol (2019) 126 (4):842–53. doi: 10.1152/japplphysiol.00761.2018
8. Crucian B, Stowe RP, Mehta S, Quiriarte H, Pierson D, Sams C. Alterations in adaptive immunity persist during long-duration spaceflight. NPJ Microgravity (2015) 1 (July):1–10. doi: 10.1038/npjmgrav.2015.13
9. Leach CS, Johnson PC. Influence of spaceflight on erythrokinetics in man. Sci (1984) 225(4658):216–8. doi: 10.1126/science.6729477
10. Trudel G, Shahin N, Ramsay T, Laneuville O, Louati H. Hemolysis contributes to anemia during long-duration space flight. Nat Med (2022) 28(1):59–62. doi: 10.1038/ s41591-021-01637-7

11. Garrett-Bakelman FE, Darshi M, Green SJ, Gur RC, Lin L, Macias BR, et al. The NASA twins study: a multidimensional analysis of a year-long human spaceflight. Sci (2019) 364(6436):eaau8650. doi: 10.1126/science.aau8650
12. Pertea M, Kim D, Pertea GM, Leek JT, Salzberg SL. Transcript-level expression analysis of RNA-seq experiments with HISAT, StringTie and ballgown. Nat Protoc [Internet] (2016) 11(9):1650–67. doi: 10.1038/nprot.2016-095
13. Anders S, Pyl PT, Huber W. HTSeq-a Python framework to work with highthroughput sequencing data. Bioinformatics (2015) 31(2):166–9. doi: 10.1093/ bioinformatics/btu638
14. Love MI, Huber W, Anders S. Moderated estimation of fold change and dispersion for RNA-seq data with DESeq2. Genome Biol (2014) 15(12):1–21. doi: 10.1186/s13059-014-0550-8
15. Ignatiadis N, Klaus B, Zaugg JB, Huber W. Data-driven hypothesis weighting increases detection power in genome-scale multiple testing. Nat Methods (2016) 13 (7):577–80. doi: 10.1038/nmeth.3885
16. Benjamini Y, Hochberg Y. Controlling the false discovery rate: a practical and powerful approach to multiple testing. Journal of the Royal Statistical Society: Series B (Methodological) (2009) 57(1):289–300. doi: 10.1111/j.2517-6161.1995.tb02031.x
17. Stephens M. False discovery rates: a new deal. Biostatistics (2017) 18(2):275–94. doi: 10.1093/biostatistics/kxw041
18. Durinck S, Spellman PT, Birney E, Huber W. Mapping identifiers for the integration of genomic datasets with the R/Bioconductor package biomaRt. Bone (2008) 23(1):1–7. doi: 10.1038/nprot.2009.97
19. Durinck S, Moreau Y, Kasprzyk A, Davis S, De Moor B, Brazma A, et al. BioMart and bioconductor: a powerful link between biological databases and microarray data analysis. Bioinformatics (2005) 21(16):3439–40. doi: 10.1093/bioinformatics/bti525

20. Boyle J. Gene-expression omnibus integration and clustering tools in SeqExpress. Bioinformatics (2005) 21(10):2550–1. doi: 10.1093/bioinformatics/bti355
21. Wu T, Hu E, Xu S, Chen M, Guo P, Dai Z, et al. clusterProfiler 4.0: a universal enrichment tool for interpreting omics data. Innovation(China) [Internet] (2021) 2 (3):100141. doi: 10.1016/j.xinn.2021.100141
22. Supek F, Bosnjak M, S˘ kunca N, Š muc T. Revigo summarizes and visualizes long lists of gene ontology terms. PloS One (2011) 6(7):e21800. doi: 10.1371/journal.pone.0021800
23. Shannon P, Andrew Markiel A, Ozier O, Baliga NS, Wang JT, Ramage D, et al. Cytoscape: a software environment for integrated models. Genome Res [Internet] (1971) 13(22):426. doi: 10.1101/gr.1239303.metabolite
24. Crucian B, Simpson RJ, Mehta S, Stowe R, Chouker A, Hwang SA, et al. Terrestrial stress analogs for spaceflight associated immune system dysregulation. Brain Behav Immun [Internet] (2014) 39:23–32. doi: 10.1016/j.bbi.2014.01.011
25. Frippiat JP, Crucian BE, de Quervain DJF, Grimm D, Montano N, Praun S, et al. Towards human exploration of space: the THESEUS review series on immunology research priorities. NPJ Microgravity (2016) 16040. doi: 10.1038/npjmgrav.2016.40
26. Buchheim JI, Matzel S, Rykova M, Vassilieva G, Ponomarev S, Nichiporuk I, et al. Stress related shift toward inflammaging in cosmonauts after long-duration space flight. Front Physiol (2019) 10(FEB):1–13. doi: 10.3389/fphys.2019.00085
27. Dietrich J, Hou X, Wegener AMK, Geisler C. CD3g contains a phosphoserinedependent di-leucine motif involved in down-regulation of the T cell receptor. EMBO J (1994) 13(9):2156–66. doi: 10.1002/j.1460-2075.1994.tb06492.x

28. Borroto A, Lama J, Niedergang F, Dautry-Varsat A, Alarcon B, Alcover A. The CD3ϵ subunit of the TCR contains endocytosis signals. J Immunol (1999) 163(1):25–31. doi: 10.4049/jimmunol.163.1.25
29. ElGindi M, Sapudom J, Laws P, Garcia-Sabaté A, Daqaq MF, Teo J. 3D microenvironment attenuates simulated microgravity-mediated changes in T cell transcriptome. Cell Mol Life Sci [Internet] (2022) 79(9):1–16. doi: 10.1007/s00018-022- 04531-8
30. Buchheim JI, Ghislin S, Ouzren N, Albuisson E, Vanet A, Matzel S, et al. Plasticity of the human IgM repertoire in response to long-term spaceflight. FASEB J (2020) 34(12):16144–62. doi: 10.1096/fj.202001403RR
31. Prasad B, Grimm D, Strauch SM, Erzinger GS, Corydon TJ, Lebert M, et al. Influence of microgravity on apoptosis in cells, tissues, and other systems in vivo and in vitro. Int J Mol Sci (2020) 21(24):1–32. doi: 10.3390/ijms21249373
32. Patel ZS, Brunstetter TJ, Tarver WJ, Whitmire AM, Zwart SR, Smith SM, et al. Red risks for a journey to the red planet: the highest priority human health risks for a mission to Mars. NPJ Microgravity [Internet] (2020) 6(1):1–13. doi: 10.1038/s41526- 020-00124-6
33. Grove D, Pishak S, Mastro A. The effect of a 10-day space flight on the function, phenotype, and adhesion molecule expression of splenocytes and lymph node lymphocytes. Exp Cell Res (1995) 219(1):102–9. doi: 10.1006/ excr.1995.1210
34. Rykova MP, Antropova EN, Larina IM, Morukov BV. Humoral and cellular immunity in cosmonauts after the ISS missions. Acta astronaut. (2008) 63(7–10):697– 705.
35. Spielmann G, Agha N, Kunz H, Simpson RJ, Crucian B, Mehta S, et al. B cell homeostasis is maintained during long-duration spaceflight. J Appl Physiol (2019) 126 (2):469–76. doi: 10.1152/japplphysiol.00789.2018

36. Reithmeier RAF, Casey JR, Kalli AC, Sansom MSP, Alguel Y, Iwata S. Band 3, the human red cell chloride/bicarbonate anion exchanger (AE1, SLC4A1), in a structural context. Biochim Biophys Acta - Biomembr (2016) 1858(7):1507–32. doi: 10.1016/j.bbamem.2016.03.030
37. Roudier N, Ripoche P, Gane P, Le Pennec PY, Daniels G, Cartron JP, et al. AQP3 deficiency in humans and the molecular basis of a novel blood group system, GIL. J Biol Chem [Internet] (2002) 277(48):45854–9. doi: 10.1074/jbc.M208999200
38. Diedrich A, Paranjape SY, Robertson D. Plasma and blood volume in space. Am J Med Sci (2007) 334(1):80–6. doi: 10.1097/MAJ.0b013e318065b89b
39. Trudel G, Shafer J, Laneuville O, Ramsay T. Characterizing the effect of exposure to microgravity on anemia: more space is worse. Am J Hematol (2020) 95(3):267–73. doi: 10.1002/ajh.25699
40. Stratis D, Trudel G, Rocheleau L, Pelchat M, Laneuville O. The characteristic response of the human leukocyte transcriptome to 60 days of bed rest and to reambulation. Med Sci Sports Exercise (2022) 55(3):365–75. doi: 10.1249/ MSS.0000000000003071
41. Pandiarajan M, Hargens AR. Ground-based analogs for human spaceflight. Front Physiol (2020) 11(June):1–6. doi: 10.3389/fphys.2020.00716
42. Hargens AR, Vico L. Long-duration bed rest as an analog to microgravity. J Appl Physiol (2016) 120(8):891–903. doi: 10.1152/japplphysiol.00935.2015
43. Trudel G, Uhthoff HK, Laneuville O. Hemolysis during and after 21 days of head-down-tilt bed rest. Physiol Rep (2017) 5(24):1–12. doi: 10.14814/phy2.13469
44. Marusic U, Narici M, Simunic B, Pisot R, Ritzmann R. Nonuniform loss of muscle strength and atrophy during bed rest: a systematic review. J Appl Physiol (2021) 131(1):194–206. doi: 10.1152/japplphysiol.00363.2020
45. Laity JH, Lee BM, Wright PE. Zinc finger proteins: new insights into structural and functional diversity. Curr Opin Struct Biol (2001) 11(1):39–46. doi: 10.1016/S0959- 440X(00)00167-6

46. Kozaki T, Takahama M, Misawa T, Matsuura Y, Akira S, Saitoh T. Role of zincfinger anti-viral protein in host defense against sindbis virus. Int Immunol (2015) 27 (7):357–64. doi: 10.1093/intimm/dxv010

Figures and tables

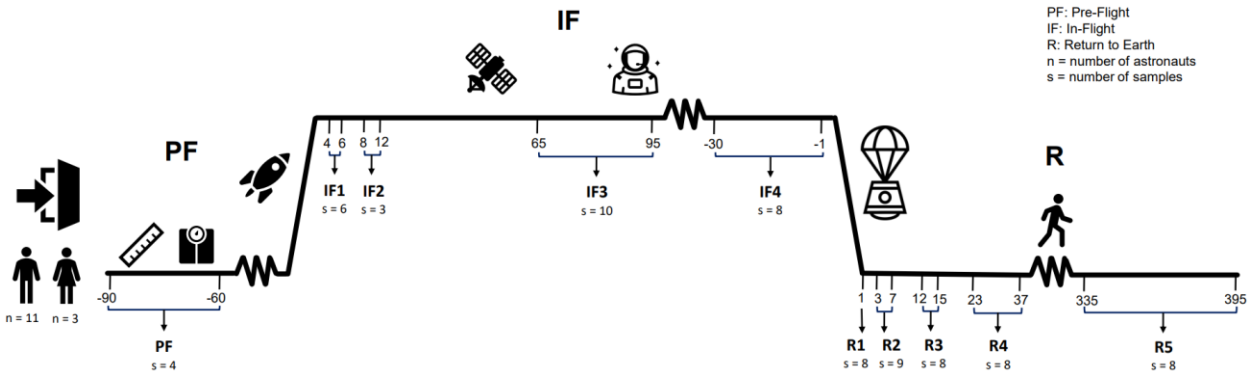

Figure 2.1 | Experimental design. Fourteen astronauts (11 men and 3 women) sojourned aboard the ISS. Ten venous blood samples were collected from each astronaut throughout the three phases of their mission: one sample at pre-flight (PF) between 90 and 60 days before liftoff, four samples in-flight (IF) onboard the ISS (IF1: between days 4 and 6; IF2: between days 8 and 12; IF3: between days 65 and 95; IF4: 30 to 1 days before returning on Earth), and five samples upon return to Earth (R) (R1: day 1; R2: between days 3 and 7; R3: between days 12 and 15; R4: between days 23 and 37; R5: between days 335 and 395). “n” is the sample size of male and female astronauts that participated in the study. “s” is the number of RNA samples with libraries that passed quality metrics and used for sequencing at each timepoint.

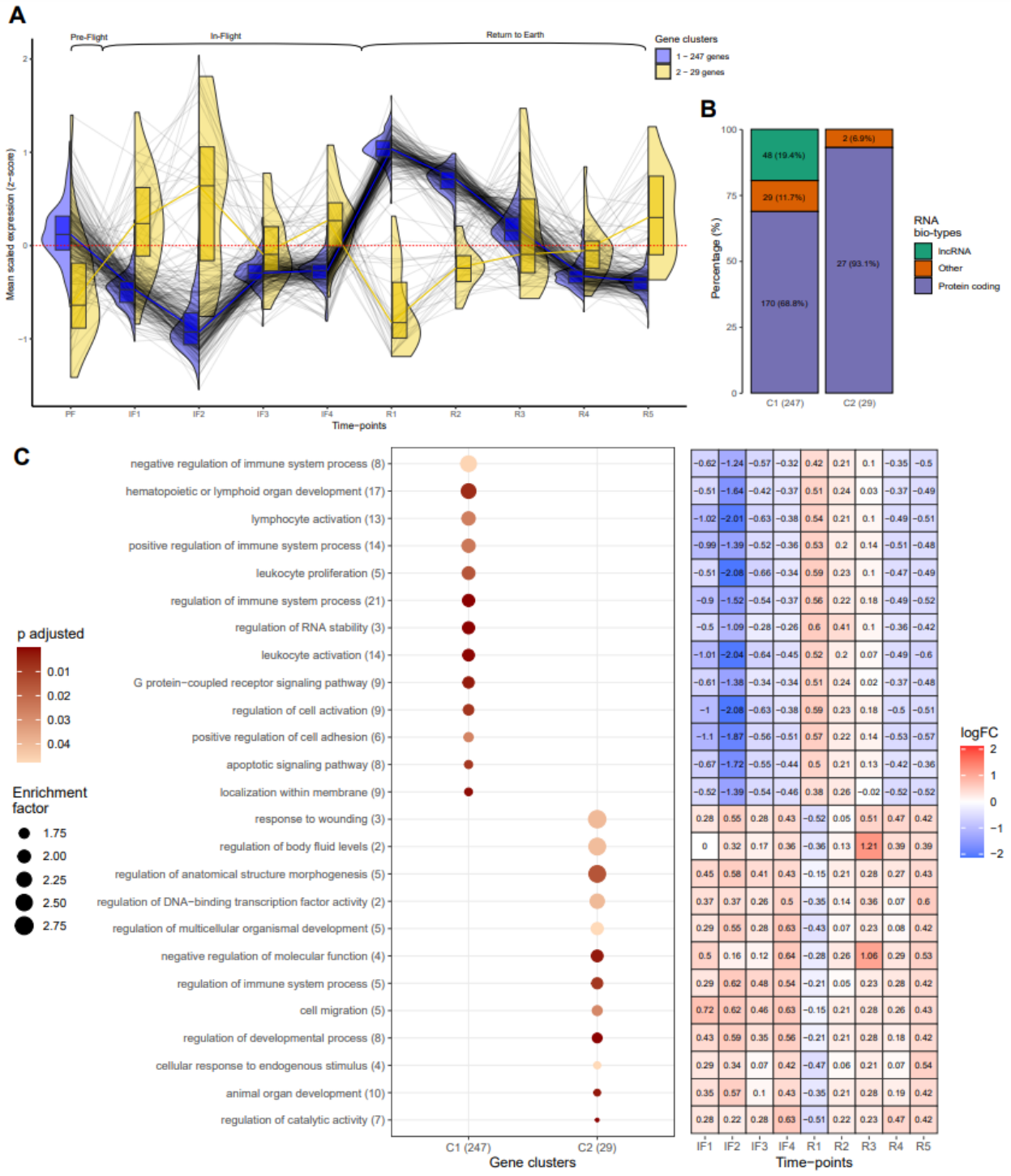

Figure 2.2 | Temporal analysis of leukocyte transcriptomes before, during, and after spaceflight. (A) Gene expression levels plotted as scaled Z-scores across individual time points. Z-scores represent the average normalized read counts scaled across the 276 temporal differentially expressed genes at each

individual time-point for the 14 astronauts. Black lines follow individual transcripts over time. Colored lines, split violin, and box plots represent the profiles of temporal gene clusters identified through hierarchical clustering. The number of genes identified in each cluster is indicated. Above brackets indicate the mission phases of time points. (B) RNA bio-type proportions for the two temporal gene cluster profiles displayed as stacked bar plots. RNA bio-type, gene counts, and percentages are indicated. The “other” category includes miscellaneous RNA, pseudogenes,and RNA to be experimentally confirmed (TEC). (C) Dot plot displaying the gene ontology (GO) terms obtained from the overrepresentation analysis (ORA) of temporal gene clusters across all mission phases. Terms with >1.5 enrichment in each temporal cluster were plotted with the number of genes mapping to that specific GO term indicated in brackets. The size of each dot is proportional to the enrichment factor (size scale) and the color represents the FDR adjusted p-values, where darker points have lower values (color scale). Enrichment corresponds to the ratio of mapped gene counts to a given GO term between each temporal gene cluster and the reference list of 15,410 genes. Enriched GO terms were grouped under “Biological Processes” at level 4. Using the Benjamini–Hochberg correction for multiple comparisons, p-values with false discovery rate (FDR) < 0.05 were considered statistically significant. The heatmap displays the median log fold change (LFC) values throughout in-flight and post-flight time points relative to baseline for the genes associated with each GO term. The color bar represents values of log2 fold changes ranging from +2 (red) to −2 (blue).

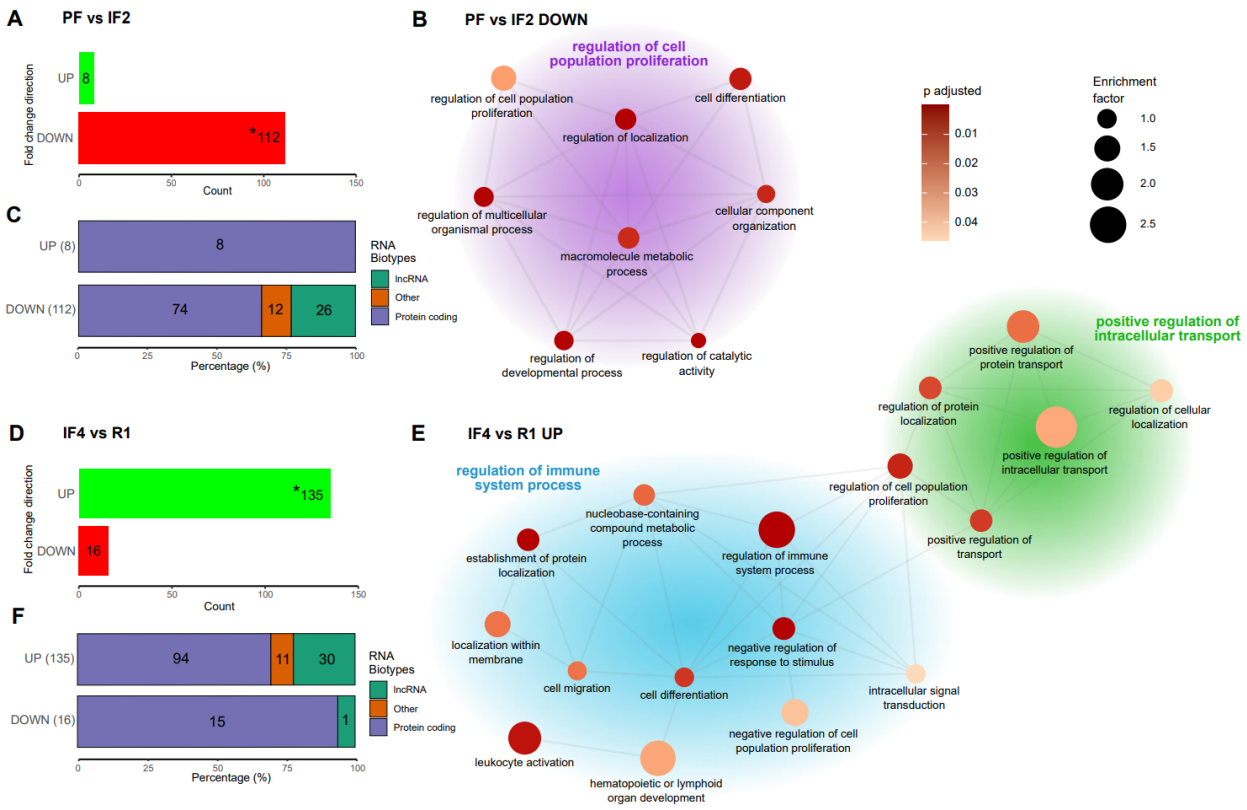

Figure 2.3 | Genes differentially expressed at spaceflight phase transitions and functional enrichment. Cluster network of gene ontology (GO) terms was obtained from the phase-specific overrepresentation analysis (ORA) of 112 downregulated genes between PF and IF2 (A, B), and 135 upregulated genes between IF4 and R1 (D, E) with stacked bar plots (C, F) displaying the RNA Bio-type proportions for these genes. RNA Bio-type, gene counts, and percentages are indicated. The "other" category includes miscellaneous RNA, pseudogenes, and RNA's to be experimentally confirmed (TEC). Networks (B, E) illustrate semantic similarity of GO terms using REVIGO. The size of each dot is proportional to the enrichment factor (size scale) and color represents the FDR adjusted p-values, where darker points have lower values (color scale). Cluster headers are the GO term with the highest enrichment factor within that cluster. Enrichment corresponds to the ratio of mapped gene counts to a given GO term between each differentially expressed gene profile [PF vs. IF2 (A) and IF4 vs. R1 (D)] and the reference list of 15,410 genes. Enriched GO terms were grouped under "Biological Processes" at level 4. Using the

Benjamini-Hochberg correction for multiple comparisons, p-values with false discovery rate (FDR) < 0.05 were considered statistically significant. Asterisk (*) in bar plots (A, D) indicate the genes use in the enrichment analysis.

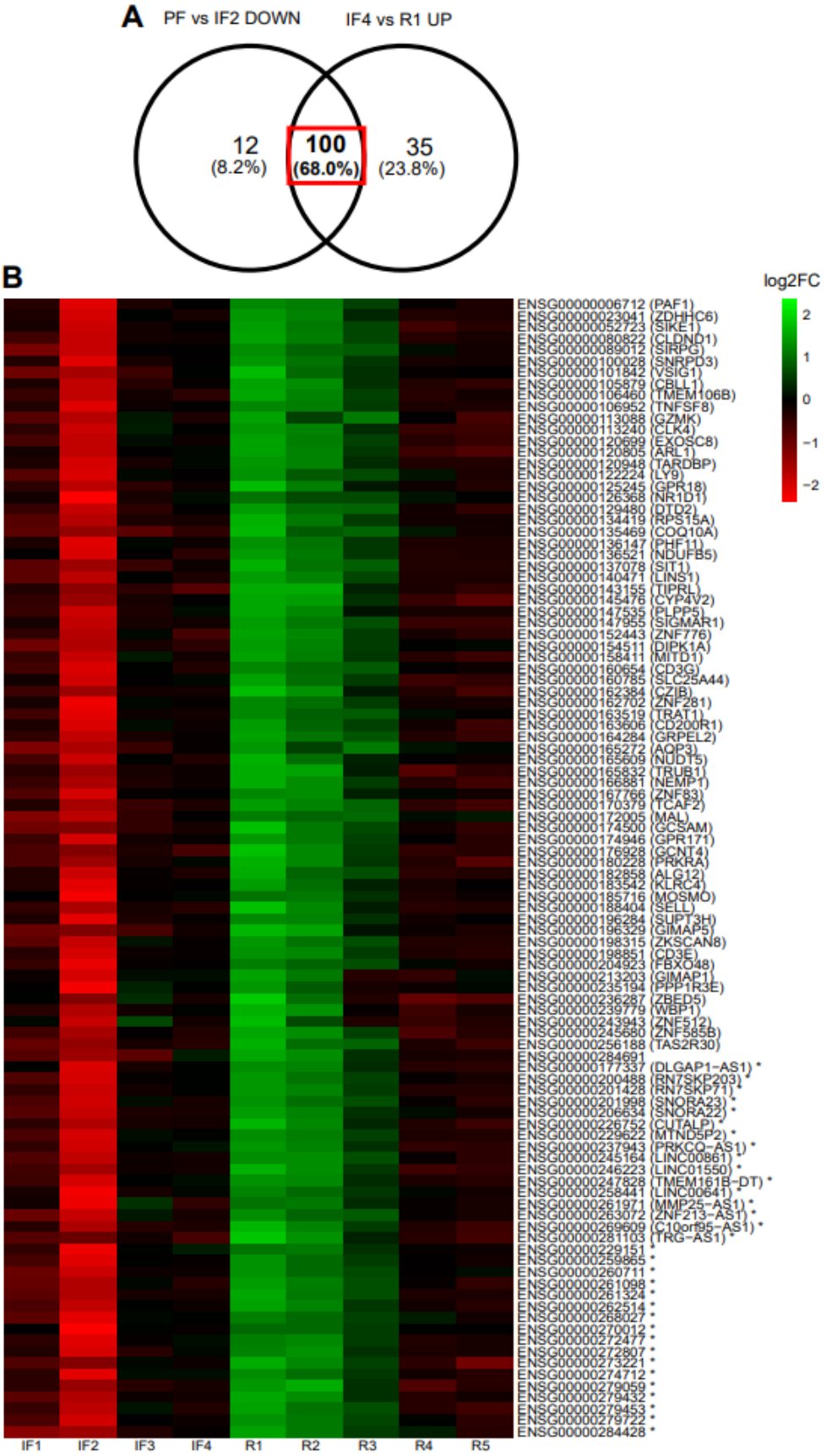
A
PF vs IF2 DOWN
IF4 vs R1 UP
12
(8.2%)
100
(68.0%)
35
(23.8%)
B
log2FC
2
1
0
−1
−2
ENSG00000006712 (PAF1)
ENSG00000023041 (ZDHHC6)
ENSG00000052723 (SIKE1)
ENSG00000080822 (CLDND1)
ENSG00000089012 (SIRPG)
ENSG00000100028 (SNRPD3)
ENSG00000101842 (VSIG1)
ENSG00000105879 (CBLL1)
ENSG00000106460 (TMEM106B)
ENSG00000106952 (TNFSF8)
ENSG00000113088 (GZMK)
ENSG00000113240 (CLK4)
ENSG00000120699 (EXOSC8)
ENSG00000120805 (ARL1)
ENSG00000120948 (TARDBP)
ENSG00000122224 (LY9)
ENSG00000125245 (GPR18)
ENSG00000126368 (NR1D1)
ENSG00000129480 (DTD2)
ENSG00000134419 (RPS15A)
ENSG00000135469 (COQ10A)
ENSG00000136147 (PHF11)
ENSG00000136521 (NDUFB5)
ENSG00000137078 (SIT1)
ENSG00000140471 (LINS1)
ENSG00000143155 (TIPRL)
ENSG00000145476 (CYP4V2)
ENSG00000147535 (PLPP5)
ENSG00000147955 (SIGMAR1)
ENSG00000152443 (ZNF776)
ENSG00000154511 (DIPK1A)
ENSG00000158411 (MITD1)
ENSG00000160654 (CD3G)
ENSG00000160785 (SLC25A44)
ENSG00000162384 (CZIB)
ENSG00000162702 (ZNF281)
ENSG00000163519 (TRAT1)
ENSG00000163606 (CD200R1)
ENSG00000164284 (GRPEL2)
ENSG00000165272 (AQP3)
ENSG00000165609 (NUDT5)
ENSG00000165832 (TRUB1)
ENSG00000166881 (NEMP1)
ENSG00000167766 (ZNF83)
ENSG00000170379 (TCAF2)
ENSG00000172005 (MAL)
ENSG00000174500 (GCSAM)
ENSG00000174946 (GPR171)
ENSG00000176928 (GCNT4)
ENSG00000180228 (PRKRA)
ENSG00000182858 (ALG12)
ENSG00000183542 (KLRC4)
ENSG00000185716 (MOSMO)
ENSG00000188404 (SELL)
ENSG00000196284 (SUPT3H)
ENSG00000196329 (GIMAP5)
ENSG00000198315 (ZKSCAN8)
ENSG00000198851 (CD3E)
ENSG00000204923 (FBXO48)
ENSG00000213203 (GIMAP1)
ENSG00000235194 (PPP1R3E)
ENSG00000236287 (ZBED5)
ENSG00000239779 (WBP1)
ENSG00000243943 (ZNF512)
ENSG00000245680 (ZNF585B)
ENSG00000256188 (TAS2R30)
ENSG00000284691
ENSG00000177337 (DLGAP1-AS1) *
ENSG00000200488 (RN7SKP203) *
ENSG00000201428 (RN7SKP71) *
ENSG00000201998 (SNORA23) *
ENSG00000206634 (SNORA22) *
ENSG00000226752 (CUTALP) *
ENSG00000229622 (MTND5P2) *
ENSG00000237943 (PRKCQ-AS1) *
ENSG00000245164 (LINC00861) *
ENSG00000246223 (LINC01550) *
ENSG00000247828 (TMEM161B-DT) *
ENSG00000258441 (LINC00641) *
ENSG00000261971 (MMP25-AS1) *
ENSG00000263072 (ZNF213-AS1) *
ENSG00000269609 (C10orf95-AS1) *
ENSG00000281103 (TRG-AS1) *
ENSG00000229151 *
ENSG00000259865 *
ENSG00000260711 *
ENSG00000261098 *
ENSG00000261324 *
ENSG00000262514 *
ENSG00000268027 *
ENSG00000270012 *
ENSG00000272477 *
ENSG00000272807 *
ENSG00000273221 *
ENSG00000274712 *
ENSG00000279059 *
ENSG00000279432 *
ENSG00000279453 *
ENSG00000279722 *
ENSG00000284428 *
IF1
IF2
IF3
IF4
R1
R2
R3
R4
R5

Figure 2.4 | Log2 fold change of 100 genes displaying downregulation when reaching space and upregulation when landing on Earth after 6 months in space. Heatmap illustration of the log2 fold changes (Log2FC) of expression relative to pre-flight across all in-flight and post-flight time points for the 100 genes both downregulated when reaching space and upregulated when landing on Earth. The Venn diagram (A) indicates the profile of genes being displayed in the heatmap (B). Expression levels of individual genes relative to pre-flight values are expressed across in-flight and post-flight time points as log2 fold changes displayed as a heatmap (B). The color bar represents values of log2 fold changes ranging from −2 (red) to +2 (green). Gene identities are shown by their ensembl ID and corresponding HGNC symbol (if applicable) in brackets. Asterisk (*) indicates non-coding genes.

Table 2.1 | Sample inventory: libraries that passed quality metrics and used for sequencing.

Astronaut n=14	Time-point									
	PF (n=3)	IF1 (n=6)	IF2 (n=3)	IF3 (n=10)	IF4 (n=8)	R1 (n=8)	R2 (n=9)	R3 (n=8)	R4 (n=8)	R5 (n=8)
a2073		*		*						
a2017				*						
a2029	*	*			*	*	*	*	*	*
a2005		*	*	*		*	*	*	*	*
a2096	*	*		*			*			
a2049			*	*	*	*	*		*	*
a2052				*	*		*	*	*	
a2020					*			*		*
a2068	*[1]		*	*	*	*	*	*		*
a2036		*			*	*	*	*	*	*
a2084				*		*	*		*	
a2091		*		*	*	*	*	*	*	*
a2057				*	*	*		*	*	*
a2031	*									

[1]Sample excluded as an outlier (Supplementary Figure 2.2).

Table 2.2 | Summary of selective time-point differential expression results.

Test[1]	Differentially expressed genes (DEGs)		
	Total	Up-regulated[2]	Down-regulated[3]
PF vs IF2	120	8	112
PF vs R5	0	0	0
IF3 vs IF4	0	0	0
IF4 vs R1	151	135	16

[1]Pairwise time-point significance testing using the Wald's test and ashr log_2fold change (LFC) shrinkage.
[2]LFC > 0.5
[3]LFC < -0.5

Supplemental Digital Content

- Supplemental Table 2.1
- Supplemental Figure 2.1
- Supplemental Figure 2.2
- Supplemental Figure 2.3
- Supplemental Figure 2.4

Discussion

My analysis of leukocyte transcriptomes extracted from twenty healthy participants to 60 days in bed rest and fourteen astronauts to ~6 months in spaceflight revealed dynamic gene expression changes in response to both altered gravity environments. In addition, the bed rest study tested a nutritional intervention for any mitigating effects on bed rest induced deconditioning; this intervention had no effect at the transcriptome level. In contrast, the spaceflight study was observational with no intervention tested and included further analysis of transcriptomes at selective timepoints. The salient findings common to both studies were: (1) temporal analyses of leukocyte transcriptomes identified clusters of genes with inverse patterns of expression changes occurring at phase transitions to and from bed rest or to and from spaceflight; (2) the expression changes were in genes related to immune system processes; and (3) transcriptome levels converged towards average levels with no differential expression during late bed rest (days 30 and 60) and late spaceflight (between ~2-6 months).

Bed rest specific findings

The high inter-individual correlations of normalized read counts between the twenty participants (Supplementary Figure 1.3) indicated high transcriptome homogeneity among this cohort. This attests to the stringent recruitment standards limited to healthy men in a controlled experimental environment minimizing the number of confounding variables, reducing transcriptome variability, and increasing statistical power and precision when measuring differentially expressed genes (66). However, transcriptome homogeneity is inconsistent with immune variability in large populations of healthy adults characterized by differences in leukocyte subpopulations, cytokine profiles, and functional responses indicating immune heterogeneity (67). Interestingly, a study on these same twenty participants showed no significant changes in leukocytes, lymphocytes, and B-cell concentrations during bed rest (40) supporting our findings of immune homogeneity in this small cohort. Consequently, generalizability or

extrapolation of our results to the broader human population is limited. Future experiments are required to validate the transcriptome homogeneity in leukocytes from larger populations of healthy adults. Additionally, correlational analysis at baseline could not be completed with the astronauts in pre-flight due to limited sample availability and sex representation differences. To prevent fluid leaks while in space, NASA protocols dictated that extracted blood samples be frozen for their journey back to Earth prior to RNA extraction. For consistency, pre-flight samples taken on Earth were also frozen. Sample freezing induces cell lysis and RNA degradation (68) resulting in only four samples collected at pre-flight having sufficient quality for sequencing. Freezing and thawing procedures of samples also introduce variability, which was measured in one pre-flight sample through PCA and consequently excluded from further analyses (Supplemental Figure 2.2). Therefore, three pre-flight samples were insufficient to characterize the transcriptome variability for all fourteen astronauts when compared to all twenty participants included in the bed rest baseline analysis.

Specific to the bed rest study was the testing of the nutritional intervention at mitigating the negative effects of bed rest. My analysis found zero differentially expressed genes between control and "cocktail" intervention groups during bed rest indicating the nutritional intervention was unable to diminish the leukocyte transcriptome changes. This is consistent with other studies reporting a lack of effect for various physiological processes including cardiovascular (69), musculoskeletal (70), hematological (71), nervous (72), and immune systems (40) on the same participants. Additionally, another 21 day bed rest study with ten healthy men found a high protein diet was not effective in mitigating the changes in lumbar vertebral fat fraction (VFF) during bed rest (73). For our study, the European Space Agency (ESA) provided funding and chose to test the nutritional intervention because of its anti-inflammatory and anti-oxidant properties. The motivation likely being to find an intervention that reduces the immune inflammation and oxidative stress experienced by astronauts during spaceflight (1). Based on our results, the nutritional intervention was not responsive to the change in the gravity vector

during bed rest. However, benefits from nutritional supplementation take time to manifest given individual differences in metabolism and microbiomes (74,75). Perhaps 60 days of the nutritional supplement was not enough time to observe any measurable improvements or differences in the "cocktail" group. Testing in astronauts during spaceflight may produce quantifiable results given their longer exposure to the space environment with additional oxidative stressors such as exposure to cosmic radiation. Regardless, prior validation of intervention effectiveness and safety using Earth based microgravity analogs such as bed rest is necessary.

Spaceflight specific findings

Leukocyte transcriptome measures in astronauts revealed the main profile of expression changes to be a decrease during the transition into spaceflight, followed by an increase in expression upon return to Earth (Figure 2.2A). Functional enrichment of genes with this increase-then-decrease pattern of expression were mainly immune related (Figure 2.2C) suggesting opposite changes of immune suppression and activation in response to the transitions to and from spaceflight. Immune suppression upon entering spaceflight may be explained in part by the 10-15% blood plasma volume reduction triggered by the fluid shift when astronauts are exposed to microgravity (9,10). Plasma volume reduction increases blood cell concentrations that must be returned to homeostatic levels through decreasing immune cell populations; mainly T cells, NK cells and neutrophils with downstream consequences on immune cell function, surveillance, cytokine secretion, and inflammatory responses (76–78). Acute stress responses induced by short durations of 3-5 g hypergravity exposure during the journey to the ISS may also play a role in immune suppression. The release of cortisol during a stress response modulates various immune processes; mainly inhibiting the production and function of T cells and reducing the release of pro-inflammatory cytokines (79,80). These effects are made worse with prolonged release of cortisol from chronic stress induced by confinement and isolation in space. Rooney et al., 2019 reported

14 out of 23 (61%) astronauts shed at least one or more herpes virus particles during long duration missions aboard the ISS measured in their saliva or urine (81). Documented viruses with latent reactivation include the Epstein-Barr virus (EBV) responsible for infectious mononucleosis, varicella-zoster virus (VZV) responsible for chickenpox and shingles, herpes simplex virus (HSV) responsible for cold sores, and cytomegalovirus (CMV) responsible for various inflammatory diseases (81). Although mostly subclinical, Crucian et al., 2016 reported clinical symptoms related to immune dysregulation in 46% of 46 ISS crew members during spaceflight missions (82); likely prompted by an immune response to the accumulation of viral herpes particles. The reactivation of latent viruses is consistent with our findings of gene expression increases in the same immune related genes suggesting immune activation when returning to Earth. The trigger for immune activation may be elucidated by the opposite fluid shift occurring in astronaut's post-flight. Normal gravity redistributes blood to the lower limbs requiring an increase in plasma volume achieved through increasing fluid intake (83). The increase in plasma volume results in blood cell dilution and subsequent increases in immune cell production and function (84); an opposite reaction to the fluid shift experienced when astronauts enter microgravity.

Additional analysis of specific timepoints found 100 genes that were both down-regulated and up-regulated at spaceflight phase transitions (Figure 2.4). This further supports the increase-then-decrease expression profile and indicates the same genes responded to both spaceflight transition periods despite opposite immune responses. Several of these differentially expressed genes coded for long non-coding (lnc) RNA's, which can regulate gene expression in many ways including: acting as transcriptional activators or repressors, control of DNA methylation, form structural scaffolds to organize chromatin, and regulate RNA processing events such as alternative splicing and mRNA stability (85). Processes influenced by regulatory lncRNA likely explain how the same genes can modulate transcriptome changes that result in different physiological responses. Unfortunately, the detection and quantification of lncRNA's may have been influenced by our library preparation method, which

prioritized the enrichment of messenger (m) RNA's leading to an underrepresentation of non-polyadenylated lncRNA's. Many lncRNA's are also still poorly annotated in the reference genome we used to align sequenced reads (86). Additionally, lncRNA's are inherently expressed at lower levels compared to protein-coding RNA from faster degradation making their detection more challenging (86). More advanced methods are required to obtain a more comprehensive understanding of the lncRNA changes occurring during spaceflight phase transitions as will be discussed in the *future directions* section below.

Bed rest and spaceflight findings

The primary finding common to both bed rest and spaceflight models was the identification of major transcriptome changes occurring at phase transitions to and from bed rest or to and from spaceflight. The timing of transcriptome changes demonstrates leukocytes are respondent to the change in gravity vectors common to both models despite being buoyant cells in the blood. Bone and muscle cells represent cell types typically under constant load from gravity and any removal or change to the gravity vector results in molecular and cellular modifications that manifest at the physiological level; mainly reduced muscle fiber sizes and lower bone density (16,38). Blood cells such as leukocytes experience buoyant forces that counteract gravity and as such do not encounter constant load, yet our results show leukocytes responding at the molecular level to gravity changes; an interesting outcome given the cells environment in blood. As discussed in the previous section, I suggest this is a consequence of the fluid shift that occurs relatively early during the transition to both bed rest and spaceflight. The characteristic profiles of gene clusters displaying inverse or opposite patterns of expression changes at phase transitions is consistent with the opposite physiological responses associated with the fluid shifts during unloading and reloading of the body.

Differences in the number of differentially expressed genes and enriched pathways between both studies can be explained mainly by the discrepancy in RNA quality. As mentioned previously, NASA

restrictions and protocols during spaceflight required astronaut blood samples to be frozen, which caused reduced RNA stability and degradation prior to its extraction resulting in overall lower quality and amount of RNA when compared to the bed rest samples that did not require sample freezing. To compensate, astronaut RNA samples underwent different library preparation steps to improve detection of protein-coding RNA's through mRNA enrichment or ribosomal (r) RNA depletion. However, many libraries did not pass quality metrics for sequencing due to the initially poor RNA quality culminating in just over half (~52%) of the astronaut RNA samples being sequenced. This resulted in unbalanced sample sizes at each timepoint producing various downstream statistical issues; mainly reduced power. This is the reason for the vast differences in independent filtering thresholds, number of identified differentially expressed genes, and p-value cutoffs between both studies. Another source of variability arises from logistical issues aboard the ISS resulting in astronaut samples being taken within a window of days rather than on a specific day. Additionally, both studies consist of different timepoints collected over different durations; 60 days of bed rest and ~6 months of spaceflight. The timing of transcriptome changes differs between both models, specifically at the transition to bed rest on day 2 and spaceflight on days 8-12. However, both studies detected consistent shifts on day 1 of reambulation and return to Earth. Lastly, the bed rest model is not a perfect analog to simulate the microgravity experienced by astronauts given there is still weight-bearing involved. Bed rest does not remove the gravity vector but merely shifts its orientation from the vertical head-to-toe position to the horizontal chest-to-back position (9). Most sampled astronauts also had previous microgravity exposures from prior missions, whereas only one participant had previously engaged in a bed rest experiment.

Functional enrichment analysis of differentially expressed genes in both studies revealed mainly immune related processes, a result not surprising given the transcriptome measures were in leukocytes. The enrichment analysis provides further support for immune system changes in response to changing gravity environments detected at the molecular level. However, comparing specific immune processes

between both studies is difficult given the vast differences in number of identified differentially expressed genes (2,415 and 276 genes for the bed rest and spaceflight studies respectively). In general, larger gene sets result in increased statistical power and likelihood of detecting more enriched biological processes with an overrepresentation analysis (64). This is evident with the bed rest model as it was able to detect more enriched biological processes including other multisystem changes outside of the immune system. The variety of biological processes identified reinforces the idea that leukocytes may reflect diverse transcriptome changes given their circulation and contact with multiple organ systems throughout the body.

The most novel and unexpected finding to both studies was the discovery of transcriptome convergence during both late bed rest and spaceflight. This finding suggests two outcomes: (1) no differential expression between late bed rest (HDT30 vs HDT60) and spaceflight timepoints (IF3 and IF4); and (2) reduced transcriptome variability at these timepoints. No differential expression is evident by the lack of change in z-score levels for both studies, which may be explained by leukocytes successfully adapting to the altered gravity environments and stabilizing their transcriptome to maintain gene expression patterns that support their adjusted physiological state. Z-score scaling transformed the normalized read counts of differentially expressed genes to a standard normal distribution, enabling comparisons and interpretations of gene expression levels relative to the overall distribution of data (87). The general reduction in spread of z-scores indicates that leukocyte transcriptomes were converging towards average levels with reduced variability between genes. Statistically, regression towards the mean may be involved but doesn't explain the greater variability observed for later reambulation and post-flight timepoints. The presence of unidentified general mechanisms specifically limiting transcript levels during late bed rest and spaceflight remains unknown. Transcription factors which tightly regulate and coordinate gene transcription in response to environmental signals are likely strong candidates. Similarly, post-transcriptional modifications regulating RNA degradation may also contribute to the

reduced variability but cannot be determined with RNA-seq data, which measures steady-state levels of transcripts and is unable to differentiate RNA synthesis from degradation (47). Global Run-On (GRO) sequencing represents an alternative method to measure nascent RNA transcription to capture RNA molecules actively being transcribed by RNA polymerase at a given time (88). Incorporating both RNA-seq steady state levels with GRO-seq transcription rates would allow RNA degradation to be inferred, providing a more complete overview of the mechanisms involved limiting RNA transcript level variability. Unfortunately, GRO-seq cannot be performed in the future as it requires the isolation of cell nuclei where transcription occurs, but RNA extraction protocols which homogenized the nuclear RNA prevent the use of this approach.

Implications and applications

Most of the evidence for immune dysfunction in astronauts occurs at the subclinical level (89). Nevertheless, immune-related changes have significant implications for the overall health of astronauts during and after space missions even if symptoms do not manifest. For instance, increased viral shedding of various herpes viruses present in the saliva and urine of astronauts (81) may evolve towards severe symptoms such as swollen lymph nodes, shingles, or flu with limited access to medical care while isolated in space (22). Issues like this may be exacerbated in longer term missions lasting years where the estimated incidence of immune-related symptomatic events is 3.4 events per year (82); a profound issue for long duration missions such as travel to Mars. Even if symptoms do not appear, presence of viral particles means astronauts are infectious to others when returning to Earth. Studying subclinical and molecular changes is therefore crucial to understand and prevent immune dysfunction during space travel. Specifically, identifying gene biomarkers to monitor and mitigate the progression of immune or multisystem deconditioning in response to microgravity would be beneficial for space travelers. A more comprehensive and comparative analysis between both bed rest and spaceflight models is required as

well as validation experiments focused on individual genes rather than GO terms to better understand the molecular response to microgravity isolated from other space stressors. Additionally, the superior quality data collected from bed rest participants represents an excellent argument for their primary use in further analyses, whereas the astronaut spaceflight data should be used for confirmational purposes. The bed rest data has the added advantage of the model being comparable to bedridden and unloaded patients suffering from injury or hospitalization. Leukocyte transcriptome changes during inpatient rehabilitation have been measured in patients with hospital acquired deconditioning (HAD) (90). However, this dataset of deconditioned patients suffers from low quality RNA and variability issues owing to wide between-patient heterogeneity from their unique health conditions, medications, interventions, and demographics. This highlights another case to prioritize the analysis of the higher quality bed rest dataset and subsequently compare to the bedridden patients for validation to identify biomarkers of systemic deconditioning. Lastly, hibernating (torpor) animals share resemblance to the unloaded state of bed rest but do not experience the same deconditioning of physiological systems (91). Bears exit the den with marginal loss in muscle mass and squirrels and bats have protective mechanisms preventing leucopenia (91,92). Coupling available transcriptome studies in both bed rest and hibernating animal models provides a thorough overview of the molecular mechanisms both causing and preventing deconditioning during unloading. This has practical applications for developing strategies to induce torpor states in humans for deep space exploration (91). Moreover, future bed rest studies provide the ideal environment for testing mitigating interventions developed from researching animal torpor.

Limitations

Several limitations from logistical and technical constraints associated with sampling exist for both studies. As previously discussed, NASA standard blood collection protocols preventing fluid leaks onboard the ISS prohibited RNA extraction while in-flight resulting in blood samples being frozen for

their journey back to Earth causing cell lysis and poor RNA quality with downstream issues in the pipeline of data analysis. Blood samples were also collected from fourteen astronauts during twelve different ISS missions. This meant that depending on specific mission objectives and astronaut commitments to other studies, samples could not be obtained on the exact same days for every astronaut and resulted in timepoints ranging within a window of days rather than specific days like the bed rest study. Many of the protocol restrictions imposed on astronaut sampling also limited the applied analyses to bed rest participants. For instance, no access to flow cytometry during spaceflight prevented cell-sorting of leukocytes into individual sub-populations. For consistency between both studies, cell-sorting was not applied for bed rest participants either preventing the identification of transcriptome changes specific to individual cell types.

Limitations were also linked to RNA-sequencing method and the pipeline of data analysis. As already mentioned, RNA-sequencing measures steady-state levels and cannot distinguish between transcriptional and post-transcriptional strategies to regulate RNA levels (47). Individual contributions from RNA transcription and degradation to changing transcript levels could not be determined. Transcriptome measures were also biased to specific RNA types; mainly protein-coding mRNA. For instance, RNA extraction missed the diverse population of small non-coding (snc) RNA's that play crucial roles in the regulation of gene expression (93). As previously discussed, library preparation for both studies employed techniques to prioritize the enrichment of mRNA leading to an underrepresentation of non-coding RNA's. In fact, the bed rest analysis ignored all other RNA biotypes, favoring the evaluation to protein-coding genes only. However, lncRNA's identified as differentially expressed in astronauts were the second most represented in the dataset. Inherent to RNA-seq data are the statistical power issues that arise during differential expression analysis owing to the high variability among low read count genes (60). Z-score scaling of normalized read counts also presents its own limitations; mainly its robustness to normality and sensitivity to outliers. Differential expression analysis with the *DESeq2* tool

assumed a negative binomial distribution of normalized read counts (58), whereas z-score scaling assumes a normal distribution (87). However, Central Limit Theorem (CLT) implies approximate normality given that the scaling calculations were done with hundreds to thousands of genes (87). Z-score scaling is also influenced by extreme values or outliers leading to significant distortions of z-scores for the remaining data (87). This was the case for one of the pre-flight astronaut samples, which contained extremely high read counts outliers for certain genes identified through PCA but was excluded from further analyses preventing any distortions in the data. Lastly, enrichment analysis with GO terms has several limitations including terms being species neutral applying to both prokaryotic and eukaryotic organisms, bias to protein-coding genes given that non-coding genes are not well annotated in the GO database, and hierarchical parent-child relationships among terms creating levels that were chosen arbitrarily and effect enrichment results (62).

Future directions

As emphasized previously, future analyses will focus on individual genes displaying characteristic expression changes to identify gene biomarkers responding to altered gravity environments. More specifically, future analyses will involve utilizing the high-quality bed rest data to complete differential expression analyses at selective timepoints, consistent with the strategy employed to analyze differential expression at specific timepoints in astronauts. This approach will subgroup the bed rest study timepoints to determine transcriptome changes in specific genes at each study phase including unloading during bed rest, reloading during reambulation, and determine the recovery back to baseline levels. Utilizing unsupervised machine learning (ML) methods that do not rely on predefined sample labels or classes would enhance differential expression analysis through improving the predictive accuracy of results (94). ML algorithms are more flexible with assumptions, can handle diverse variables with complex relationships, and are robust to noisy or incomplete data compared to traditional linear

modelling strategies used in the current studies (87). Applying ML based analyses has the potential to improve the shortcoming of low read count variability inherent to RNA-seq data and identify differentially expressed genes normally missed by conventional methods (94). To verify the gene expression changes are manifesting at the protein level, Enzyme-Linked Immunosorbent Assays (ELISA) could be employed to measure the protein concentration changes and facilitate the development of gene biomarkers. Unfortunately, these validation experiments would be limited to secreted proteins outside of cells because only the flow-through of blood plasma were frozen and saved following leukocyte extraction. Blood plasma also contains secreted extracellular vesicles (sEVs), which contain a reservoir of small and long non-coding RNAs (27). Extracting the sEVs from frozen plasma samples and employing specialized sequencing techniques more sensitive to short RNA sequences such as small RNA-seq could prove valuable to further characterize transcriptomes (95). Measuring expression changes in both small and long non-coding RNAs would provide a more thorough overview of the transcriptome modulations occurring during bed rest and spaceflight. Another future prospect made possible through the increased resolution of paired-end sequencing is the analysis of alternative splicing variants. Re-mapping of sequenced raw reads at the transcript and exon-level would provide deeper insights into alternative splicing patterns and expression changes of different isoforms in response to altered gravity (96). However, this would only be possible with the bed rest data given that adequate sequencing depth is required to improve sensitivity for accurate re-mapping.

Conclusion

The altered gravity environments consistent with both bed rest and spaceflight models significantly modulated the leukocyte transcriptome composition in humans confined to 60 days of bed rest and to ~6 months in spaceflight. The transcriptome changes reflected multisystem shifts including dynamic expression alterations in immune related genes responding to the transition to and from bed rest and spaceflight environments. Conversely, an unexpected trend towards stable RNA levels with no differential expression was measured during later timepoints in bed rest and spaceflight. The nutritional intervention tested in the bed rest study had no mitigating effect on transcriptome changes and the high transcriptome homogeneity among bed rest participants at baseline emphasizes the datasets superior quality and power to characterize transcriptome changes. The spaceflight study revealed opposite gene expression patterns of down and up-regulation in response to the transition to and from spaceflight suggesting immune suppression during spaceflight and activation upon return to Earth. My analyses emphasize the importance of utilizing temporal investigations that take advantage of multiple timepoints to reveal a comprehensive overview of gene expression trajectories during bed rest and spaceflight. Measuring the leukocyte transcriptome provided further insight into the immune dysfunction and multisystem deconditioning experienced by astronauts during space travel. Additional analyses and validation experiments using the bed rest dataset are required to develop gene biomarkers indicative of immune dysfunction and isolate the effect of microgravity from other space stressors.

References

1. Afshinnekoo E, Scott RT, MacKay MJ, Pariset E, Cekanaviciute E, Barker R, et al. Fundamental Biological Features of Spaceflight: Advancing the Field to Enable Deep-Space Exploration. Vol. 183, Cell. Cell Press; 2020. p. 1162–84.
2. Demontis GC, Germani MM, Caiani EG, Barravecchia I, Passino C, Angeloni D. Human pathophysiological adaptations to the space environment. Vol. 8, Frontiers in Physiology. Frontiers Media S.A.; 2017.
3. Norsk P, Asmar A, Damgaard M, Christensen NJ. Fluid shifts, vasodilatation and ambulatory blood pressure reduction during long duration spaceflight. Journal of Physiology. 2015 Feb 1;593(3):573–84.
4. Thornton WE, Moore TP, Pool SL. Fluid shifts in weightlessness. Aviat Space Environ Med [Internet]. 1987.
5. Watenpaugh DE, Hargens AR. The Cardiovascular System in Microgravity. In: Comprehensive Physiology. Wiley; 1996. p. 631–74.
6. Katkov VE, Chestukhin V V. Blood pressure and oxygenation in different cardiovascular compartments of a normal man during postural exposures. Aviat Space Environ Med. 1980 Nov;51(11):1234–42.
7. Mader T, Gibson C, Miller N, Subramanian P, Patel N, Lee A. An overview of spaceflight-associated neuro-ocular syndrome (SANS). Vol. 67, Neurology India. 2019.
8. Wostyn P, De Deyn PP. The ‘“ocular glymphatic system”’: An important missing piece in the puzzle of optic disc edema in astronauts? Vol. 59, Investigative Ophthalmology and Visual Science. Association for Research in Vision and Ophthalmology Inc.; 2018. p. 2090–1.

9. Hargens AR, Vico L. HIGHLIGHTED TOPIC Analogs of Microgravity: Space Research without Leaving the Planet Long-duration bed rest as an analog to microgravity. J Appl Physiol [Internet]. 2016;120:891–903.

10. Convfrtino VA. Clinical aspects of the control of plasma volume at miorogravity and during return to one gravity.

11. Trudel G, Shafer J, Laneuville O, Ramsay T. Characterizing the effect of exposure to microgravity on anemia: more space is worse. Am J Hematol. 2020 Mar 1;95(3):267–73.

12. Trudel G, Shahin N, Ramsay T, Laneuville O, Louati H. Hemolysis contributes to anemia during long-duration space flight. Nat Med. 2022 Jan 1;28(1):59–62.

13. Vico L, Hargens A. Skeletal changes during and after spaceflight. Vol. 14, Nature Reviews Rheumatology. Nature Publishing Group; 2018. p. 229–45.

14. Fitts RH, Riley DR, Widrick JJ. highlighted topics Physiology of a Microgravity Environment Invited Review: Microgravity and skeletal muscle [Internet]. 2000.

15. McNamara KP, Greene KA, Moore AM, Lenchik L, Weaver AA. Lumbopelvic muscle changes following long-duration spaceflight. Front Physiol. 2019;10(MAY).

16. Stavnichuk M, Mikolajewicz N, Corlett T, Morris M, Komarova S V. A systematic review and meta-analysis of bone loss in space travelers. NPJ Microgravity. 2020 Dec 1;6(1).

17. Sibonga JD, Evans HJ, Sung HG, Spector ER, Lang TF, Oganov VS, et al. Recovery of spaceflight-induced bone loss: Bone mineral density after long-duration missions as fitted with an exponential function. Bone. 2007 Dec;41(6):973–8.

18. Smith SM, Zwart SR, Block G, Rice BL, Davis-Street JE. Human Nutrition and Metabolism The Nutritional Status of Astronauts Is Altered after Long-Term Space Flight Aboard the International Space Station 1 [Internet]. 2005.

19. Sibonga JD, Spector ER, Johnston SL, Tarver WJ, Reeves JM. Evaluating bone loss in ISS astronauts. Aerosp Med Hum Perform. 2015 Dec 1;86:A38–44.

20. Garrett-Bakelman FE, Darshi M, Green SJ, Gur RC, Lin L, Macias BR, et al. The NASA twins study: A multidimensional analysis of a year-long human spaceflight. Science (1979). 2019;364(6436).

21. Gertz ML, Chin CR, Tomoiaga D, MacKay M, Chang C, Butler D, et al. Multi-omic, Single-Cell, and Biochemical Profiles of Astronauts Guide Pharmacological Strategies for Returning to Gravity. Cell Rep. 2020 Dec 8;33(10).

22. Crucian B, Johnston S, Mehta S, Stowe R, Uchakin P, Quiriarte H, et al. Clinical Communications A case of persistent skin rash and rhinitis with immune system dysregulation onboard the International Space Station [Internet]. 2016.

23. Ponomarev SA, Berendeeva TA, Kalinin SA, Muranova A V. The State of the System of Signaling Pattern Recognition Receptors of Monocytes and Granulocytes in the Cosmonauts' Peripheral Blood before and after Long-Term Flights on Board the International Space Station. Hum Physiol. 2017 Dec 1;43(7):808–12.

24. Mehta SK, Laudenslager ML, Stowe RP, Crucian BE, Feiveson AH, Sams CF, et al. Latent virus reactivation in astronauts on the international space station. NPJ Microgravity. 2017 Dec 1;3(1).

25. Crucian BE, Zwart SR, Mehta S, Uchakin P, Quiriarte HD, Pierson D, et al. Plasma cytokine concentrations indicate that in vivo hormonal regulation of immunity is altered during long-duration spaceflight. Journal of Interferon and Cytokine Research. 2014 Oct 1;34(10):778–86.

26. Barrila J, Ott CM, Leblanc C, Mehta SK, Crabbé A, Stafford P, et al. Spaceflight modulates gene expression in the whole blood of astronauts. NPJ Microgravity. 2016 Jan 7;2.

27. Bisserier M, Saffran N, Brojakowska A, Sebastian A, Evans AC, Coleman MA, et al. Emerging Role of Exosomal Long Non-coding RNAs in Spaceflight-Associated Risks in Astronauts. Front Genet. 2022 Jan 17;12.

28. Lee RG, Worthy ES, Willis EM, Brown GL, Cipriani F, Barker DC. Development of a comprehensive physics-based model for study of NASA gateway lunar dust contamination. Acta Astronaut. 2023 Sep 1.

29. Mallapaty S. Mars mission is China's "first step" in planetary exploration. Nature. 2021 Dec 24.

30. Stratis D, Trudel G, Rocheleau L, Pelchat M, Laneuville O. The transcriptome response of astronaut leukocytes to long missions aboard the International Space Station reveals immune modulation. Front Immunol [Internet]. 2023 Jun 22;14.

31. Sundblad P, Orlov O, Angerer O, Larina I, Cromwell R. Standardization of bed rest studies in the spaceflight context. Vol. 121, Journal of Applied Physiology. American Physiological Society; 2016. p. 348–9.

32. Pandiarajan M, Hargens AR. Ground-Based Analogs for Human Spaceflight. Vol. 11, Frontiers in Physiology. Frontiers Media S.A.; 2020.

33. Trudel G, Payne M, Mädler B, Ramachandran N, Lecompte M, Wade C, et al. Bone marrow fat accumulation after 60 days of bed rest persisted 1 year after activities were resumed along with hemopoietic stimulation: the Women International Space Simulation for Exploration study. J Appl Physiol [Internet]. 2009;107:540–8.

34. Lawley JS, Babu G, J E Janssen SL, Petersen LG, Hearon CM, Dias KA, et al. Daily generation of a footward fluid shift attenuates ocular changes associated with head-down tilt bed rest. J Appl Physiol [Internet]. 2020;129:1220–31.

35. Taibbi G, Cromwell RL, Zanello SB, Yarbough PO, Ploutz-Snyder RJ, Godley BF, et al. Ocular outcomes comparison between 14- and 70-day head-down-tilt bed rest. Invest Ophthalmol Vis Sci. 2016 Feb 1;57(2):495–501.

36. Trudel G, Uhthoff HK, Laneuville O. Hemolysis during and after 21 days of head-down-tilt bed rest. Physiol Rep. 2017 Dec 1;5(24).

37. Pavy-Le Traon A, Heer M, Narici M V., Rittweger J, Vernikos J. From space to Earth: Advances in human physiology from 20 years of bed rest studies (1986-2006). Vol. 101, European Journal of Applied Physiology. 2007. p. 143–94.

38. Mulder ER, Horstman AMH, Stegeman DF, dde Haan A, Belavy D, Miokovic T, et al. Influence of vibration resistance training on knee extensor and plantar flexor size, strength, and contractile speed characteristics after 60 days of bed rest. J Appl Physiol. 2009;107(6):1789–98.

39. Marusic U, Narici M, Simunic B, Pisot R, Ritzmann R. Nonuniform loss of muscle strength and atrophy during bed rest: A systematic review. J Appl Physiol. 2021 Jul 1;131(1):194–206.

40. Bonnefoy J, Baselet B, Moser D, Ghislin S, Miranda S, Riant E, et al. B-Cell Homeostasis Is Maintained During Two Months of Head-Down Tilt Bed Rest With or Without Antioxidant Supplementation. Front Immunol. 2022 Feb 16;13.

41. Crucian BE, Stowe RP, Mehta SK, Yetman DL, Leal MJ, Quiriarte HD, et al. Immune status, latent viral reactivation, and stress during long-duration head-down bed rest. Aviat Space Environ Med. 2009 May;80(5 Suppl):A37-44.

42. Hoff P, Belavý DL, Huscher D, Lang A, Hahne M, Kuhlmey AK, et al. Effects of 60-day bed rest with and without exercise on cellular and humoral immunological parameters. Cell Mol Immunol. 2015 Jul 7;12(4):483–92.

43. Chouke`r A, Chouke`r C, Thiel M, Baranov V, Meshkov D, Kotov A, et al. Downloaded from journals.physiology.org/journal/jappl [Internet]. Vol. 90, J Appl Physiol. 2001.

44. Schmitt A, Jouault H, Guichard J, Wendling F, Drouin A, Cramer EM. Pathologic interaction between megakaryocytes and polymorphonuclear leukocytes in myelofibrosis [Internet]. 2000.

45. Stratis D, Trudel G, Rocheleau L, Pelchat M, Laneuville O. The Characteristic Response of the Human Leukocyte Transcriptome to 60 Days of Bed Rest and to Reambulation. Med Sci Sports Exerc. 2023 Mar 1;55(3):365–75.

46. Rodrigues DF, Costa VM, Silvestre R, Bastos ML, Carvalho F. Methods for the analysis of transcriptome dynamics. Vol. 8, Toxicology Research. Royal Society of Chemistry; 2019. p. 597–612.

47. Rabani M, Levin JZ, Fan L, Adiconis X, Raychowdhury R, Garber M, et al. Metabolic labeling of RNA uncovers principles of RNA production and degradation dynamics in mammalian cells. Nat Biotechnol. 2011 May;29(5):436–42.

48. Rädle B, Rutkoswki A, Ruzsics Z, Friedel CC, Koszinowski UH, Dölken L. Metabolic labeling of newly transcribed RNA for high resolution gene expression profiling of RNA synthesis, processing and decay in cell culture. Journal of Visualized Experiments. 2013 Aug 8;(78).

49. Li YY, Zhang S, Wang H, Zhang SX, Xu T, Chen SW, et al. Identification of crucial genes and pathways associated with atherosclerotic plaque in diabetic patients. Pharmgenomics Pers Med. 2021;14:211–20.

50. Lowe R, Shirley N, Bleackley M, Dolan S, Shafee T. Transcriptomics technologies. PLoS Comput Biol. 2017 May 1;13(5).

51. Mortazavi A, Williams BA, McCue K, Schaeffer L, Wold B. Mapping and quantifying mammalian transcriptomes by RNA-Seq. Nat Methods. 2008 Jul;5(7):621–8.

52. Nakazato T, Ohta T, Bono H. Experimental Design-Based Functional Mining and Characterization of High-Throughput Sequencing Data in the Sequence Read Archive. PLoS One. 2013 Oct 22;8(10).

53. Zhong Wang, Mark Gerstein, Michael Snyder. RNA-Seq: a revolutionary tool for transcriptomics. Nat Rev Genet. 2009;10.

54. Sun Y, Xiao H. Identification of alternative splicing events by RNA sequencing in early growth tomato fruits. BMC Genomics. 2015 Nov 16;16(1).

55. Evans C, Hardin J, Stoebel DM. Selecting between-sample RNA-Seq normalization methods from the perspective of their assumptions. Brief Bioinform. 2018 Sep 28;19(5):776–92.

56. Dillies MA, Rau A, Aubert J, Hennequet-Antier C, Jeanmougin M, Servant N, et al. A comprehensive evaluation of normalization methods for Illumina high-throughput RNA sequencing data analysis. Brief Bioinform. 2013 Nov;14(6):671–83.

57. Robinson MD, Oshlack A. A scaling normalization method for differential expression analysis of RNA-seq data [Internet]. 2010.

58. Love MI, Huber W, Anders S. Moderated estimation of fold change and dispersion for RNA-seq data with DESeq2. Genome Biol. 2014 Dec 5;15(12).

59. Anders S, Huber W. Differential expression analysis for sequence count data. Genome Biol. 2010 Oct 27;11(10).

60. Seyednasrollah F, Laiho A, Elo LL. Comparison of software packages for detecting differential expression in RNA-seq studies. Brief Bioinform. 2013 Oct 5;16(1):59–70.

61. Bullard JH, Purdom E, Hansen KD, Dudoit S. Evaluation of statistical methods for normalization and differential expression in mRNA-Seq experiments. BMC Bioinformatics. 2010 Feb 18;11:94.

62. Ashburner M, Ball CA, Blake JA, Botstein D, Butler H, Cherry JM, et al. Gene ontology: tool for the unification of biology. The Gene Ontology Consortium. Nat Genet. 2000 May;25(1):25–9.

63. Aleksander SA, Balhoff J, Carbon S, Cherry JM, Drabkin HJ, Ebert D, et al. The Gene Ontology knowledgebase in 2023. Baryshnikova A, editor. Genetics [Internet]. 2023 May 4;224(1).

64. Alexa A, Rahnenführer J, Lengauer T. Improved scoring of functional groups from gene expression data by decorrelating GO graph structure. Bioinformatics. 2006 Jul 1;22(13):1600–7.

65. Subramanian A, Tamayo P, Mootha VK, Mukherjee S, Ebert BL, Gillette MA, et al. Gene set enrichment analysis: A knowledge-based approach for interpreting genome-wide expression profiles [Internet]. 2005.

66. Wu H, Wang C, Wu Z. PROPER: Comprehensive power evaluation for differential expression using RNA-seq. Bioinformatics. 2015 Jan 15;31(2):233–41.

67. Kaczorowski KJ, Shekhar K, Nkulikiyimfura D, Dekker CL, Maecker H, Davis MM, et al. Continuous immunotypes describe human immune variation and predict diverse responses. Source. 2017;114(30):6097–106.

68. Zou C, Ji C, Zhu Y, Liu N, Zhang S, Peng H, et al. Effects of Freezing and Rewarming Methods on RNA Quality of Blood Samples. Biopreserv Biobank. 2022 Apr 1.

69. Solbiati S, Landreani F, Turcato M, Martin-Yebra A, Costantini L, Vaida P, et al. Analysis of changes in cardiac circadian rhythms of RR and QT induced by a 60-day head-down bed rest with and without nutritional countermeasure. Eur J Appl Physiol. 2020 Jul;120(7):1699–710.

70. Arc-Chagnaud C, Py G, Fovet T, Roumanille R, Demangel R, Pagano AF, et al. Evaluation of an Antioxidant and Anti-inflammatory Cocktail Against Human Hypoactivity-Induced Skeletal Muscle Deconditioning. Front Physiol. 2020;11:71.

71. Culliton K, Louati H, Laneuville O, Ramsay T, Trudel G. Six degrees head-down tilt bed rest caused low-grade hemolysis: a prospective randomized clinical trial. NPJ Microgravity. 2021 Dec 1;7(1).

72. Brauns K, Friedl-Werner A, Gunga HC, Stahn AC. Effects of two months of bed rest and antioxidant supplementation on attentional processing. Cortex. 2021 Aug;141:81–93.

73. Trudel G, Melkus G, Sheikh A, Ramsay T, Laneuville O. Marrow adipose tissue gradient is preserved through high protein diet and bed rest. A randomized crossover study. Bone Rep. 2019 Dec 1;11.

74. Ball D, Athanasiadou S. Understanding the interplay between the gut microbiome, nutrition and health. In: Proceedings of the Nutrition Society. Cambridge University Press; 2021. p. 383–5.

75. Rosenbaum M, Leibel RL. Adaptive thermogenesis in humans. Int J Obes (Lond). 2010 Oct;34 Suppl 1(0 1):S47-55.

76. Bigley AB, Agha NH, Baker FL, Spielmann G, Kunz HE, Mylabathula PL, et al. NK cell function is impaired during long-duration spaceflight. J Appl Physiol [Internet]. 2019;126:842–53.

77. Paul AM, Mhatre SD, Cekanaviciute E, Schreurs AS, Tahimic CGT, Globus RK, et al. Neutrophil-to-Lymphocyte Ratio: A Biomarker to Monitor the Immune Status of Astronauts. Front Immunol. 2020 Nov 2;11.

78. Crucian B, Stowe R, Mehta S, Uchakin P, Quiriarte H, Pierson D, et al. Immune system dysregulation occurs during short duration spaceflight on board the space shuttle. J Clin Immunol. 2013 Feb;33(2):456–65.

79. Miller AH. NEUROENDOCRINE AND IMMUNE SYSTEM INTERACTIONS IN STRESS AND DEPRESSION. 1998.

80. Dhabhar FS. Enhancing versus suppressive effects of stress on immune function: Implications for immunoprotection versus immunopathology. Vol. 4, Allergy, Asthma and Clinical Immunology. 2008. p. 2–11.

81. Rooney B V., Crucian BE, Pierson DL, Laudenslager ML, Mehta SK. Herpes virus reactivation in astronauts during spaceflight and its application on earth. Vol. 10, Frontiers in Microbiology. Frontiers Media S.A.; 2019.

82. Crucian B, Babiak-Vazquez A, Johnston S, Pierson DL, Ott CM, Sams C. Incidence of clinical symptoms during long-duration orbital spaceflight. Int J Gen Med. 2016 Nov 3;9:383–91.

83. Hargens AR, Richardson S. Cardiovascular adaptations, fluid shifts, and countermeasures related to space flight. Respir Physiol Neurobiol. 2009;169:S30–3.

84. Kaur I, Simons ER, Castro VA, Mark Ott C, Pierson DL. Changes in neutrophil functions in astronauts. Brain Behav Immun. 2004 Sep;18(5):443–50.

85. West KA, Lagos D. Long non-coding RNA function in CD4+ T cells: What we know and what next? Vol. 5, Non-coding RNA. MDPI AG; 2019.

86. Cabili MN, Trapnell C, Goff L, Koziol M, Tazon-Vega B, Regev A, et al. Integrative annotation of human large intergenic noncoding RNAs reveals global properties and specific subclasses. Genes Dev. 2011 Sep 15;25(18):1915–27.

87. Hastie T, Tibshirani R, Friedman J. The Elements of Statistical Learning. New York, NY: Springer New York; 2009.

88. Danko CG, Hyland SL, Core LJ, Martins AL, Waters CT, Lee HW, et al. Identification of active transcriptional regulatory elements from GRO-seq data. Nat Methods. 2015 Apr 29;12(5):433–8.

89. Crucian BE, Choukèr A, Simpson RJ, Mehta S, Marshall G, Smith SM, et al. Immune system dysregulation during spaceflight: Potential countermeasures for deep space exploration missions. Vol. 9, Frontiers in Immunology. Frontiers Media S.A.; 2018.

90. Laneuville O, Rocheleau L, Chan Chun Kong D, Pelchat M, Trudel G. Effect of rehabilitation on biologic and transcriptomic responses after hospital-acquired deconditioning: a prospective longitudinal feasibility study. Disabil Rehabil. 2022;44(14):3623–31.

91. Choukér A, Ngo-Anh TJ, Biesbroek R, Heldmaier G, Heppener M, Bereiter-Hahn J. European space agency's hibernation (torpor) strategy for deep space missions: Linking biology to engineering. Vol. 131, Neuroscience and Biobehavioral Reviews. Elsevier Ltd; 2021. p. 618–26.

92. Bouma HR, Henning RH, Kroese FGM, Carey H V. Hibernation is associated with depression of T-cell independent humoral immune responses in the 13-lined ground squirrel. Dev Comp Immunol. 2013 Mar;39(3):154–60.

93. Martens-Uzunova ES, Olvedy M, Jenster G. Beyond microRNA--novel RNAs derived from small non-coding RNA and their implication in cancer. Cancer Lett. 2013 Nov 1;340(2):201–11.

94. Wang L, Xi Y, Sung S, Qiao H. RNA-seq assistant: Machine learning based methods to identify more transcriptional regulated genes. BMC Genomics. 2018 Jul 20;19(1).

95. Zhao F, Cheng L, Shao Q, Chen Z, Lv X, Li J, et al. Characterization of serum small extracellular vesicles and their small RNA contents across humans, rats, and mice. Sci Rep. 2020 Dec 1;10(1).

96. Trapnell C, Pachter L, Salzberg SL. TopHat: Discovering splice junctions with RNA-Seq. Bioinformatics. 2009;25(9):1105–11.

Appendix I

Supplementary Material for Published Articles

Chapter 1: Medicine & Science in Sports & Exercise

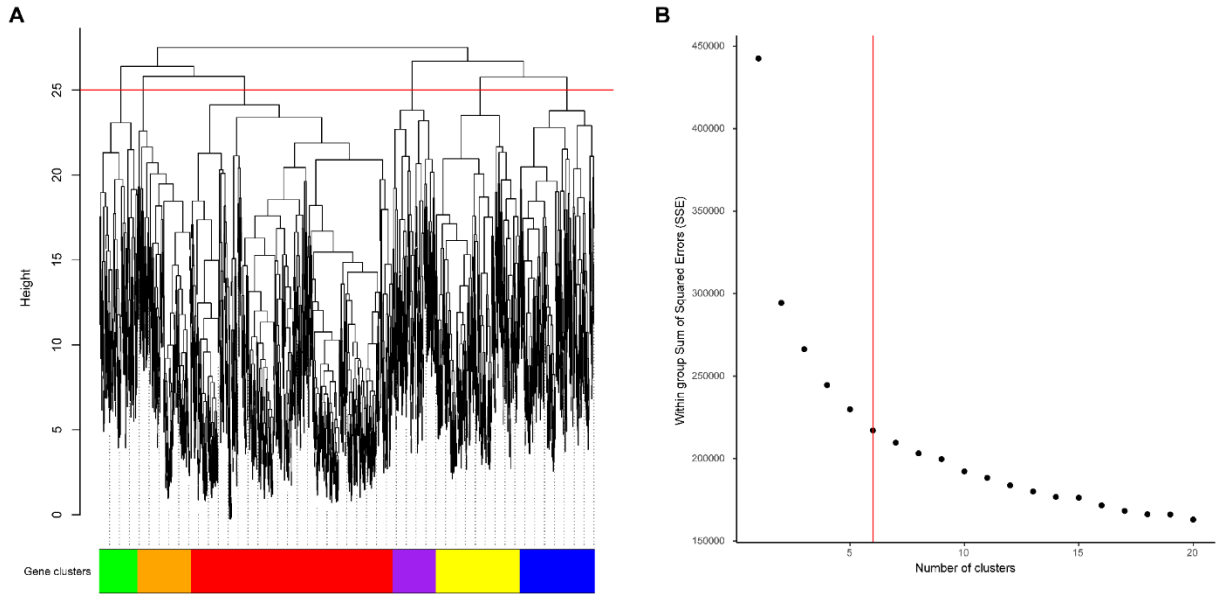

Supplemental Figure 1.1 | Gene cluster analysis. (A) Dendrogram representing the hierarchical clustering results of the 2,415 protein-coding differentially expressed genes across any time-point of the study identified from Model 1. The Euclidean distance was calculated between each gene candidate using their normalized read counts, which were then hierarchically clustered into the resulting tree dendrogram revealing 6 gene clusters characterized similar patterns of expression changes throughout the bed rest study. The horizontal red line represents where the static tree cut was made to separate and define the 6 clusters of differentially expressed genes across time. Each cluster is represented in the colored bar and identified by colors corresponding to cluster number (Figure 1.2A). (B) Elbow plot displaying the within group sum of squared error (SSE) of the normalized read counts for the 2,415 protein-coding gene candidates as a function of the number of gene clusters. The “elbow” of the curve determines the optimal number of gene clusters and increasing the number of clusters no longer

substantially decreases the SSE. The vertical red line represents the “elbow” of the plot, which further supports the identification of 6 gene clusters across time.

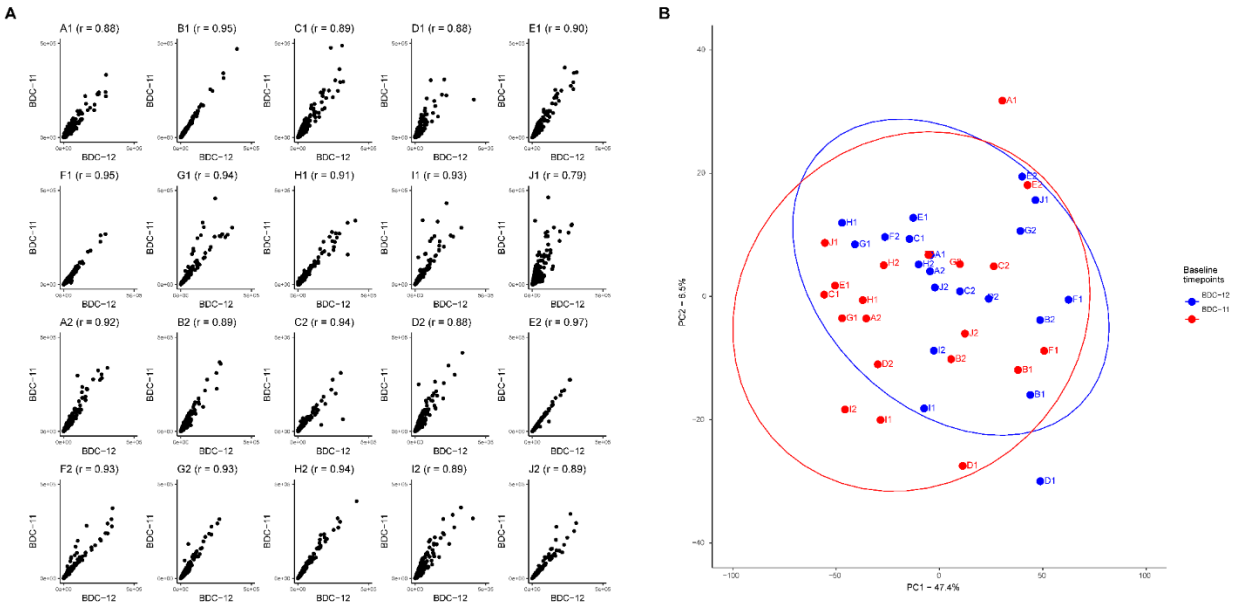

Supplemental Figure 1.2 | Baseline intra-individual variability of transcriptomes. (A) Correlation plots visualizing the Kendall correlation coefficients of normalized read counts from the 14,624 protein-coding gene list obtained through independent filtering using DESeq2. Each plot represents the two baseline time-points; BDC-12 and BDC-11, for the 20 individual participants. The Kendall rank correlation coefficient (r) for each individual participant is displayed above each plot. (B) Principal component analysis of the variance stabilizing transformation of normalized read counts from the 14,624 protein-coding gene list and the 95% confidence ellipses. Each point represents a participant at the two baseline time-points; BDC-12 in blue and BDC-11 in red.

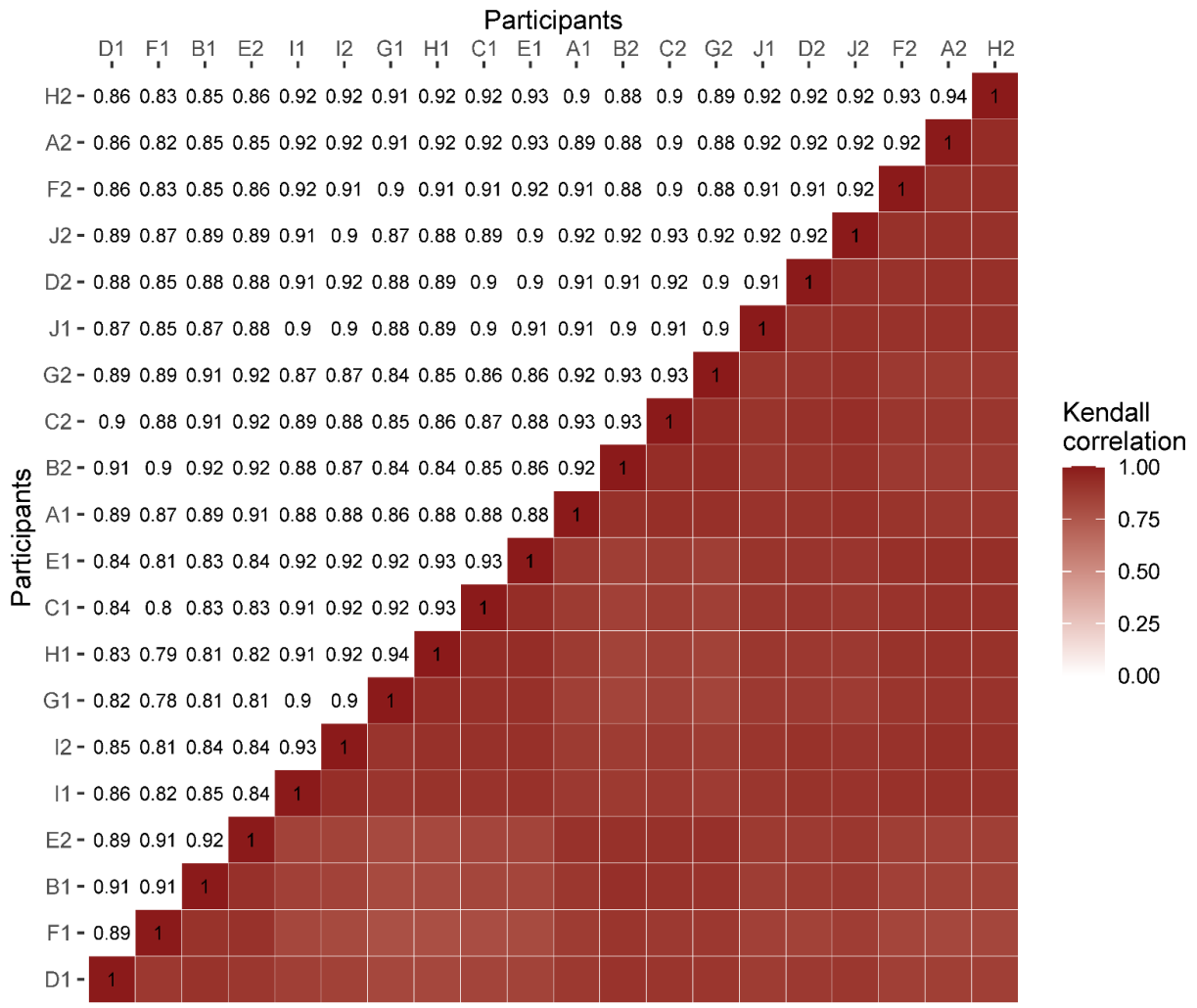

Supplemental Figure 1.3 | Baseline inter-individual variability of transcriptomes. For each participant, the average normalized read counts across both baseline time-points (BDC-12 and BDC-11) for the 14,624 protein-coding gene list obtained through independent filtering using *DESeq2* was used to compare the transcriptomes of the 20 participants. Results of all pairwise comparisons are reported as Kendall correlation coefficients displayed as a symmetrical correlation heatmap including both numbers and colored squares. The color bar represents values of Kendall correlation coefficients.

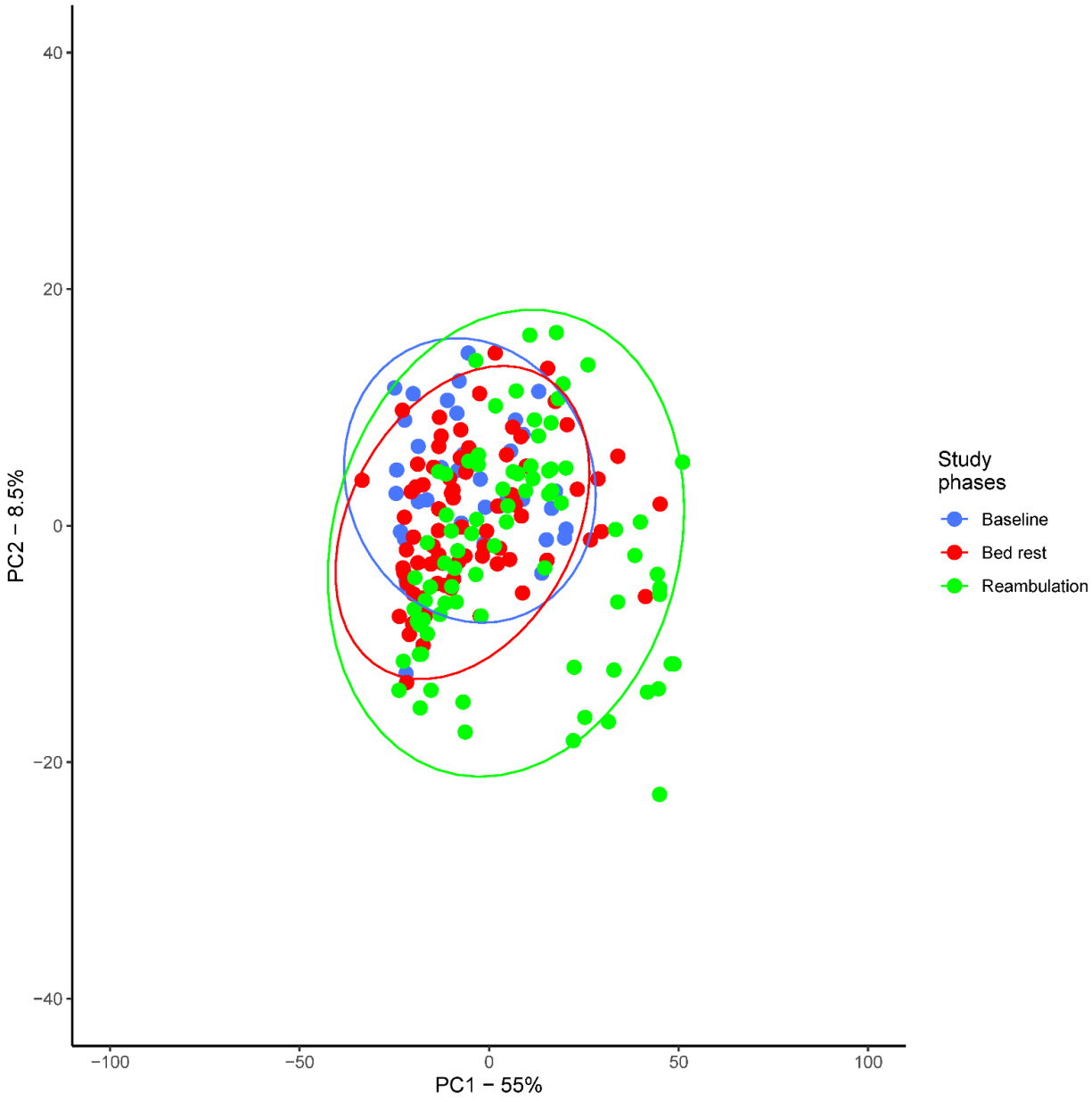

Supplemental Figure 1.4 | Principal component analysis of the differentially expressed genes across study phases. Principal component analysis of the variance stabilizing transformation from normalized read counts from the 2,415 protein-coding gene candidates identified from Model 1: read counts ~ replicate + group + time point + ε. Each point corresponds to a sample and colored based on the study phase; baseline (blue), bedrest HDT (red), and reambulation (green). The 95% confidence ellipses for each phase are indicated.

Supplemental Table 2.1 | Scaled expression summary statistics of 15,410 expressed genes.

Time-point	Mean scaled expression (z-score)						
	Min	**Max**	**Max-Min**	**25% quartile**	**Median**	**75% quartile**	**IQR**[1]
PF	-1.51	2.07	3.58	-0.35	-0.11	0.14	0.49
IF1	-1.13	1.46	2.59	-0.40	-0.20	0.24	0.64
IF2	-1.85	2.63	4.48	-1.01	-0.61	0.90	1.91
IF3	-0.90	0.91	1.81	-0.20	-0.05	0.09	0.29
IF4	-1.21	1.20	2.41	-0.23	-0.08	0.09	0.32
R1	-1.19	1.40	2.59	-0.51	0.20	0.63	1.14
R2	-1.02	1.05	2.07	-0.27	0.12	0.39	0.66
R3	-0.78	1.47	2.25	-0.15	0.17	0.36	0.51
R4	-0.84	1.06	1.90	-0.25	-0.05	0.19	0.44
R5	-0.86	1.27	2.13	-0.25	-0.05	0.17	0.42

[1]Inter-quartile range.

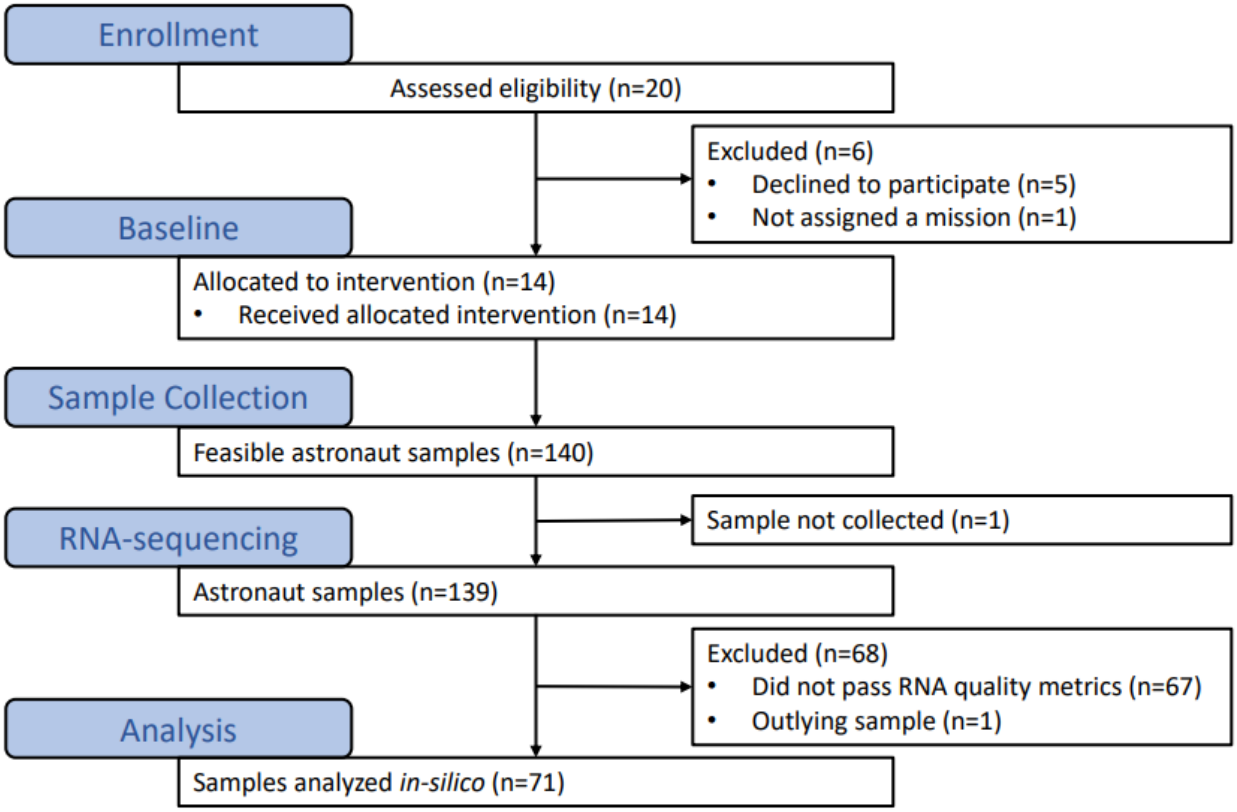

Supplemental Figure 2.1 | Astronaut sample inventory. Twenty astronauts listened to an informed consent briefing session approximately one year before an astronaut's scheduled flight. Fourteen astronauts, 11 men and 3 women consented to participating in the study. With 10 time-points (Figure 2.1) and 14 astronauts', there were 140 potential blood samples for collection. One sample was not collected leaving 139 blood samples for RNA-sequencing. RNA quality control excluded 67 samples (RIN <8.0) and one sample was removed as an outlier (Supplementary Figure 2.2), leaving 71 samples for analysis *in silico*.

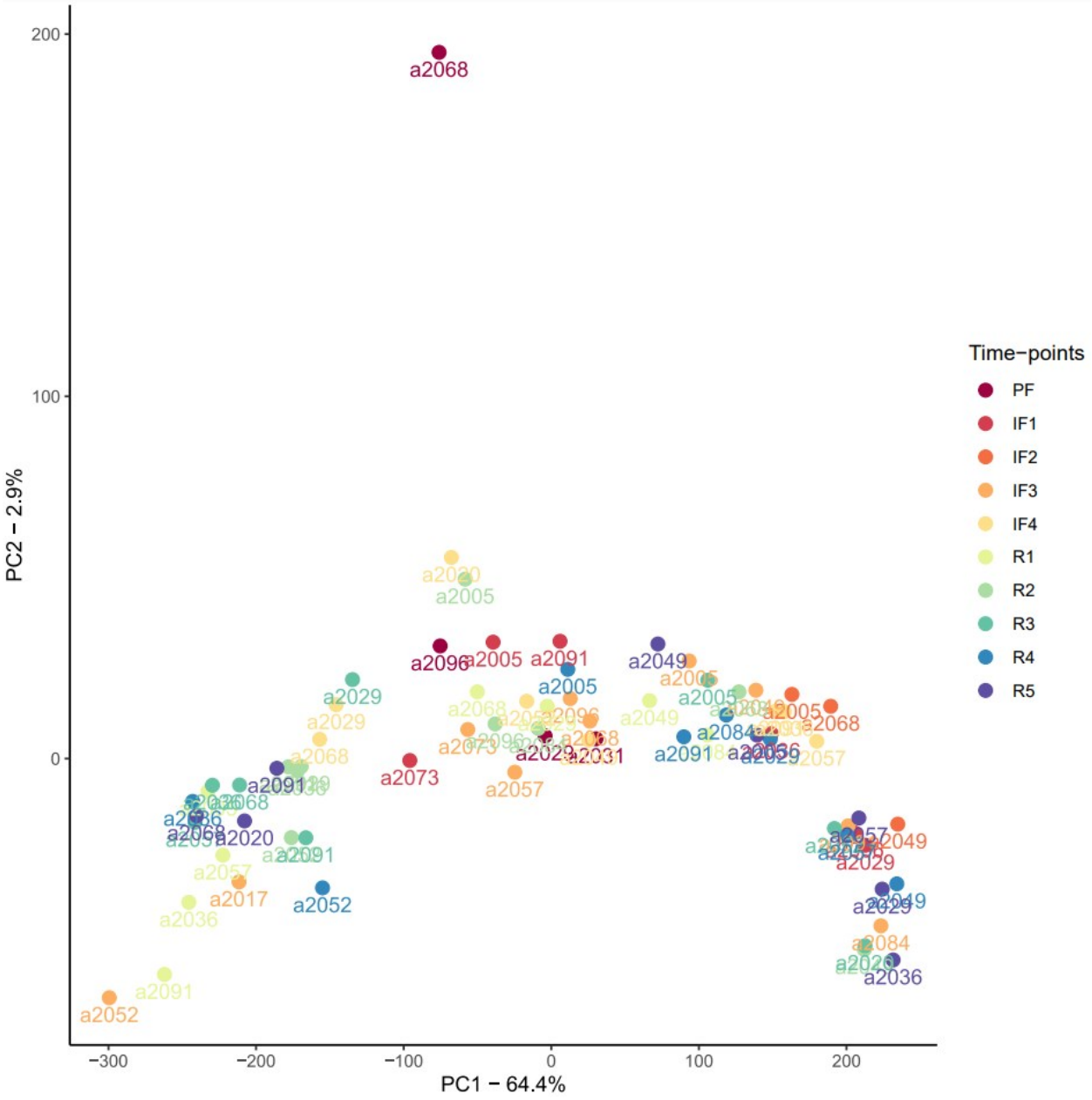

Supplemental Figure 2.2 | Pre-flight sample outlier. Principal component analysis (PCA) of all 72 samples passing RNA quality metrics (RIN ≥8.0). Sample principal component scores were calculated from the variance stabilizing transformation (VST) of normalized read counts for the 59,901 genes. Each point represents an astronaut RNA sample (Table 2.1) and colors indicates the time-point for sample collection (Figure 2.1).

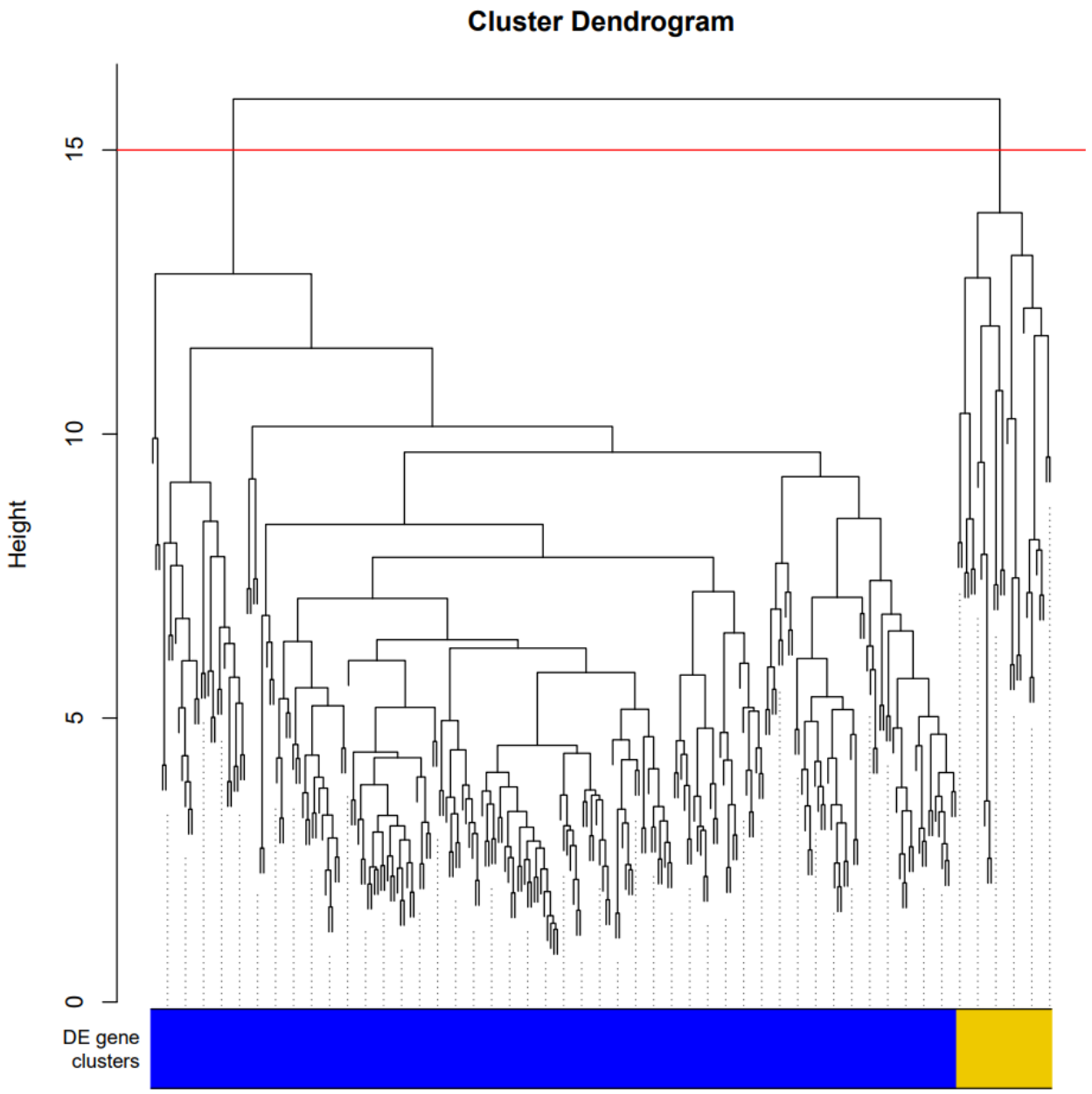

Supplemental Figure 2.3 | Gene cluster dendrogram of the 276 differentially expressed genes identified from the temporal analysis leukocyte transcriptomes. The Euclidean distance was calculated between each of the 276 gene candidates using their z-scores scaled normalized read counts, which were then hierarchically clustered into the resulting tree dendrogram revealing two distinct gene clusters characterized by similar patterns of expression changes throughout the study. The horizontal red line represents where the static tree cut was made to separate and define the two clusters of differentially

expressed genes across time. Each cluster is represented in the colored bar and identified by cluster number (Figure 2.2A).

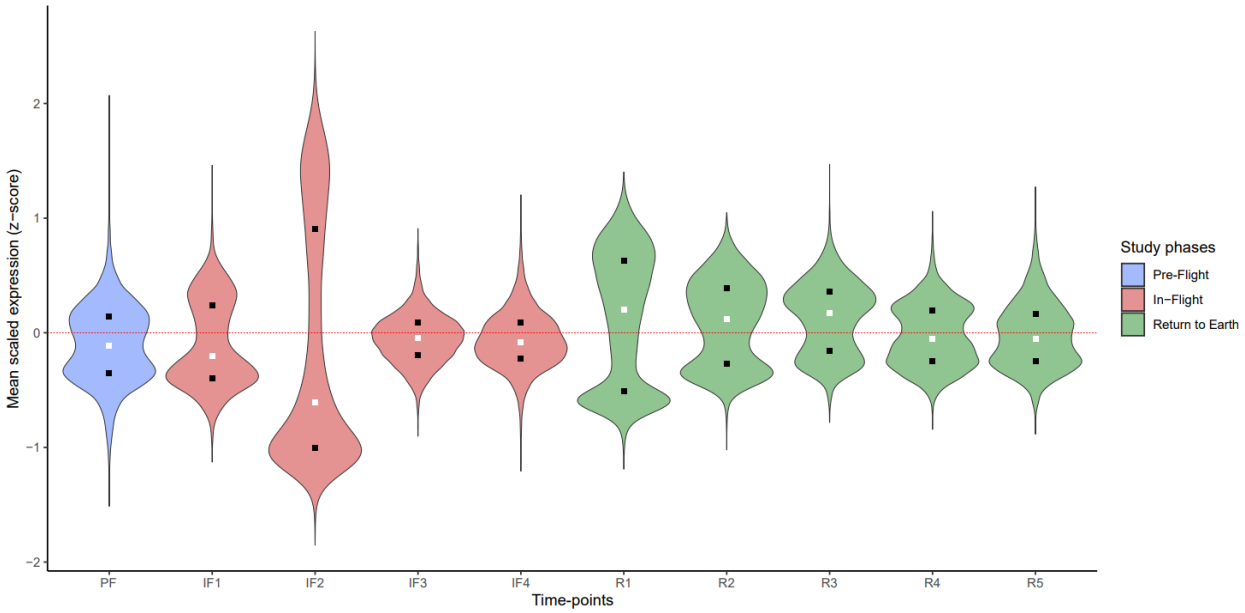

Supplemental Figure 2.4 | Expression profile of 15,410 genes expressed before, during and after long-duration spaceflight. Relative gene expression levels for the profile of 15,410 expressed transcripts (genes with mean normalized read count >45) displayed as violin plots of scaled z-scores across time. Z-scores represent the average normalized read counts for the 14 astronauts scaled across the 15,410 genes at each individual time-point. Medians indicated by white squares and upper and lower quartiles indicated by black squares. Colors denote the study phase.

Appendix II

Copyright Permissions

Chapter 1: *Medicine & Science in Sports & Exercise*

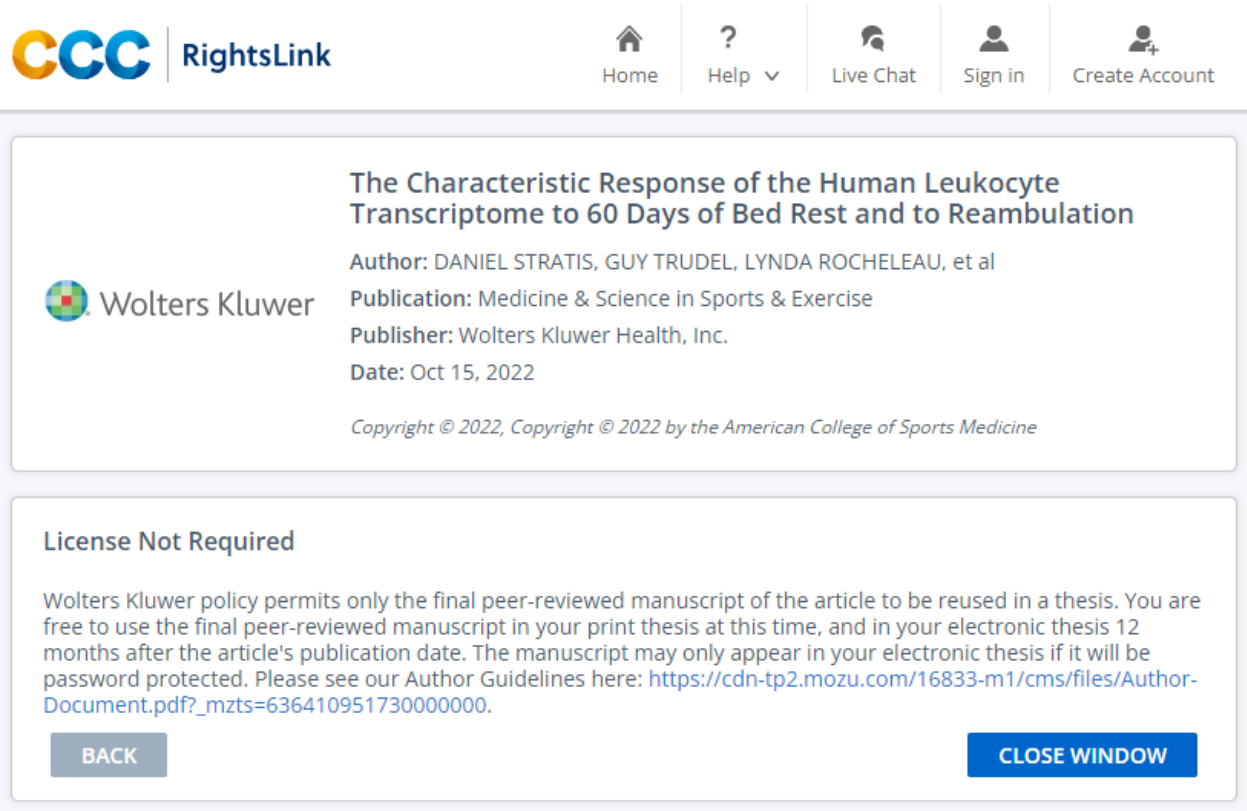

Chapter 2: *Frontiers in Immunology*

https://creativecommons.org/licenses/by/4.0/

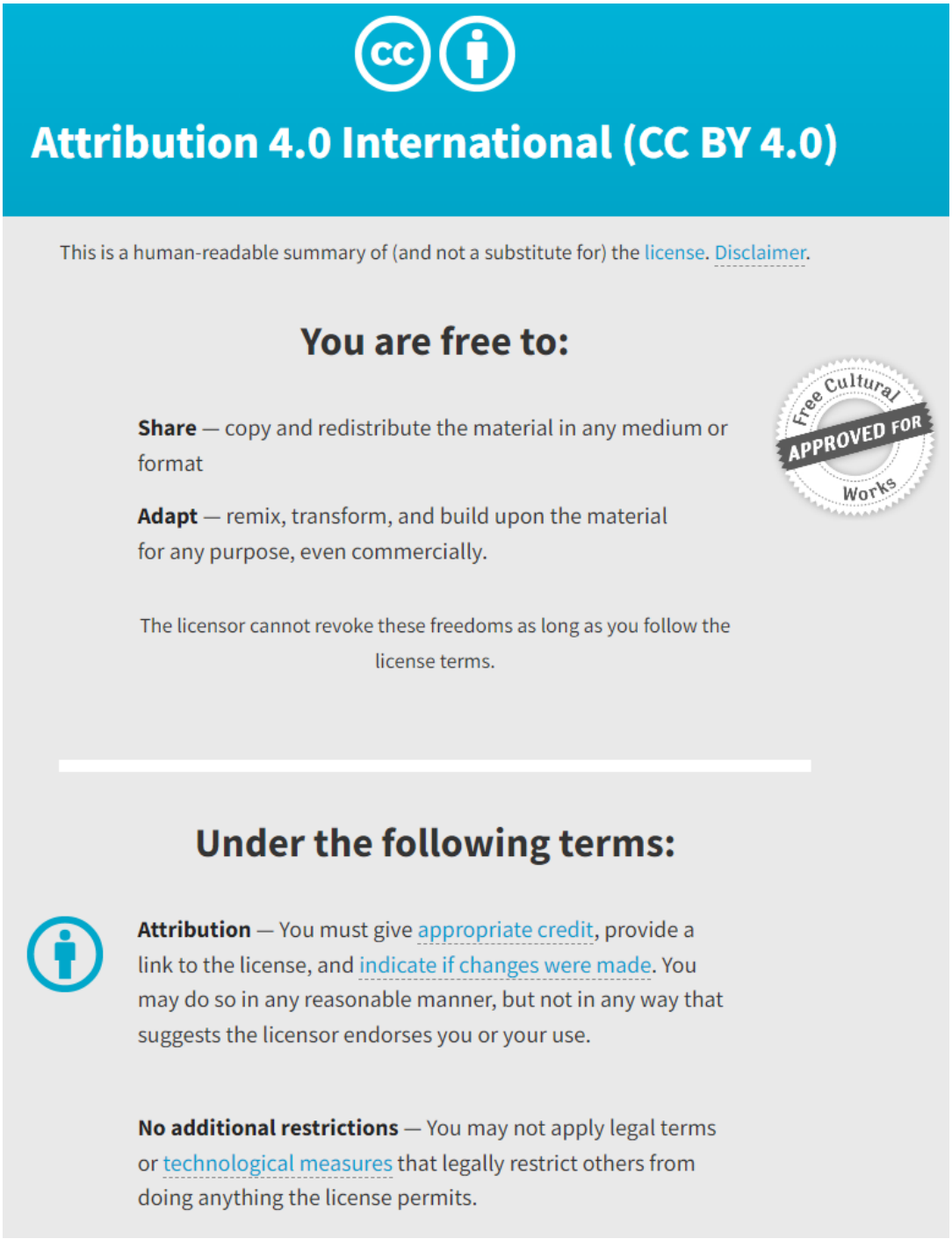

Attribution 4.0 International (CC BY 4.0)

This is a human-readable summary of (and not a substitute for) the license. Disclaimer.

You are free to:

Share — copy and redistribute the material in any medium or format

Adapt — remix, transform, and build upon the material for any purpose, even commercially.

The licensor cannot revoke these freedoms as long as you follow the license terms.

Under the following terms:

Attribution — You must give appropriate credit, provide a link to the license, and indicate if changes were made. You may do so in any reasonable manner, but not in any way that suggests the licensor endorses you or your use.

No additional restrictions — You may not apply legal terms or technological measures that legally restrict others from doing anything the license permits.

Notices:

You do not have to comply with the license for elements of the material in the public domain or where your use is permitted by an applicable exception or limitation.

No warranties are given. The license may not give you all of the permissions necessary for your intended use. For example, other rights such as publicity, privacy, or moral rights may limit how you use the material.